Centro de Investigación en Alimentación y Desarrollo, A.C.

PRODUCCIÓN Y CARACTERIZACIÓN DE ANTICUERPOS CONTRA SARS-COV-2, ANÁLISIS TRANSCRIPTÓMICO DE LINFOCITOS B EN SUJETOS CONVALECIENTES Y EVALUACIÓN DE LA INMUNIDAD HÍBRIDA INDUCIDA POR VACUNAS COVID-19

Por:

Ana Melissa García Vega

TESIS APROBADA POR LA

COORDINACIÓN DE NUTRICIÓN

Como requisito parcial para obtener el grado de

DOCTORA EN CIENCIAS

Hermosillo, Sonora Agosto, 2024

APROBACIÓN

Los miembros del comité designado para la revisión de la tesis de Ana Melissa García Vega la han encontrado satisfactoria y recomiendan que sea aceptada como requisito parcial para obtener el grado de Doctora en Ciencias.

Dr. Jesús Hemández López
Director de tesis

Dra. Verónica Mata Haro
Integrante del comité de tesis

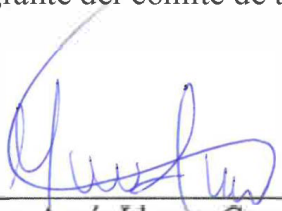

Dra. Mara Anaís Llamas Covarrubias
Integrante del comité de tesis

Dra. Adriana Karina Chávez Rueda
Integrante del comité de tesis

Dr. Miguel Ángel Hernández Oñate
Integrante del comité de tesis

DECLARACIÓN INSTITUCIONAL

La información generada en la tesis "Producción y Caracterización de Anticuerpos contra SARS-CoV-2, Análisis Transcriptónico de Linfocitos B en Sujetos Convalecientes y Evaluación de la Innunidad Híbrida Inducida por Vacunas COVID-19" es propiedad intelectual del Centro de Investigación en Alimentación y Desarrollo, A.C. (CIAD). Se permiten y agradecen las citas breves del material contenido en esta tesis sin permiso especial de la autora Ana Melissa García Vega, siempre y cuando se dé crédito correspondiente. Para la reproducción parcial o total de la tesis con fines académicos, se deberá contar con la autorización escrita de quien ocupe la titularidad de la Dirección General del CIAD.

La publicación en comunicaciones científicas o de divulgación popular de los datos contenidos en esta tesis, deberá dar los créditos al CIAD, previa autorización escrita del director(a) de tesis.

CENTRO DE INVESTIGACIÓN EN ALIMENTACIÓN Y DESARROLLO, A.C.
Coordinación de Programas Académicos

CIAD

Dra. Graciela Caire Juvera
Directora General

AGRADECIMIENTOS

Agradezco al Consejo Nacional de Humanidades, Ciencias y Tecnologías (CONAHCYT) por el apoyo prestado durante el posgrado.

Agradezco al Centro de Investigación en Alimentación y Desarrollo, A.C. (CIAD), por haber proporcionado todo lo necesario para mi completa formación doctoral.

Al financiamiento otorgado por CONAHCYT, con la subvención número 312677. Así como al Consejo Sueco de Investigación y al programa de Investigación e Innovación Horizonte 2020 de la Unión Europea, bajo la subvención número 101003650 (ATAC).

Al Dr. Jesús Hernández, mi director de tesis, por todo el apoyo brindado a lo largo de este trayecto. Se convirtió en un gran guía académico, de quien he aprendido mucho y a quien siempre estaré agradecida. Sus enseñanzas me motivaron a siempre ir por más y dar lo mejor de mi.

A la Dra. Mara Anaís Llamas Covarrubias por su gran aporte en este proyecto, además de recibirme en Japón durante mi estancia doctoral. Todas las herramientas y enseñanzas proporcionadas en el ámbito de la bioinformática abrieron un nuevo camino para mí en la investigación.

A la Dra. Verónica Mata, por sus consejos, recomendaciones y gran disposición para el enriquecimiento de este proyecto.

A la Dra. Karina Chávez, por su gran aporte en el tema de linfocitos B durante las reuniones de comité.

Al Dr. Miguel Hernández por sus conocimientos y aporte en el área de la transcriptómica, tanto en clase como en las reuniones de comité.

También quiero agradecer a todos los miembros del Laboratorio de Inmunología de CIAD, quienes

comenzaron siendo mis compañeros y se han vuelto grandes amigos. Todos han contribuido significativamente a este proyecto y con ellos he aprendido la importancia del trabajo en equipo. Gracias a Edgar y Diana por su apoyo y esas convivencias tan amenas que hemos compartido.

I especially want to thank Qiang Pan-Hammarström and Harold Marcotte, as well as Hui Wan, Rui Sun, and Fanglei Zou, from the Karolinska Institutet in Sweden, for their invaluable support in my thesis.

Además extiendo mis agradecimientos a Martín Loza de la Universidad de Tokio en Japón, por sus valiosas contribuciones y enseñanzas en los análisis bioinformáticos.

Gracias a cada uno de ustedes por ser parte fundamental de este gran proyecto; sus aportaciones hicieron posible todo esto.

DEDICATORIA

Este trabajo está dedicado a mi familia.

CONTENIDO

RESUMEN

Desde el inicio de la pandemia de COVID-19, se han realizado múltiples esfuerzos para comprender la respuesta inmune contra SARS-CoV-2, impulsando el rápido desarrollo de vacunas y terapias, incluyendo el uso de anticuerpos monoclonales. El objetivo de este trabajo fue producir y caracterizar anticuerpos monoclonales contra SARS-CoV-2 utilizando linfocitos B de sujetos convalecientes de COVID-19, así como el estudio de estas células en la respuesta al virus. Se seleccionaron nueve sujetos convalecientes con diferentes cuadros clínicos. Se aislaron los linfocitos B específicos para las proteínas S1 y RBD del SARS-CoV-2 y se utilizó la secuenciación de ARN unicelular (single-cell RNAseq) para generar librerías VDJ y de expresión génica. Después del análisis de las secuencias VDJ, se seleccionaron 44 anticuerpos y se produjeron, por métodos recombinantes, anticuerpos de cadena sencilla o formato completo IgG. El anticuerpo identificado como 19n01 mostró una potente y amplia capacidad neutralizante en ensayos de neutralización y competencia contra diversas variantes incluyendo Ómicron BA.1, BA.2 y BA.4/5. Por otro lado, el análisis de expresión génica en linfocitos B mostró una regulación positiva de genes proinflamatorios en sujetos con cuadros severos. Además, se identificó una población de linfocitos B de memoria atípicos que sugiere tener una vía de diferenciación en centros germinales por su expresión de genes *CXCR4*, *BCL2* y *MYC*, así como elevada expresión de genes característicos en respuesta a COVID-19, como *IRF1* e *IFNGR2*. Estos resultados indican que la diferenciación de linfocitos B de memoria atípicos está influenciada por la exposición al virus y podrían contribuir a la respuesta inmune antiviral.

Adicionalmente, se realizó un análisis comparativo de la inmunidad inducida por vacunas COVID-19 de CansinoBio y AstraZeneca, así como de la inmunidad híbrida desarrollada en personas infectadas y vacunadas. Se reclutaron veintisiete sujetos para obtener sus células mononucleares de sangre periférica para realizar análisis utilizando single-cell RNAseq. Los resultados muestran que la vacuna de AstraZeneca generó una respuesta de anticuerpos más robusta comparada con CansinoBio. Mientras que CansinoBio mostró fuerte activación de linfocitos T $CD4^+$ y $CD8^+$ citotóxicos y elevada expresión de genes *GZMB* y *GZMH*. Estos resultados indican que ambas vacunas generan una fuerte inmunidad híbrida pero con características diferentes.

En resumen, este trabajo contribuye al desarrollo de anticuerpos con potencial terapéutico contra

SARS-CoV-2, a la comprensión de la respuesta antiviral en linfocitos B, y la inmunidad inducida por vacunas contra COVID-19. Estos hallazgos podrían ser útiles para futuras estrategias terapéuticas y de vacunación.

Palabras clave: COVID-19, anticuerpos neutralizantes, SARS-CoV-2, linfocitos B, single-cell RNAseq, inmunidad híbrida, vacunas.

ABSTRACT

Since the beginning of the COVID-19 pandemic, multiple efforts have been made to understand the immune response against SARS-CoV-2, which has driven the rapid development of vaccines and therapies, including monoclonal antibodies. The aim of this work was to produce and characterize monoclonal antibodies against SARS-CoV-2, using B cells from convalescent COVID-19 subjects, as well as to study these cells in the antiviral response. Nine convalescent subjects who exhibited different clinical manifestations were selected for the study. The specific B cells for the SARS-CoV-2 S1 and RBD proteins were isolated from these subjects, and single-cell RNA sequencing (single-cell RNAseq) technology was used to generate VDJ and gene expression libraries. After VDJ sequence analysis, 44 antibodies were selected to produce single-chain or full-format IgG recombinant antibodies. Notably, antibody 19n01 demonstrated potent and broad neutralizing capacity in neutralization and competition assays against several variants, including Omicron BA.1, BA.2, and BA.4/5.

The gene expression analysis in B cells showed upregulation of pro-inflammatory-related genes in subjects with severe conditions. Additionally, an atypical memory B cells subset was identified, suggesting a germinal center differentiation pathway due to the expression of *CXCR4*, *BCL2*, and *MYC* genes, as well as the elevated expression of characteristic genes in response to COVID-19 such as *IRF1* and *IFNGR2*. These results indicate that the differentiation of atypical memory B lymphocytes is influenced by virus exposure and could contribute to the antiviral immune response. In addition, comparative analyses of the immune response induced by COVID-19 vaccines from CansinoBio, and AstraZeneca were conducted, as well as the hybrid immunity developed in infected and vaccinated individuals. Twenty-seven subjects were recruited to collect their peripheral blood mononuclear cells for analysis using single-cell RNA sequencing technology. The findings revealed that the AstraZeneca vaccine elicited a stronger antibody response compared to CansinoBio. Conversely, CansinoBio demonstrated robust activation of $CD4^+$ T and cytotoxic $CD8^+$ T cells and elevated expression levels of *GZMB* and *GZMH*. These results indicate that both vaccines generate strong hybrid immunity but with different characteristics. In summary, this work contributes to the development of antibodies with therapeutic potential against SARS-CoV-2, understanding the antiviral response of B cells, and the immunity induced by COVID-19 vaccines.

These findings could be valuable for future therapeutic and vaccination strategies.

Key words: COVID-19, neutralizing antibodies, SARS-CoV-2, B cells, single-cell RNAseq, hybrid immunity, COVID-19 vaccines.

1. SINOPSIS

1.1. Justificación

La pandemia por COVID-19 provocó una crisis de salud pública excepcional, lo que generó una necesidad urgente de medidas para contrarrestar la situación. En respuesta, investigadores de todo el mundo unieron sus esfuerzos para desarrollar pruebas para su detección, terapias y vacunas para controlar el SARS-CoV-2. Los anticuerpos monoclonales (mAbs) representan una herramienta terapéutica efectiva y viable para el tratamiento de diversos tipos de cáncer, trastornos autoinmunes y enfermedades infecciosas[1-3]. Por lo tanto, los mAbs fueron considerados candidatos prometedores desde el inicio de la pandemia de COVID-19.

Los mAbs terapéuticos contra SARS-CoV-2, van dirigidos principalmente hacia el dominio de unión al receptor (RBD) de la proteína spike (S) del virus. Por lo tanto, los mAb anti-RBD previenen la unión de la proteína S a su receptor la enzima convertidora de angiotensina 2 (ACE2), neutralizando el virus y evitando la infección. Este tipo de tratamiento ha sido fundamental para pacientes con comorbilidades, ya que en las etapas tempranas de la infección pueden prevenir la progresión a formas más graves de COVID-19, reduciendo así el riesgo de hospitalización y muerte[4]. Aunque se han aprobado diversas terapias basadas en anticuerpos, como la combinación de los mAbs Bamlanivimab/Etesevimab y Casirivimab/Imdevimab, actualmente no están en uso debido a la pérdida de efectividad frente a las nuevas variantes de SARS-CoV-2[5]. Por lo tanto, es importante la búsqueda y caracterización continua de mAbs dirigidos a sitios altamente conservados de la proteína S, con la finalidad de desarrollar estrategias terapéuticas que puedan neutralizar nuevas mutaciones del virus. Este enfoque no solo podría prolongar su eficacia en el tratamiento de la COVID-19, sino que también sería de utilidad para futuras estrategias en el desarrollo de anticuerpos contra otras infecciones virales emergentes.

Por otro lado, parte de los esfuerzos que se han realizado durante la pandemia han estado orientados a la comprensión de la respuesta inmune frente a SARS-CoV-2. Particularmente, la respuesta de los linfocitos B va más allá del estudio de la producción de anticuerpos. Se ha reportado que estas células presentan alteraciones relacionadas con la severidad de la enfermedad y un aumento en la activación de la respuesta inmune extrafolicular de linfocitos B. Esta activación se asocia con la

presencia de marcadores proinflamatorios y la producción de autoanticuerpos, lo que potencialmente contribuye a un peor pronóstico[6,7]. Además, se ha observado una expansión de diversas subpoblaciones celulares asociadas a cuadros de mayor severidad, como los linfocitos B atípicos de memoria[8]. Sin embargo, estas células han sido poco estudiadas en el contexto de COVID-19, por lo que la vía de desarrollo y funciones de los linfocitos B atípicos de memoria siguen sin estar claros, incluso en otras condiciones como malaria y VIH[9]. Por lo tanto, surge la necesidad de realizar estudios que utilicen tecnologías avanzadas como el single-cell RNAseq para analizar a profundidad la respuesta de linfocitos B en COVID-19 en los diversos cuadros clínicos de la enfermedad. Esto además, permite evaluar la heterogeneidad de las células y sus posibles vías de desarrollo.

Otro aspecto crucial durante la pandemia ha sido el rápido desarrollo de vacunas contra el COVID-19, empleando diversas plataformas tecnológicas como ARNm, virus inactivados, unidades proteicas y vectores adenovirales. En Hermosillo, Sonora, las primeras vacunas disponibles fueron la de AstraZeneca, administrada en dos dosis, y la vacuna de CansinoBio, administrada en una sola dosis, ambas desarrolladas utilizando vectores adenovirales. A diferencia de la vacuna de Pfizer/BioNTech, ampliamente estudiada por su innovadora plataforma de ARNm[10-13], las vacunas basadas en vectores adenovirales han sido relativamente poco estudiadas a nivel de single-cell RNAseq. Estos estudios son fundamentales ya que permiten comprender como estas vacunas activan y actúan sobre la respuesta inmune a nivel unicelular. Además, estudiar vacunas con la misma plataforma, pero con esquemas diferentes, como es el caso de AstraZeneca y CansinoBio, permite evaluar y comparar sus respuestas inmunitarias, incluyendo la inmunidad híbrida inducida en sujetos con infección previa. Comprender estos aspectos podría ser de utilidad para el desarrollo de futuras estrategias de vacunación.

1.2. Antecedentes

1.2.1. COVID-19

La enfermedad por coronavirus 19 (COVID-19), es un proceso infeccioso causada por el

coronavirus del síndrome respiratorio agudo severo tipo 2 (SARS-CoV-2). Esta enfermedad ha causado grandes estragos a nivel mundial, provocando más de 6 millones de muertes. Los primeros casos se reportaron en Wuhan, provincia de Hubei, China a finales de diciembre de 2019 y a partir de entonces, el virus se diseminó rápidamente en todo el mundo. En enero del 2020, la Organización Mundial de la Salud (OMS) declaró que la COVID-19 era una emergencia sanitaria de salud pública mundial, y en marzo de 2020 la calificó como pandemia[14].

El SARS-CoV-2 es un virus de ARN monocatenario que codifica para 4 proteínas estructurales: spike (S), envoltura, nucleocápside y membrana. La proteína S es una glicoproteína trimérica y tiene la capacidad de ser escindida en dos subunidades: S1, responsable de la unión al receptor de la célula a través del RBD y en S2, que se encarga de la fusión a la membrana celular. Se trata de una proteína altamente inmunogénica, capaz de inducir una potente respuesta de anticuerpos neutralizantes, por lo tanto, es un objetivo clave para el desarrollo de vacunas y terapias[15,16]. El principal modo de transmisión de SARS-CoV-2 es a través de microgotas respiratorias que transportan el virus infeccioso por contacto cercano o transmisión directa de personas que albergan el virus.

Una vez que el virus entra a las células hospederas mediante la unión de la proteína S al receptor celular ACE2, el virus comienza la replicación viral en una fase temprana de la infección. Se estima que entre el 17% y el 33% de los pacientes infectados permanecen asintomáticos[17]. Dependiendo de los síntomas clínicos, así como diversas pruebas radiológicas y de laboratorio, la OMS clasificó la severidad de la enfermedad en 4 tipos: leve, moderado, severo y crítico.

Se ha observado que todas las personas sin distinción de edad corren el riesgo de contraer esta infección, la mayoría experimentan una enfermedad respiratoria leve a moderada y se recuperarán sin requerir un tratamiento especial[18]. Sin embargo, existen poblaciones vulnerables con mayor riesgo a desarrollar COVID-19 grave. Algunas de estas poblaciones son pacientes mayores a 60 años y aquellos con comorbilidades médicas como obesidad, enfermedad cardiovascular, enfermedad renal crónica, diabetes, asma, cáncer, entre otros[19]. Los resultados clínicos, ingreso a unidades de cuidados intensivos y la duración de la estadía se correlacionan directamente con estas condiciones subyacentes y edad del paciente[19,20]. Por otro lado, el surgimiento de variantes de preocupación (VOCs) del SARS-CoV-2 ha sido otro factor que incrementa la severidad de la enfermedad[21,22]. No obstante, el uso de vacunas y terapias contra COVID-19, ha demostrado disminuir la severidad, incluso en personas con comorbilidades, así como también se ha reducido

la tasa de hospitalización y muertes ocasionadas por SARS-CoV-2[23].

1.2.2. Variantes de Preocupación del SARS-CoV-2 (VOCs)

La mutación es una característica inherente a la mayoría de los virus, sin embargo, aquellos con un genoma de ARN, como lo es el SARS-CoV-2 presentan tasas de mutación mucho más altas comparada con aquellos virus con genoma de ADN. La primera variante identificada en 2020 fue la denominada D614, la cual se asoció con un incremento en la transmisión pero sin cambios en su virulencia[24]. Desde entonces, múltiples variantes de SARS-CoV-2 se han descrito, algunas se han considerado VOC por su mayor transmisibilidad, capacidad de evadir el sistema inmune y virulencia. Entre ellas se encuentran las variantes Alfa, Beta, Gamma y Delta, que presentan desde 1 hasta 3 mutaciones en el RBD, favoreciendo la evasión inmune. En el caso de la variante Ómicron, esta provocó un incremento de casos en un corto periodo, desde su aparición en noviembre de 2021. La evolución de Ómicron ha dado lugar al surgimiento de múltiples subvariantes, las cuales presentan de 12 a 14 mutaciones en su RBD y más de 57 mutaciones en la proteína S[25].

Ómicron ha sido una causa importante de preocupación mundial dado su alta transmisibilidad, la cual reemplazó rápidamente las VOC anteriores[25]. Las mutaciones que presenta ha dado como resultado una mayor afinidad de la proteína S hacía el receptor ACE2, generando cambios en la infección celular y tropismo, aumentando su transmisibilidad[26,27]. No obstante, se ha demostrado que Ómicron presenta menor patogenicidad comparada con variantes anteriores, debido a que infecta preferentemente el tracto respiratorio superior, lo que a menudo resulta en casos asintomáticos o cuadros leves[28,29]. Actualmente, las últimas subvariantes de Ómicron con mayor prevalencia en los meses de mayo y junio de 2024 han sido KP.2, KP.3, JN.1.7, KP.1.1 y JN.1, según los reportes del Centro para el Control y la Prevención de Enfermedades (CDC). Por otro lado, la alta seroprevalencia e inmunidad inducida por la infección, vacunación o una combinación de ambas (inmunidad híbrida), proporciona protección contra estas subvariantes, reduciendo la gravedad y tasa de hospitalizaciones. Sin embargo, las personas con comorbilidades continúan siendo vulnerables a infecciones severas y complicaciones por COVID-19, siendo fundamental el desarrollo y actualización continua de terapias y vacunas para esta enfermedad.

1.2.3. Respuesta Inmune Contra SARS-CoV-2

Al igual que en otras infecciones, la respuesta inmune contra el SARS-CoV-2 se divide en dos fases principales: la respuesta inmune innata y la respuesta inmune adaptativa. La respuesta inmune innata actúa como la primera línea de defensa, encargándose de reconocer al virus de manera rápida y activando el sistema inmune para contener la enfermedad en sus etapas iniciales. Esta fase incluye la participación de células como monocitos, macrófagos, neutrófilos y células dendríticas, que detectan la presencia del patógeno a través de receptores de reconocimiento de patrones (PRRs) y desencadenan una serie de respuestas para limitar la propagación del virus. Sin embargo, una activación exacerbada de monocitos y macrófagos, principalmente, puede contribuir a la tormenta de citocinas, característica en pacientes con cuadros más severos de COVID-19. Esta situación se asocia con niveles elevados de citocinas como IL-2, IL-7, IL-10, G-CSF, IFN-γ, TNF-α e IL-6, lo cual puede desencadenar fallo multiorgánico y resultados fatales en estos pacientes[30,31].

A medida que la infección progresa, las células dendríticas procesan y presentan el antígeno viral a los linfocitos T para iniciar la respuesta inmune adaptativa. En esta fase, la respuesta celular mediada por linfocitos T y la respuesta humoral por linfocitos B, juegan roles fundamentales para proporcionar una defensa robusta y específica contra SARS-CoV-2. En la respuesta celular, los linfocitos T $CD8^+$ se encargan de eliminar las células infectadas por el virus, mientras que los linfocitos T $CD4^+$ desempeñan un papel crucial en la cooperación y potenciación de la activación de otras células mediante la producción de citocinas. Un ejemplo de esta cooperación es la activación y diferenciación de los linfocitos B en células plasmáticas productoras de anticuerpos y linfocitos B de memoria[32]. Diversos estudios han reportado que pacientes con cuadros graves por COVID-19 presentan reducción de linfocitos T y un aumento en la expresión de receptores de inhibición como PD-1, TIM-3, LAG-3, CTLA-4 y NKG2A[33-35]. La expresión de estos receptores se ha observado principalmente en linfocitos T $CD8^+$ y refleja un perfil de células exhaustas, lo que hace reducir su funcionalidad ante la respuesta antiviral y es un predictor de severidad en COVID-19[34,36].

En la inmunidad humoral en respuesta a COVID-19 la participación de los linfocitos B en la producción de anticuerpos neutralizantes contra SARS-CoV-2 es fundamental. Durante la fase inicial de la infección, los anticuerpos IgM suelen aparecer en la primera semana y alcanzan su

punto máximo entre el día 8 y 10[37,38]. Por otro lado, los anticuerpos IgG comienzan a detectarse aproximadamente a partir de la segunda semana después de la infección y alcanzan su punto máximo entre las 3 y 4 semanas posteriores al inicio de los síntomas[37,39]. Sin embargo, la duración y la magnitud de la respuesta de los anticuerpos pueden variar entre individuos y están influenciadas por varios factores, incluyendo la severidad de la infección, la edad y el estado inmunológico previo del paciente[37-39].

Los pacientes con cuadros severos, han evidenciado alteraciones en las subpoblaciones de linfocitos B relacionadas a la severidad. Además, se ha observado que en estos pacientes existe una fuerte activación de la vía extrafolicular[6,7]. Esta vía está asociada con una diferenciación rápida de linfocitos B y producción de anticuerpos contra el virus, aunque estos anticuerpos tienden a tener una afinidad menor hacia el antígeno y ser menos duraderos. En contraste, la diferenciación de los linfocitos B a través de la vía de centros germinales es crucial para la formación de linfocitos B de memoria y células plasmáticas productoras de anticuerpos con alta afinidad hacia el antígeno y mayor capacidad neutralizante[40]. Sin embargo, en estudios postmortem se ha identificado la ausencia de centros germinales en pacientes que fallecieron a causa de COVID-19, lo que explica la activación preferencial de la vía extrafolicular en los pacientes con cuadros severos de la enfermedad[7]. Además, la gravedad de COVID-19 se ha asociado con la producción de autoanticuerpos, lo cual, junto con las alteraciones mencionadas anteriormente, contribuye a un peor pronóstico.

1.2.4. Inmunidad Híbrida

La inmunidad híbrida resulta de la combinación de la inmunidad natural por una infección de SARS-CoV-2 y la inmunidad adquirida por vacunación, produciendo una respuesta sinérgica[41].

Tras la aprobación de vacunas contra COVID-19 desarrolladas con diversas plataformas tecnológicas, como ARNm (Pfizer/BioNTech y Moderna), subunidades proteicas (Novavax), virus inactivado (CoronaVac), y vectores adenovirales (AstraZeneca, Johnson & Johnson y CanSinoBio), se ha observado esta respuesta sinérgica en la mayoría de las investigaciones con individuos previamente infectados[42-47].

Estudios con vacunas como Pfizer/BioNTech y AstraZeneca indican que después de una sola dosis, los sujetos con infección previa muestran niveles significativamente más altos de anticuerpos neutralizantes en comparación con aquellos que recibieron dos dosis sin infección previa[42,48,49]. Además, con la vacuna Pfizer/BioNTech se ha observado que la dosis de refuerzo en sujetos previamente infectados aumenta la frecuencia de linfocitos B de memoria de las líneas germinales IGHV3-53, IGHV3-66 y IGHV2-5, los cuales tienen la capacidad de producir anticuerpos neutralizantes contra diversas variantes[47]. De manera similar, se ha observado que después de 3 meses de la segunda dosis de Pfizer/BioNTech o Moderna, los sujetos con infección previa mantienen niveles más altos de anticuerpos, linfocitos B de memoria y linfocitos T $CD4^+$ con perfil Th1 en comparación con aquellos sin infección previa. Sin embargo, una tercera dosis proporciona un incremento de anticuerpos circulantes, pero no de linfocitos B o T de memoria, lo que sugiere que la memoria inmunitaria se maximiza después de dos dosis para el caso de estas vacunas en sujetos previamente infectados[50].

1.3 Hipótesis

Los anticuerpos monoclonales aislados a partir de linfocitos B de memoria de pacientes convalecientes, tienen la capacidad de neutralizar a SARS-CoV-2 y sus variantes de preocupación. Además, la respuesta de linfocitos B y la activación de sus subpoblaciones es diferente en los distintos cuadros clínicos que se presentan en la enfermedad de COVID-19. Por otro lado, las vacunas basadas en vectores adenovirales tienen la capacidad de inducir una respuesta inmune híbrida robusta en sujetos previamente infectados por SARS-CoV-2.

1.4 Objetivo General

Producir y caracterizar anticuerpos monoclonales específicos a la proteína S de SARS-CoV-2, a partir de linfocitos B de memoria de personas convalecientes y realizar un análisis de expresión

diferencial de estas células, en distintos cuadros clínicos de COVID-19. Así como también evaluar la inmunidad híbrida inducida por vacunas basadas en vectores adenovirales en sujetos previamente infectados por SARS-CoV-2.

1.5. Objetivos Específicos

1. Establecer y validar las condiciones para identificar y aislar linfocitos B de memoria de personas convalecientes que reconozcan las proteínas S1 y RBD de SARS-CoV-2.
2. Secuenciar el ARNm de células individuales de linfocitos B de memoria específicos a las proteínas S1 y RBD de SARS-CoV-2, y analizar sus regiones VDJ para identificar las secuencias codificantes de anticuerpos contra el virus.
3. Producir y caracterizar anticuerpos monoclonales que reconocen a SARS-CoV-2 y las variantes de preocupación.
4. Realizar un análisis de expresión diferencial, a partir de la secuenciación de ARNm de células individuales de linfocitos B de personas convalecientes con distintos cuadros clínicos de COVID-19.
5. Realizar un estudio comparativo de la inmunidad híbrida inducida por las vacunas COVID-19 de CansinoBio y AstraZeneca.

1.6 Sección Integradora

El trabajo realizado durante este proyecto doctoral comenzó con la validación de condiciones para aislar linfocitos B específicos para las proteínas S1 y RBD de sujetos convalecientes de COVID-19. Esto fue seguido de un single-cell RNAseq a partir de linfocitos B para obtener datos de expresión génica y las secuencias VDJ en estas células, cumpliendo así con los dos primeros objetivos del proyecto. Partiendo de estos resultados, se prosiguió con el cumplimiento del tercer y cuarto objetivo. En el tercer objetivo se realizó la producción y caracterización de anticuerpos

neutralizantes contra el SARS-CoV-2 y sus variantes circulantes a partir de las secuencias VDJ. En el cuarto objetivo se profundizó en los análisis de la expresión génica y el repertorio VDJ de los linfocitos B en sujetos convalecientes, con el propósito de estudiar las características de estas células en diversos cuadros clínicos. Además, se estudiaron las diferentes subpoblaciones de linfocitos B que predominaba en los sujetos con los diferentes cuadros clínicos de la enfermedad. Como quinto objetivo, se realizó un estudio comparativo usando single-cell RNAseq de la inmunidad híbrida generada por las vacunas basadas en vectores adenovirales AstraZeneca (AZD1222) y CansinoBio (Ad5-nCoV). Este estudio se realizó debido a la necesidad de evaluar la respuesta inmune tras la introducción de estas vacunas, las cuales fueron utilizadas desde un principio en los esquemas de vacunación en Hermosillo, Sonora.

En la primera fase de resultados, como parte de la producción y caracterización de anticuerpos neutralizantes contra el SARS-CoV-2, se incluye un artículo publicado titulado "*19n01, a broadly neutralizing antibody against omicron BA.1, BA.2, BA.4/5, and other SARS-CoV-2 variants of concern*". En este trabajo, se obtuvieron 25,621 secuencias VDJ de linfocitos B de sujetos convalecientes de COVID-19 infectados con la cepa original del SARS-CoV-2. De estas, se seleccionaron las secuencias para producir anticuerpos, para ellos se definieron cinco criterios: 1) secuencias con isotipo IgG, 2) cadenas ligeras y pesadas pareadas, 3) clonotipo con frecuencia ≥2, 4) genes *IGHV* comunes en anticuerpos neutralizantes contra SARS-CoV-2, y 5) >70% de identidad con anticuerpos reportados contra SARS-CoV-2. En total, se seleccionaron 44 anticuerpos para producirlos con tecnología recombinante en formato de cadena sencilla. De estos anticuerpos, solo 9 mostraron reconocimiento hacia la cepa ancestral del SARS-CoV-2, y 5 anticuerpos (19n01, 01n21, 01n01, 20n01 y 20n18) reconocieron tanto la cepa ancestral como al menos una VOC. Por lo tanto, estos 5 anticuerpos se produjeron en formato completo IgG para continuar con su caracterización.

Los resultados de caracterización demostraron que, de los 5 anticuerpos, el 19n01 fue el más potente, mostrando una alta capacidad de unión y neutralización de las variantes Alfa, Beta, Gamma, Delta, Kappa, Zeta, así como de las subvariantes Ómicron BA.1, BA.2 y BA.4/5. Los ensayos de neutralización con pseudovirus mostraron que el 19n01 tenía una alta capacidad para neutralizar la variante G614 y las subvariantes Ómicron BA.1, BA.2 y BA.4/5, con valores de concentración inhibitoria (IC50) entre 0.0035 y 0.0164 μg/mL. En los estudios de microneutralización con el virus de la cepa ancestral de SARS-CoV-2 y las variantes G614, Alfa,

Beta, Delta, y Ómicron BA.1 y BA.5, el 19n01 mostró valores IC50 entre 0.013 y 0.267 µg/mL. Además, se realizaron análisis biofísicos de competencia y estructurales, evidenciando que el anticuerpo 19n01 compite con el receptor ACE2 por la unión al RBD, lo que explica su capacidad neutralizante. Los resultados de resonancia de plasmón superficial (SPR) confirman la elevada afinidad hacia Ómicron BA.2 y BA.4/5 con K_D de 61 a 31 nM, respectivamente. Sin embargo, la afinidad que mostró contra Ómicron BA.1 se vio reducida presentando un K_D de 441 nM. Por otro lado, el modelado molecular mostró que parte del sitio de unión del 19n01 está en contacto cercano con la posición G446 de la proteína S, lo que explica la baja afinidad contra Ómicron BA.1 ya que esta subvariante presenta una mutación en este sitio (G446S). Además, se observó que las posiciones K444 y V445 de la proteína S tienen contacto directo con el sitio de unión del anticuerpo 19n01. Por lo tanto, las subvariantes de Ómicron con mutaciones en esas posiciones ya no son susceptibles a su neutralización, como es el caso de las subvariantes BQ.1.1, XBB.1.5, JN.1.7, KP.3, entre otras.

Fue interesante observar que el anticuerpo 19n01 provenía de un paciente con un cuadro moderado de COVID-19, quien se había infectado con la cepa ancestral del SARS-CoV-2 antes de la circulación de variantes VOC en Hermosillo, Sonora. Esto sugiere que la infección natural puede estimular la activación y expansión de linfocitos B capaces de producir anticuerpos con una amplia capacidad neutralizante. Así mismo, el anticuerpo 19n01 demostró una capacidad neutralizante amplia y superior en comparación con los demás, resultando ser un anticuerpo con potencial terapéutico, hasta el surgimiento de subvariantes Ómicron con mutaciones en los sitios K444 y V445. Finalmente, la base de datos generada, que contiene 25,621 secuencias, podría ser de gran utilidad para seguir explorando potenciales anticuerpos neutralizantes contra variantes emergentes de preocupación. Las estrategias de selección y caracterización empleadas en este trabajo podrían servir para la identificación y estudio de futuros anticuerpos, no solo contra el SARS-CoV-2, sino también contra otros agentes infecciosos.

La segunda fase de los resultados abarcó el análisis de expresión génica en linfocitos B de sujetos convalecientes de COVID-19, y la caracterización de linfocitos B de memoria atípicos. Estos resultados se presentan en el artículo "*Single-cell transcriptomic analysis of B cells reveals new insights into atypical memory B cells in COVID-19*", el cual se encuentra publicado en la revista Journal of Medical Virology. Los análisis transcriptómicos a nivel unicelular de este estudio permitieron identificar una población heterogénea de linfocitos B en sujetos convalecientes con

cuadros críticos, severos, moderados y leves. Dentro de la población heterogénea, se identificaron 10 subpoblaciones, incluyendo linfocitos B transicionales (T1, T2 y T3), naïve activados, 5 subtipos de linfocitos B de memoria, entre ellos un grupo de memoria atípica, y finalmente uno de células secretoras de anticuerpos. Notablemente, se observó un incremento de linfocitos B transicionales en sujetos con cuadros críticos y severos, asociado a la necesidad de desarrollar linfocitos B maduros debido a la persistencia antigénica. Sin embargo, la evidencia de que una alta proporción de estas células permanecieron en estados de transición durante la convalecencia en cuadros críticos y severos sugiere una posible relación con la progresión de la enfermedad, ya que fueron células que no alcanzaron estadios más diferenciadas.

Los análisis de expresión génica diferencial revelaron una firma proinflamatoria en grupos convalecientes con cuadros críticos y severos, destacando una elevada expresión de diversos genes proinflamatorios como *GADD45B*, *MAP3K8*, *NFKBIA*, *JUNB*, *AREG*, *PPP1R15A* y *FOSB*, en la mayoría de las subpoblaciones. En contraste, los grupos convalecientes con cuadros moderados y leves mostraron incremento en la expresión de genes antivirales como *IFI16*, *IFI30*, *ISG20*, *AIM2*, además de genes de activación incluyendo *SPIB*, *PTPRCAP*, los cuales estaban reprimidos en los grupos críticos y severos. Esto sugiere que diversas subpoblaciones, incluyendo linfocitos B transicionales, naïve, de memoria y células secretoras de anticuerpos, pueden contribuir a la respuesta proinflamatoria en casos severos. Sin embargo, su adecuada activación también puede cooperar en la respuesta antiviral en casos leves y moderados.

Tras la identificación de una subpoblación de linfocitos B de memoria atípicos, se observaron diferencias en su repertorio en comparación con las diferentes subpoblaciones de linfocitos B de memoria convencionales. Los análisis de hipermutación somática (SHM) revelaron que los linfocitos B de memoria atípicos mostraban una tasa de SHM menor que las células de memoria clásicas con cambio de isotipo, pero una tasa mayor de SHM en comparación con las células de memoria clásica sin cambio de isotipo. Así mismo, se observó que los linfocitos B de memoria atípicos presentaban diferencias en la combinación de uso de genes *IGHV/IGHJ* al compararlos con los de memoria convencional. Algunos de estos genes mayormente expresados en las células atípicas incluyen *IGHV3-11/IGHJ4*, *IGHV6-1/IGHJ4* y *IGHV1-18/IGHJ5*. Lo que indica que estas células presentan un perfil transcripcional y de repertorio diferente a las convencionales.

Los linfocitos B de memoria atípicos representan una población poco estudiada en COVID-19, por lo que aún se desconoce su desarrollo y funciones específicas en esta enfermedad. El análisis de

trayectoria revela que estas células atípicas siguen una vía de diferenciación similar a las convencionales de memoria. Además, pasan por procesos de diferenciación en centros germinales (CG) dado a la regulación positiva de genes *CXCR5*, *CXCR4*, *MYC*, *BCL2* y *MCL1*, importantes para la circulación y mantenimiento de CG. Los análisis de enriquecimiento de los genes expresados diferencialmente en los linfocitos B atípicos de memoria indican que participan en procesos biológicos de células activas y de señalización del receptor de células B (BCR), contrario a lo que se ha sugerido en algunas patologías que podrían tratarse de células anérgicas o exhaustas. Finalmente, se identificó una incremento de expresión de genes ampliamente reportados en COVID-19, como *IFNGR2*, *DUSP1*, *ZFP36* y *IFITM3*, en estas células. Esto sugiere que su desarrollo podría verse influenciado por la exposición antigénica y el entorno inmunológico en respuesta al virus. Por lo tanto, es probable que estas células sean funcionalmente activas y contribuyan a la respuesta inmune contra COVID-19.

El análisis transcriptómico de linfocitos B a nivel unicelular en sujetos convalecientes reveló una gran heterogeneidad de estas células entre los diferentes cuadros clínicos. Los resultados destacan la capacidad de los linfocitos B para contribuir a la respuesta proinflamatoria, particularmente en los casos críticos y severos. Además, los hallazgos de este estudio indican que los linfocitos B de memoria atípicos presentan un perfil transcripcional y de repertorio distintos en comparación con los linfocitos B de memoria convencionales. Así mismo, los análisis sugieren que estas células siguen una vía de diferenciación a través de centros germinales, similar a los linfocitos B de memoria convencionales. Sin embargo, su diferenciación y activación podrían estar influenciadas por genes y factores de transcripción característicos de la exposición antigénica al SARS-CoV-2. Estos resultados proporcionan una mayor comprensión de los linfocitos B de memoria atípicos, así como del rol de las subpoblaciones de linfocitos B en los diversos cuadros clínicos de COVID-19.

Como último objetivo en este trabajo doctoral, se realizó un estudio comparativo de la inmunidad híbrida generada por las vacunas basadas en vectores adenovirales. Los resultados de este trabajo se encuentran ya publicados bajo el título "*Comparative single-cell transcriptomic profile of hybrid immunity induced by adenovirus vector-based COVID-19 vaccines*". En este estudio se evaluó la respuesta de anticuerpos y se realizaron análisis transcriptómicos unicelulares en sujetos vacunados con AstraZeneca (AZD1222) y CansinoBio (Ad5-nCoV). Para este propósito se estudiaron 5 grupos: vacunados con Ad5-nCoV (Cso, n = 6), vacunados con AZD1222 (AZ, n = 4), previamente infectados y vacunados con Ad5-nCoV (Cso-hb, n = 6) o AZD1222 (AZ-hb, n = 6), y por último

un grupo de infectados sin vacunación (Inf, n = 5). El esquema de vacunación de Ad5-nCoV consistió en una sola dosis, mientras que AZD1222 incluyeron dos dosis, con intervalo de un mes entre dosis.

Los resultados de la evaluación de anticuerpos por ELISA y microneutralización mostraron que la inmunidad híbrida observada en los grupos AZ-hb y Cso-hb, se asoció con una mejor respuesta de anticuerpos neutralizantes (nAbs) en comparación con los grupos sin infección AZ y Cso. Además, la vacuna AZD1222 mostró un mayor incremento de nAbs en general, tanto en los grupos de inmunidad híbrida o sin infección (AZ-hb y AZ), en comparación aquellos vacunados con Ad5-nCoV. Los análisis de single-cell RNAseq se centraron en evaluar el perfil de linfocitos B y linfocitos T en respuesta a ambas vacunas. En el caso de los linfocitos B, se identificaron cuatro subpoblaciones: dos asociadas a células naïve (Bnaïve-1 y Bnaïve-2), uno de células de memoria y otro de plasmablastos. Además, se observó una elevada frecuencia de linfocitos B de memoria en los grupos Cso y Cso-hb. En contraste, en los grupos AZ y AZ-hb se identificó una población naïve (Bnaïve-1) caracterizada por el incremento de la expresión de *CXCR4* y genes de activación como *CD83* y *CD69*, lo que sugiere una población de linfocitos B naïve con capacidad migratoria para continuar su diferenciación. Por lo tanto, mientras los grupos vacunados con Ad5-nCoV habían desarrollado ya mayor proporción de linfocitos B de memoria, los grupos vacunados con AZD1222 continuaban con la activación y diferenciación de linfocitos B naïve.

El perfil transcriptómico de linfocitos T, reveló 17 subpoblaciones, incluyendo 9 subpoblaciones de linfocitos T $CD4^+$, 7 subpoblaciones de linfocitos T $CD8^+$ y 1 subpoblación de linfocitos T γδ. Estas subpoblaciones mostraron una respuesta celular heterogénea después de la vacunación, la inmunidad híbrida o la infección natural. En el caso de los grupos Cso, se observó que una sola dosis de Ad5-nCoV fue capaz de activar algunas subpoblaciones de manera similar a los grupos de inmunidad híbrida AZ-hb, que habían experimentado previamente una infección y recibido dos dosis de AZD1222. Esta respuesta fue notable principalmente en las subpoblaciones CD4.Tm-3, CD4.Tn-2 y CD8.Te-2. También, se observó una expansión significativa de la subpoblación CD8.Te-4 exclusivamente en el grupo Cso-hb, caracterizada por un perfil citotóxico con un incremento de la expresión de *GZMB*, *GZMH* y *IFNG*, genes cruciales para una respuesta antiviral efectiva. Sin embargo, estas células también mostraron la expresión de genes que codifican para receptores de inhibición como PD-1 (*PDCD1*), TIM-3 (*HAVCR2*) y *LAG-3*, asociados a una respuesta de células exhaustas. Por lo tanto, esto sugiere que la activación robusta de la respuesta

celular inducida por la vacuna Ad5-nCoV activó la expresión de genes asociados con agotamiento celular, posiblemente como un mecanismo de equilibrio para mantener la homeostasis del sistema inmune en respuesta a la vacunación.

Este estudio demuestra que ambas vacunas estimulan eficazmente la inmunidad híbrida con características distintas, resaltando la capacidad de la vacuna AZD1222 para generar una respuesta humoral robusta de anticuerpos neutralizantes. Mientras que Ad5-nCoV se destacó por inducir una respuesta celular robusta con una sola dosis. Estos hallazgos muestran la diversidad en la respuesta inmune inducida por dos vacunas desarrolladas a partir de vectores adenovirales, Ad5-nCoV utiliza el adenovirus tipo 5 (Ad5), mientras que AZD1222 emplea el adenovirus de chimpancé ChAdOx1. Además, ambas vacunas presentan esquemas de vacunación diferente.

En resumen, este proyecto doctoral contribuye significativamente al entendimiento de la respuesta inmune frente al SARS-CoV-2, ya que logró el descubrimiento, producción y caracterización de un anticuerpo con alto potencial terapéutico. Esto se debió a su amplia capacidad neutralizante tanto contra la cepa ancestral como contra múltiples variantes de preocupación, incluyendo las últimas subvariantes de Ómicron, previas al surgimiento de mutaciones en los sitios K444 y V445. Además, presenta un estudio de transcritos a nivel unicelular en individuos convalecientes con diversos cuadros clínicos como en sujetos inmunizados con distintos esquemas de vacunación. Este trabajo integral revela la complejidad y adaptabilidad del sistema inmune frente al virus, sus variantes, diversas condiciones clínicas y vacunas empleadas contra COVID-19. Finalmente, estos hallazgos ayudarán en el desarrollo de futuras estrategias terapéuticas y de vacunación.

2. 19N01, A BROADLY NEUTRALIZING ANTIBODY AGAINST OMICRON BA.1, BA.2, BA.4/5, AND OTHER SARS-COV-2 VARIANTS OF CONCERN

Melissa García-Vega,[1] Edgar A. Melgoza-González,[1] Sofía Hernández-Valenzuela,[1] Diana Hinojosa-Trujillo,[1] Mónica Reséndiz-Sandoval,[1] Mara Anais Llamas-Covarrubias,[2] Martín Loza-Lopez,[3] Olivia Valenzuela,[4] Alan Soto-Gaxiola,[5] Miguel A. Hernández-Oñate,[1] Verónica Mata-Haro[1], Irene Cassaniti,[6] Josè Camilla Sammartino,[6] Alessandro Ferrari,[6] Luca Simonelli,[7] Mattia Pedotti,[7] Rui Sun,[8] Fanglei Zuo,[8] Fausto Baldanti,[8,9]Luca Varani,[9] Harold Marcotte,[8] Qiang Pan-Hammarström,[8] Jesús Hernández[1]

[1]Centro de Investigación en Alimentación y Desarrollo, A.C. Hermosillo, Sonora, Mexico.
[2]Research Institute for Microbial Diseases, Osaka University, 3-1 Yamadaoka, Suita, Japan.
[3]Laboratory of Functional Analysis in silico, The University of Tokyo, Shirokanedai, Tokyo, Japan.
[4]Departamento de Ciencias Químico Biológicas, División de Ciencias de la Salud, Universidad de Sonora, Mexico.
[5]Hospital General del Estado de Sonora "Dr. Ernesto Ramos Bours", Secretaria de Salud del Estado de Sonora, Mexico.
[6]Microbiology and Virology Department, Fondazione IRCCS Policlinico San Matteo, Pavia, Italy
[7]Institute for Research in Biomedicine, Università della Svizzera Italiana (USI), Bellinzona, Switzerland.
[8]Department of Biosciences and Nutrition, Karolinska Institutet, Huddinge, Sweden
[9]Department of Clinical, Surgical, Diagnostics and Pediatric Sciences, University of Pavia, Pavia, Italy.

Publicado en la revista
iScience

Fecha de publicación:
1 de abril del 2023

DOI: 10.1016/j.isci.2023.106562

iScience

CellPress
OPEN ACCESS

Article

19n01, a broadly neutralizing antibody against omicron BA.1, BA.2, BA.4/5, and other SARS-CoV-2 variants of concern

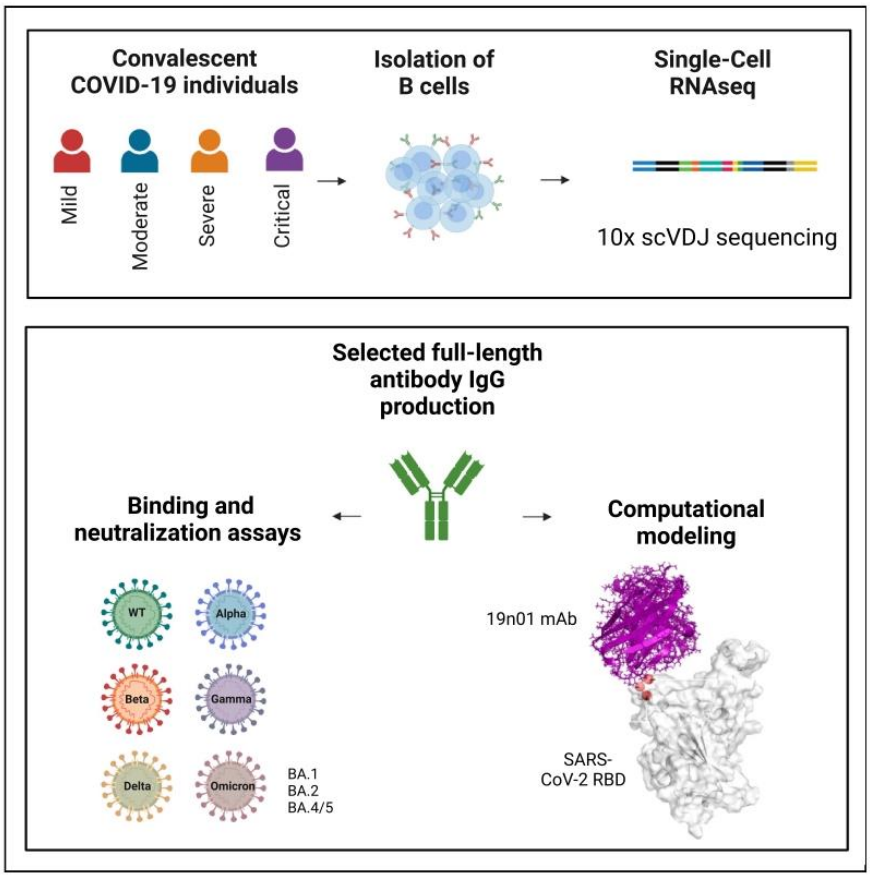

Melissa García-Vega, Edgar A. Melgoza-González, Sofía Hernández-Valenzuela, ..., Harold Marcotte, Qiang Pan-Hammarström, Jesús Hernández

jhdez@ciad.mx

Highlights

Single-cell RNAseq was done in B cells from donors infected with the ancestral strain

Selected mAbs were produced and characterized against SARS-COV-2 VOCs

19n01 mAb neutralizes SARS-CoV-2 VOCs, including Omicron BA.1, BA.2, and BA.4/5

19n01 mAb cross-competes with ACE2 binding to the RBD

García-Vega et al., iScience 26, 106562
April 21, 2023
https://doi.org/10.1016/j.isci.2023.106562

iScience

CellPress
OPEN ACCESS

Article

19n01, a broadly neutralizing antibody against omicron BA.1, BA.2, BA.4/5, and other SARS-CoV-2 variants of concern

Melissa García-Vega,[1] Edgar A. Melgoza-González,[1] Sofía Hernández-Valenzuela,[1] Diana Hinojosa-Trujillo,[1] Mónica Reséndiz-Sandoval,[1] Mara Anais Llamas-Covarrubias,[2] Martín Loza-López,[3] Olivia Valenzuela,[4] Alan Soto-Gaxiola,[5] Miguel A. Hernández-Oñate,[6] Verónica Mata-Haro,[7] Irene Cassaniti,[8] Josè Camilla Sammartino,[8] Alessandro Ferrari,[8] Luca Simonelli,[9] Mattia Pedotti,[9] Rui Sun,[10] Fanglei Zuo,[10] Fausto Baldanti,[8,11] Luca Varani,[9] Harold Marcotte,[10] Qiang Pan-Hammarström,[10] and Jesús Hernández[1,12,*]

SUMMARY

This study reports the isolation and characterization of a human monoclonal antibody (mAb) called 19n01. This mAb was isolated by using single-cell RNAseq of B cells from donors infected with the ancestral strain. This mAb possesses a potent and broad capacity to bind and neutralize all previously circulating variants of concern (VOCs), including Omicron sublineages BA.1, BA.2, and BA.4/5. The pseudovirus neutralization assay revealed robust neutralization capacity against the G614 strain, BA.1, BA.2, and BA.4/5, with inhibitory concentration (IC50) values ranging from 0.0035 to 0.0164 μg/mL. The microneutralization assay using the G614 strain and VOCs demonstrated IC50 values of 0.013–0.267 μg/mL. Biophysical and structural analysis showed that 19n01 cross-competes with ACE2 binding to the receptor-binding domain (RBD) and the kinetic parameters confirmed the high affinity against the Omicron sublineages (K_D of 61 and 30 nM for BA.2 and BA.4/5, respectively). These results suggest that the 19n01 is a remarkably potent and broadly reactive mAb.

INTRODUCTION

The spike protein is the main surface antigen of SARS-CoV-2 and utilizes its receptor-binding domain (RBD) to engage the host receptors ACE2 and TMPRSS2 for viral entry.[1,2] Based on this knowledge, the spike protein has been a central target for vaccine and drug design. Nonetheless, SARS-CoV-2 is constantly evolving due to high replication rates provoking new variants characterized by different mutations, particularly in the RBD domain.[3] These variants are characterized by increased transmissibility, reduced vaccine efficacy, and increased risk of reinfection.[4,5] The latest variant described Omicron, carries over 30 mutations in the spike and possesses a high infectivity rate that provokes rapid global dissemination. This variant comprises several major sublineages, such as BA.1, BA.2, BA.3, BA.4, and BA.5.[6,7] Many cases caused by BA.2, BA.4, and BA.5 and descendant sublineages have been detected in some countries, and the European Center for Diseases Prevention and Control (ECDC) classified these sublineages in the list of variants of concern (VOCs).[8]

Most vaccines elicit antibody responses with decreased neutralizing activity against Omicron and other variants, and two or three boosters are needed to increase the neutralizing response.[9,10] Monoclonal antibodies (mAbs) represent an important therapeutic option that provides clinical benefit in mild to moderate COVID-19, reducing the risk of hospitalization and severe disease.[11,12] There are multiple mAbs in preclinical and clinical phases; nevertheless, most FDA-approved mAbs show reduced effectiveness against certain variants and have lost approval.

RBD-targeting mAbs have been divided into four major classes based on their epitopes. Class 1 and class 2 recognize epitopes overlapping the ACE2-binding site. Class 3 is potent neutralizing antibodies that do not directly bind to the ACE2 contact surface. Class 4 antibodies target an epitope outside the receptor-binding motif and are generally less powerful.[13] This characterization and classification have been

[1]Laboratorio de Inmunología, Centro de Investigación en Alimentación y Desarrollo, A.C. Hermosillo, Sonora, Mexico

[2]Research Institute for Microbial Diseases, Osaka University, 3-1 Yamadaoka, Suita, Japan

[3]Laboratory of Functional Analysis in silico, The University of Tokyo, Shirokanedai, Tokyo, Japan

[4]Departamento de Ciencias Químico Biológicas, División de Ciencias de la Salud, Universidad de Sonora, Hermosillo, Sonora, Mexico

[5]Hospital General del Estado de Sonora "Dr. Ernesto Ramos Bours", Secretaria de Salud del Estado de Sonora, Hermosillo, Sonora, Mexico

[6]Laboratorio de Fisiología y Biología Molecular de Plantas, Centro de Investigación en Alimentación y Desarrollo, A.C. Hermosillo, Sonora, Mexico

[7]Laboratorio de Microbiología e Inmunología, Centro de Investigación en Alimentación y Desarrollo, A.C. Hermosillo, Sonora, Mexico

[8]Microbiology and Virology Department, Fondazione IRCCS Policlinico San Matteo, Pavia, Italy

[9]Institute for Research in Biomedicine, Università della Svizzera italiana (USI), Bellinzona, Switzerland

[10]Division of Immunology, Department of Medical Biochemistry and Biophysics, Karolinska Institutet, Stockholm, Sweden

Continued

necessary for identifying the best candidates, possible combinations, and mapping mutations that escape RBD-targeting mAbs.[14] In this study, we report the isolation and characterization of mAbs against SARS-CoV-2 obtained from convalescent patients infected with the ancestral strain of SARS-CoV-2. By using single-cell RNA-Seq (scRNA-Seq) of enriched or sorted S1/RBD-specific B cells, we isolated five mAbs (19n01, 20n01, 20n18, 01n03, and 01n21) able to recognize SARS-CoV-2 and its VOCs; remarkably, the 19n01 mAb neutralizes all variants, including the Omicron sublineages BA.1, BA.2, and BA.4/5. Structural and surface plasmon resonance (SPR) analysis showed that 19n01 mAb competes with ACE2 binding to the RBD, suggesting that the 19n01 epitope partially overlaps the receptor binding site.

RESULTS

Identification and production of antibodies against SARS-CoV-2 from convalescent patients

To identify SARS-CoV-2 neutralizing antibodies, we collected blood samples from nine COVID-19 convalescent patients with a positive qRT−PCR test. Samples were collected 3 and 8 weeks after symptom onset from patients who experienced different clinical manifestations (Figures S1A and S1B). All patients were from Northwest Mexico (Hermosillo, Sonora, Mexico) and had COVID-19 from October to November 2020, before the emergence of VOCs.

We performed two scRNA-seq experiments. We obtained an enriched population of S1/RBD-specific B cells from the nine convalescent patients in the first experiment using biotinylated RBD and S1 protein and a magnetic bead separation system (Figure S1). In the second experiment, we used fluorescent activated cell sorter (FACS) to sort antigen-specific memory B cells ($CD19^+IgD^-CD27^+RBD^+S1^+$, $CD19^+IgD^-CD27^+RBD^+S1^-$, and $CD19^+IgD^-CD27^+RBD^-S1^+$ B cells). We sorted 4,660 cells from five convalescent patients and merged them into a single pool. Once these cells were obtained, we performed scRNA-seq using 10x genomics technology. The cells were placed into 10x chromium for gel bead-in-emulsion (gel bead emulsion (GEM) preparation, library construction, and V(D)J library sequencing to obtain paired heavy (H) and light (L) chain sequences for antibody production and characterization.

We obtained 25,621 VDJ sequences from enriched S1/RBD-specific B cells; 16,483 were IgM, 4,253 were IgG, 4,664 were IgA, and 221 were IgD. From the sorted cells, we obtained 528 VDJ sequences; 299 were IgG, 115 IgM, 112 IgA, and 2 IgD. We defined five selection criteria to increase the efficiency in identifying mAbs against SARS-CoV-2: (1) sequences with IgG1 isotype; (2) heavy and light chains with paired sequences; (3) sequences with clonotypes with a frequency ≥2; (4) predominance of immunoglobulin heavy variable region (IGHV) genes of SARS-CoV-2 neutralizing antibodies (nAbs) previously reported; (5) heavy and light chain sequences with >70% identity with antibodies reported against SARS-CoV-2 in The Coronavirus Antibody Database (CoV-AbDab)[15] (Figure S1C). Based on these criteria, we obtained 44 antibody sequences that can potentially recognize SARS-CoV-2 (Table S1). We produced a single-chain variable fragment (scFv) from the selected sequences to test its recognition against the Wuhan-Hu-1 and RBD VOCs by ELISA. Fourteen scFvs were positive for Wuhan-Hu-1 (Wild-Type, WT), but only 5 recognized at least one VOC and were selected to produce them in full-length IgG format to continue their characterization. The 19n01, 20n01, and 20n18 mAbs were derived from enriched S1/RBD-specific B cells, while the 01n03 and 01n21 mAbs were derived from FACS-sorted S1/RBD-specific memory B cells.

Binding and neutralization of SARS-CoV-2 VOCs

The full-length IgG1 format of 19n01, 20n01, 20n18, 01n21, and 01n03 mAbs was produced by transient transfection of Expi293 cells and purified by protein G affinity chromatography. First, we performed ELISAs to evaluate the binding capacity against several SARS-CoV-2 variants (Figure 1A). The 19n01 mAb showed recognition against all variants, including the Omicron sublineages BA.1, BA.2, and BA.4/5. The half-maximal effective concentrations (EC50) ranged from 0.028 to 0.121 μg/mL, with an EC50 of 28.82 ng/mL for BA.4/5. The 01n21 mAb binds to all variants tested except Omicron. The 01n03 mAb recognized all variants, excluding Beta and Omicron. 20n01 showed recognition against Wuhan-hu-1 and Alpha. Additionally, 20n18 only recognized these two variants, but the binding was weak. The 19n01 mAb showed strong RBD binding affinity against all variants; its CDRH3 is composed of a relatively short sequence (12 amino acids), and this mAb had a paired germline IGHV2-5/IGLV1-47. IGHV2-5 has already been reported as a gene for broadly neutralizing antibodies against SARS-CoV-2 variants in convalescent patients.[16] The 20n01 mAb was derived from the IGHV1-69/IGLV2-23 germline genes, whereas the next three mAbs were derived from the same IGHV gene: 01n21 (IGHV3-53/IGKV3-20), 01n03 (IGHV3-53/IGKV1-33) and 20n18 (IGHV3-53/IGKV3-15) (Table S1).

[11]Department of Clinical, Surgical, Diagnostics and Pediatric Sciences, University of Pavia, Pavia, Italy

[12]Lead contact

*Correspondence: jhdez@ciad.mx

https://doi.org/10.1016/j.isci.2023.106562

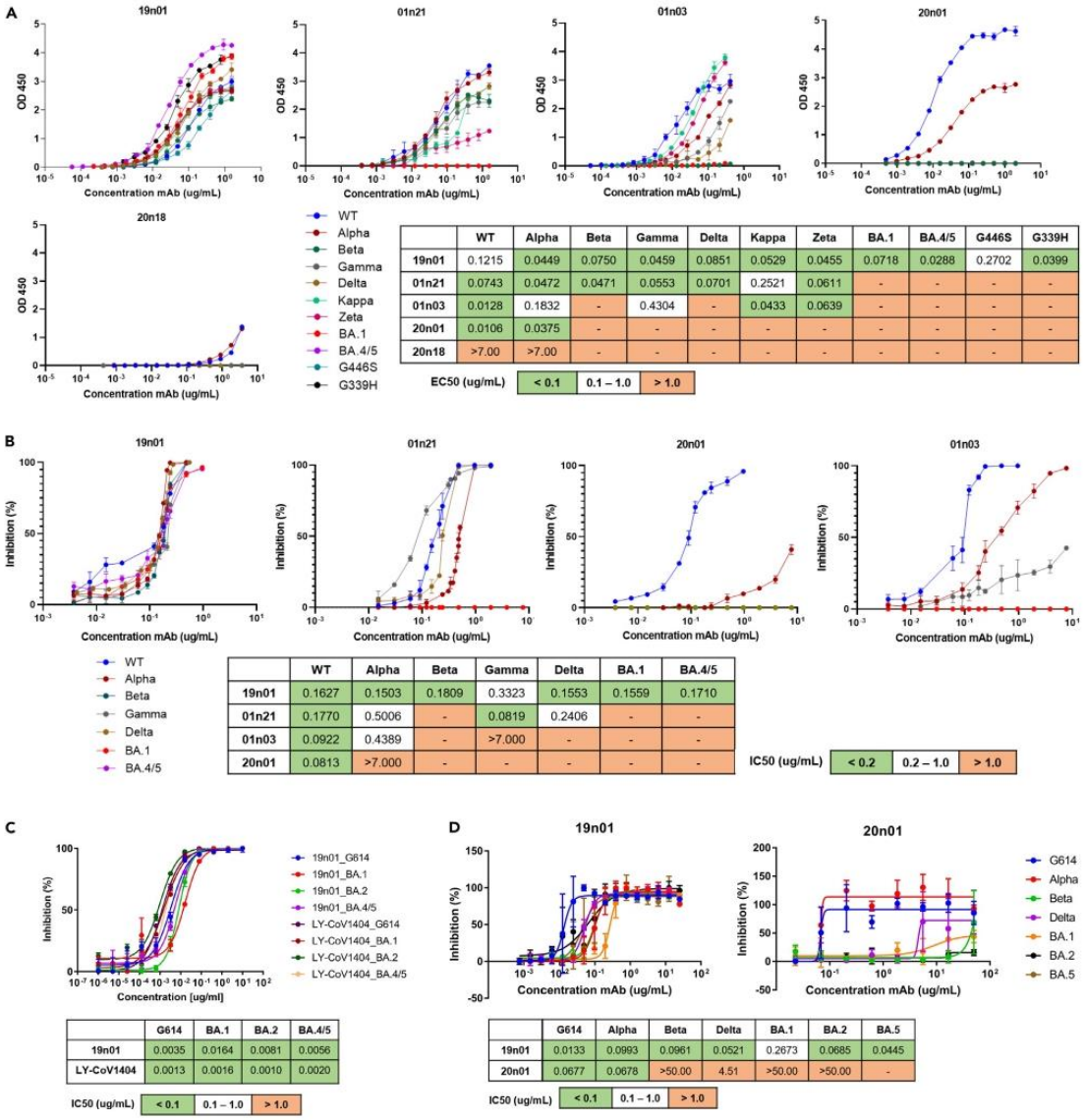

	WT	Alpha	Beta	Gamma	Delta	Kappa	Zeta	BA.1	BA.4/5	G446S	G339H
19n01	0.1215	0.0449	0.0750	0.0459	0.0851	0.0529	0.0455	0.0718	0.0288	0.2702	0.0399
01n21	0.0743	0.0472	0.0471	0.0553	0.0701	0.2521	0.0611	-	-	-	-
01n03	0.0128	0.1832	-	0.4304	-	0.0433	0.0639	-	-	-	-
20n01	0.0106	0.0375	-	-	-	-	-	-	-	-	-
20n18	>7.00	>7.00	-	-	-	-	-	-	-	-	-

EC50 (ug/mL) | < 0.1 | 0.1 – 1.0 | > 1.0

	WT	Alpha	Beta	Gamma	Delta	BA.1	BA.4/5
19n01	0.1627	0.1503	0.1809	0.3323	0.1553	0.1559	0.1710
01n21	0.1770	0.5006	-	0.0819	0.2406	-	-
01n03	0.0922	0.4389	-	>7.000	-	-	-
20n01	0.0813	>7.000	-	-	-	-	-

IC50 (ug/mL) | < 0.2 | 0.2 – 1.0 | > 1.0

	G614	BA.1	BA.2	BA.4/5
19n01	0.0035	0.0164	0.0081	0.0056
LY-CoV1404	0.0013	0.0016	0.0010	0.0020

IC50 (ug/mL) | < 0.1 | 0.1 – 1.0 | > 1.0

	G614	Alpha	Beta	Delta	BA.1	BA.2	BA.5
19n01	0.0133	0.0993	0.0961	0.0521	0.2673	0.0685	0.0445
20n01	0.0677	0.0678	>50.00	4.51	>50.00	>50.00	-

IC50 (ug/mL) | < 0.1 | 0.1 – 1.0 | > 1.0

Figure 1. RBD binding characterization of mAbs and SARS-CoV-2 neutralization

(A) ELISA binding of 19n01, 01n21, 01n03, 20n01, and 20n18 mAbs against RBDs from different SARS-CoV-2 variants (Alpha, Beta, Gamma, Delta, Kappa, Zeta, Omicron BA.1, BA.4/5, and Wuhan-Hu-1 [WT]). EC50 values were determined for antibodies that showed high binding affinity.

(B) RBD-hACE2 inhibition assay in Expi293 cells expressing hACE2. The inhibition capacity of 19n01, 01n21, 01n03, and 20n01 mAbs was evaluated by flow cytometry against SARS-CoV-2 RBD from Alpha, Beta, Gamma, Delta, Omicron BA.1, BA.4/5, and Wuhan-Hu-1. IC50 values were determined for each antibody that could inhibit RBD-hACE2 binding.

(C) Pseudovirus neutralization assay with 19n01 by using spike of G614 strain, and Omicron BA.1, BA.2, and BA.4/5. The mean values and SDs of two replicates are shown for each experiment.

(D) Authentic virus neutralization assay was determined for 19n01 and 20n01 mAbs by microneutralization from isolates of SARS-CoV-2 G614 strain and Alpha, Beta, Delta, Omicron BA.1, and BA2 variants. EC_{50} values were calculated for both antibodies in all tested variants.

Next, we performed RBD-hACE2 inhibition assays by flow cytometry using Expi293F cells that express hACE2. We observed that 19n01 mAb inhibits the RBD-hACE2 binding of Omicron and other VOCs with half-maximal inhibitory concentration (IC50) ranging from 0.150 to 0.332 μg/mL (Gamma showing the maximum and Alpha the minimum IC50). The 01n21 mAb could block RBD-hACE2 binding in the variants evaluated. The 01n03 and 20n01 mAbs inhibited only Alpha and Wuhan-Hu-1 RBD (Figure 1B). We confirmed RBD-hACE2 inhibition by blocking ELISAs (Figure S2). We observed that the 19n01 mAb could block RBD-hACE2 binding of all variants and that the 20n01 mAb blocked the binding of Alpha and Wuhan-Hu-1 RBD (Figure S3).

Then, we performed a neutralizing assay with live virus (microneutralization test) with the two most promising Abs, 19n01, and 20n01 (Figure 1D). mAb 20n01 was only effective against G614 and Alpha, with an IC50 of 0.06 μg/mL. The 19n01 mAb neutralizes the G614 strain and Alpha, Beta, Delta, and Omicron BA.1, BA.2, and BA5. The IC50 ranged from 0.013 to 0.267 μg/mL, with a lower IC50 against G614 and a higher IC50 against Omicron BA.1. The neutralizing activity against Omicron BA.2 and BA.5 was 0.068 and 0.0445 μg/mL, respectively. Similarly, 19n01 could neutralize BA.1, BA.2, and BA.5 pseudoviruses with IC50 values ranging from 0.0035 to 0.0164 μg/mL, with a lower IC50 against G614 and the highest against BA.1 (Figure 1C). In comparison, the well-characterized nAbs, LY-CoV1404, showed IC50 values ranging from 0.0010 to 0.0020 μg/mL, representing a 2.69-to-10.25-fold difference. These results agree with the binding results, where 19n01 showed reduced recognition against BA.1.

SPR competition on RBD SD1 with different antibodies

SARS-CoV-2 has shown a remarkable ability to mutate and evade the immune response. Resistant escape mutants quickly develop when the virus is exposed to neutralizing antibodies both *in vitro*, in animals, and in humans.[17] A combination of multiple antibodies, either in a cocktail or multispecific format, can curtain the problem since the virus is far less likely to simultaneously generate escape mutants in more than one epitope. To assess the possibility to combine 19n01 with other antibodies, we compared its binding to a panel of potently neutralizing and well-characterized anti-spike antibodies. An SPR-based cross-competition assay revealed that 19n01 cannot bind the RBD in the presence of C121, an Ab directed against the ACE2 binding site. Intriguingly, cross-competition was also detected against C135 (Figure 2A), which does not itself cross-compete with C121 and whose epitope is outside the ACE2 binding site (Class 3) (Figure 2B). In contrast, 19n01 does not compete with an anti-subdomain 1 (SD1 domain) antibody that binds spike protein outside the RBD. The complementarity of 19n01, which neutralizes the virus by inhibiting receptor binding, and antibodies that act through different mechanisms, such as anti-SD1 Abs, would be beneficial.

Cross-competition and the ability of 19n01 to recognize all variants and different RBD-SD1 point mutations (Figure S2) suggest that its epitope may lie in a conserved RBD region partially overlapping both C121 and C135 (Figure 2C) as well as the ACE2 binding site. We employed computational docking and atomistic molecular dynamics (MD) simulations to model the 3D structure of 19n01 on the RBD (Figure 3). No constraints were imposed on the relative position of 19n01 and RBD during the docking protocols, but the results were filtered to select solutions in which 19n01 overlapped with C121, C135, and ACE2, in agreement with the experimental data. Such solutions were then subjected to MD simulation to better refine the local geometry and confirm the stability of the RBD-19n01 model (Figures 3A and 3C). The simulation positions of 19n01 are in close contact with Gly446 and Gly496; these are mutated to Ser in BA.1 but not in other omicron sublineages. In line with experimental evidence, the mutations are likely to affect antibody binding to BA.1 (K_D 441 nM observed by SPR) but not BA.2 (K_D 61 nM) or BA.4/5 (K_D 30 nM) (Figures 3A and 3B). To provide additional evidence about the 19n01 epitope, we evaluated mutants at positions G339H, K444E, V445P, and G446S (Figures 1A and S4). A mutation at positions K444 or V445 was sufficient to abolish 19n01 binding; in contrast, a mutation at position G446 reduced the 19n01 binding. These results confirm that residues at positions K444, V445, and G446 are part of the 19n01 epitope. The epitope is otherwise conserved in all variants, in further agreement with experimental data showing strong binding to the ancestral strain (K_D 15 nM), D614G (K_D 4.7 nM), and Delta (K_D 23 nM) (Figure S5) as well as all others characterized by ELISA.

DISCUSSION

Since the emergence of SARS-CoV-2, the virus has accumulated many mutations acquiring the capacity to evade the immune response induced by vaccination or natural infection, provoking reduced neutralization against new

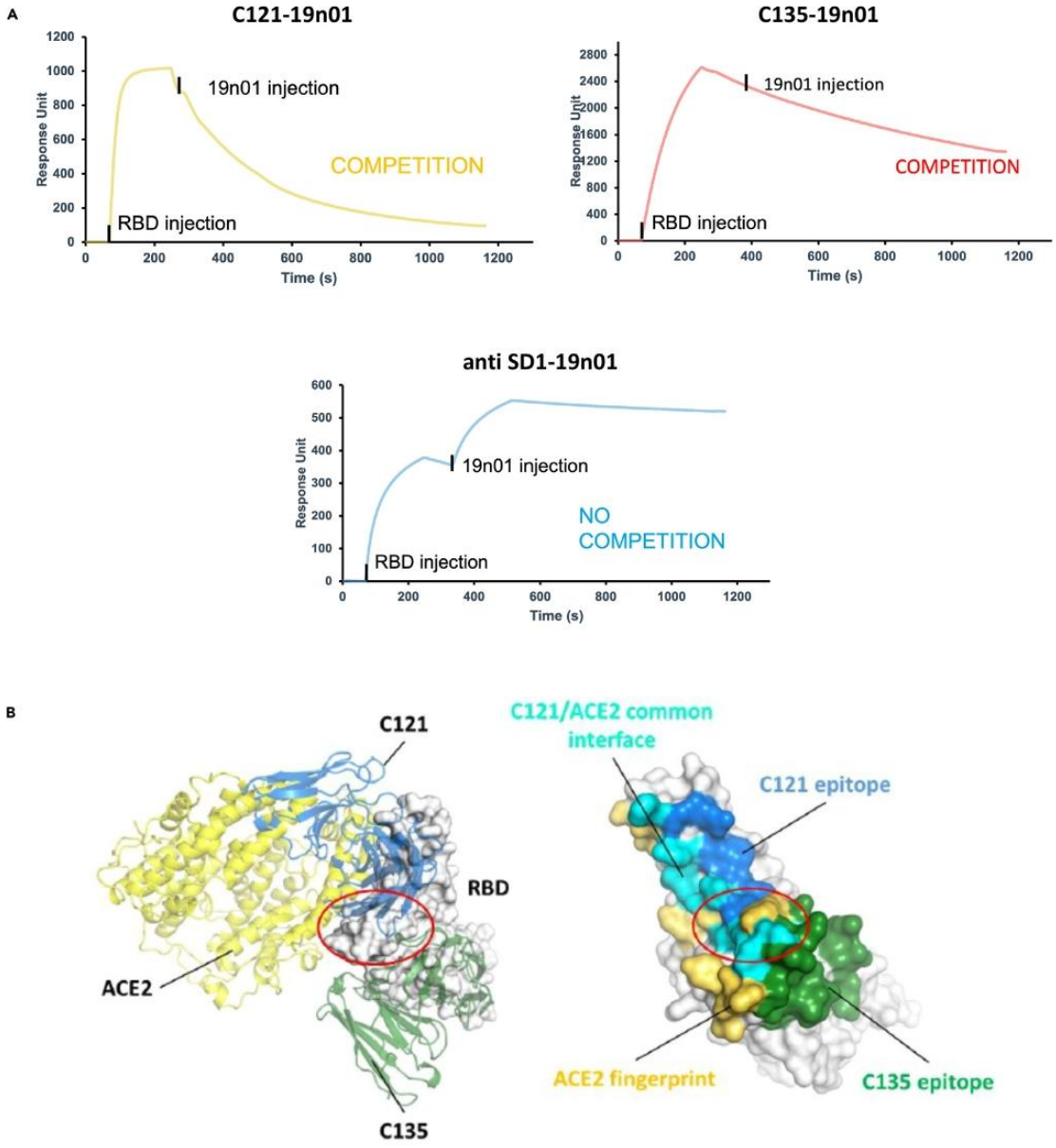

Figure 2. Binding competition between 19n01 and other characterized monoclonal antibodies against SARS-CoV-2

(A) SPR cross-competition assay. C121, C135, and an anti-SD1 antibody were immobilized on the chip surface; RBD-SD1 was then flowed forming a complex with the immobilized antibody (RBD injection), and finally, 19n01 was added (19n01 injection). 19n01 binding was detected only with the immobilized anti-SD1 antibody; instead, no signal was detected for both C121 and C135 suggesting at least partially overlapping epitopes with these antibodies.

(B) Structures of C121 (blue), C135 (green), and ACE2 (yellow) in complex with RBD (gray). The red circle indicates the putative region where 19n01 might bind to RBD.

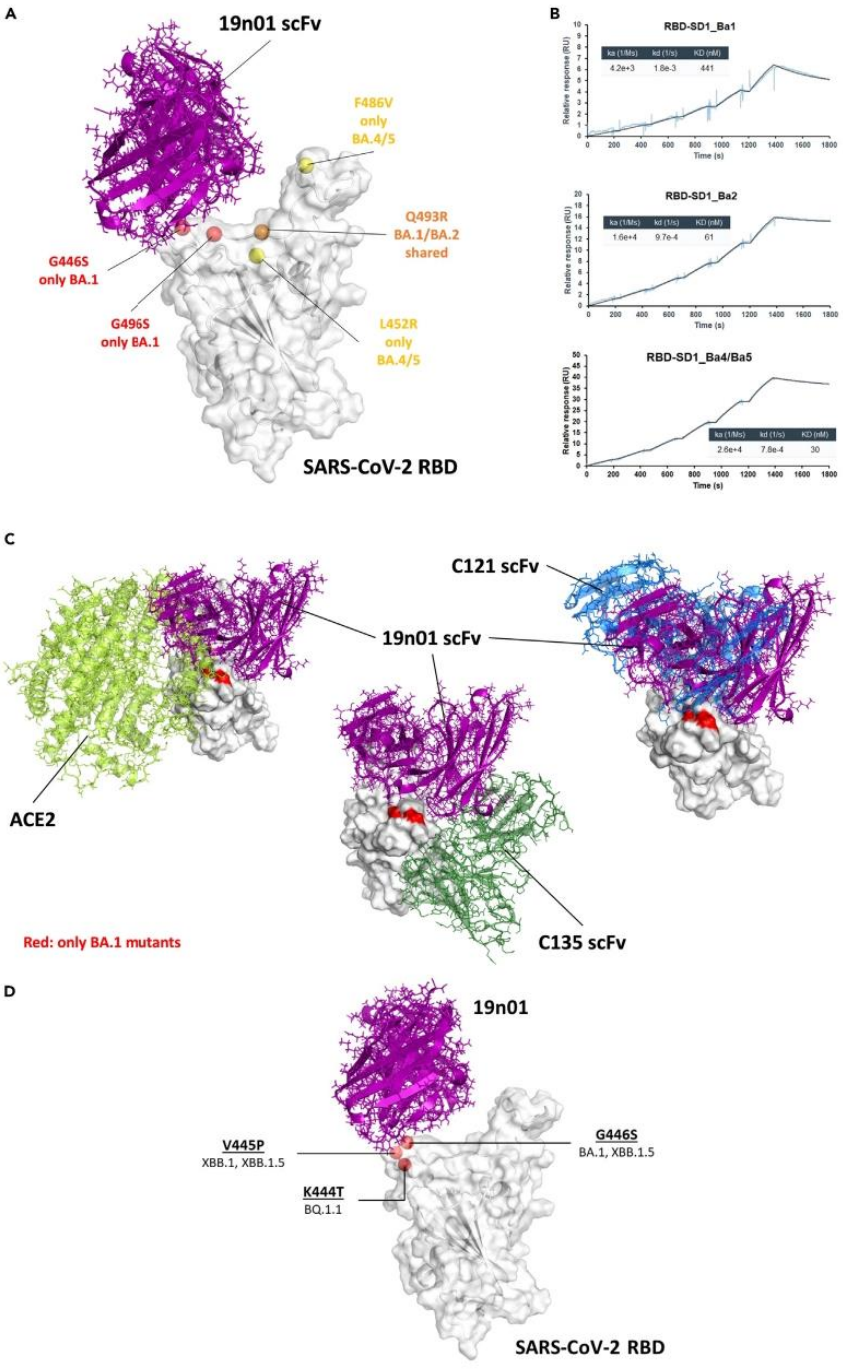
A
19n01 scFv
F486V
only
BA.4/5
Q493R
BA.1/BA.2
shared
G446S
only BA.1
G496S
only BA.1
L452R
only
BA.4/5
SARS-CoV-2 RBD
B
RBD-SD1_Ba1
ka (1/Ms) kd (1/s) KD (nM)
4.2e+3 1.8e-3 441
RBD-SD1_Ba2
ka (1/Ms) kd (1/s) KD (nM)
1.6e+4 9.7e-4 61
RBD-SD1_Ba4/Ba5
ka (1/Ms) kd (1/s) KD (nM)
2.6e+4 7.8e-4 30
Relative response (RU)
Time (s)
C
C121 scFv
19n01 scFv
ACE2
C135 scFv
Red: only BA.1 mutants
D
19n01
V445P
XBB.1, XBB.1.5
G446S
BA.1, XBB.1.5
K444T
BQ.1.1
SARS-CoV-2 RBD

Figure 3. The structural complex of 19n01 with SARS-CoV-2 RBD and binding affinities to Omicron BA.1, BA.2, and BA.4/5

(A) Structure of 19n01 (violet) in complex with SARS-CoV-2 RBD (white surface). Red spheres indicate mutations present only in BA.1 (G446S and G496S), yellow spheres are mutations present only in BA4/5 (F486V and L452R), and orange spheres are mutations shared between BA.1 and BA.2 (Q493R).

(B) Binding kinetics of 19n01 with SARS-CoV-2 RBD Omicron BA.1, BA.2, and BA.4/5 were determined by SPR.

(C) Superposition of the structures of ACE2 (lime), C135 (green), and C121 (blue) on the 19n01-RBD complex shows steric clashes between the molecules, in line with the cross-competition results.

(D) Structure of 19n01 (violet) in complex with SARS-CoV-2 RBD (white surface). The red spheres indicate mutations K444T (present in BQ.1.1), V445P (present in XBB.1 and XBB1.5), and G446S (present in BA.1 and XBB.1.5).

variants, such as Omicron.[18,19] Several reports coincide that booster-dose vaccines or hybrid immunity is needed to generate a robust humoral response to neutralize Omicron and their sublineages.[20–25] However, some patients cannot develop a potent humoral response and can be susceptible to the new variants and subvariants.[26–28] In this scenario, the use of therapies with mAbs has represented an opportunity for these patients. Nevertheless, emerging variants have also evaded neutralization by some mAbs, provoking some to lose the approval for their use in humans. Continued exploration for new, potent, and broad antibodies is needed to develop suitable treatments for the emerging variants of SARS-CoV-2. The present study aimed to isolate potent mAbs with broad neutralization capacity against several variants of SARS-CoV-2. We studied B cells from convalescent patients infected with the ancestral SARS-CoV-2 and using single-cell RNA-seq, five mAbs that bind the Wuhan-hu-1 RBD and at least one VOC were isolated. However, 19n01 was the only one able to bind and neutralize all VOCs tested, including Omicron BA.1, BA.2, and BA.4/5. On the other hand, mAbs 01n21 and 01n03 also bind several VOCs, except Omicron.

19n01 was isolated from pooled B cells of patients with moderate COVID-19 who rapidly controlled their infection. Previous reports confirm that patients with moderate symptoms generate robust antibody responses to the spike protein, which is highly correlated with neutralizing the SARS-CoV-2 virus.[29,30] Samples were collected before the emergence of Omicron, even before Alpha, and we could isolate a potent and broadly neutralizing antibody. As previously reported, neutralizing antibodies against Delta and BA.1 were obtained from early memory B cell repertoires of convalescent donors infected with the ancestral strain.[31] These results suggest that natural infection can stimulate the production of several B cells producing antibodies with broad neutralizing capacity, but not all clones are properly expanded, and therefore, infected or vaccinated persons showed a reduced response of antibodies in sera against Omicron subvariants. These clones originally activated could acquire a memory phenotype that has low or null antibody production, but it can be expanded after vaccine booster or re-infections and produce higher levels of Omicron-neutralizing antibodies.[31] These results suggest that natural infection induces memory clones of B cells producing antibodies able to neutralize future variants. 19n01 possesses an IGHV2-5/IGLV1-47 paired germline, which is common in convalescent people and is prevalent in potent and broadly neutralizing antibodies.[16] The other mAb expressed IGHV1-69 and IGHV3-53, also described as potent neutralizing antibodies, but it seems not to be very effective against Omicron.[32,33] Most mAbs reported to have broad activity against SARS-CoV-2 present short CDR3 sequences,[34] similar to 19n01, which seems to be a characteristic of broadly neutralizing antibodies.

There are many reports describing mAbs against SARS-CoV-2.[9,32,35,36] However, mAbs capable of neutralizing Omicron variants and subvariants are reduced[37]; reports describing mAbs able to neutralize BA.4/5 subvariants are particularly limited. 19n01 is potent and broad, as demonstrated by ELISA and SPR binding assays, inhibition of the RBD-ACE2 interaction and, most importantly, neutralization of pseudoviral particles and live viruses. 19n01 is active against all VOCs tested, including Omicron BA.1, BA.2, and BA.4/5. 19n01 was isolated from human donors not yet exposed to VOCs, and yet it can neutralize all of them, suggesting that the immune system induced antibodies against a region that is important to the virus and showed a low mutation rate. Computational modeling revealed that 19n01 did not interact with the RBD mutations in the Omicron BA.2, BA.3, and BA.4/5 subvariants, in addition to other VOCs, explaining its broad binding and potency. BA.1 is a partial exception to this, with mutations that decrease but do not abolish binding. The analysis of several mutants to evaluate the epitope of 19n01 revealed that positions K444 and V445 abolish 19n01 binding; confirming that 19n01 is inactive against Omicron subvariant XBB.1 and XBB.1.5 (mutation V445P), as well as BQ.1.1 (mutation K444T) (Figure 3E). The mutation G446S only decreases the binding. These results provide important information regarding the residues that are part of the 19n01 epitope and confirm the computational model.

19n01 binds the region of the RBD, recognizing the ACE2 protein used as a receptor for cell entry, like other class 1 antibodies, which tend to be particularly potent. In contrast to other class 1 antibodies, however, 19n01 is remarkably broadly reactive. Competition experiments using potent mAb previously characterized[38,39] showed that 19n01 competes with antibodies that bind RBD in the hACE2 binding site (C121 mAb) and with a mAb (C135) that binds outside this region but not with anti-SD1 antibodies, suggesting a featured venue for combination therapy. In conclusion, we isolated a mAb with the capacity to neutralize all VOCs tested, including BA.1, BA.2, and BA.4/5, making 19n01 a remarkably potent and broadly reactive mAb.

Limitations of the study

While the *in vitro* results demonstrate 19n01 mAb is potent and broadly neutralizing, *in vivo* experiments are required to prove the efficacy in an animal model. Although *in vitro* experiments suggest that 19n01 mAb binds a conserved epitope, the antibody-RBD binding structure needs to be solved.

STAR★METHODS

Detailed methods are provided in the online version of this paper and include the following:

- KEY RESOURCES TABLE
- RESOURCE AVAILABILITY
  - Lead contact
  - Materials availability
  - Data and code availability
- EXPERIMENTAL MODEL AND SUBJECT DETAILS
  - Study design
- METHOD DETAILS
  - Isolation of B cells
  - S1/RBD-specific B-cell enrichment
  - S1/RBD-specific B-Cell sorting
  - Production and purification of recombinant proteins
  - Single-cell RNA-Seq
  - Data processing
  - ELISA
  - Surface plasmon resonance
  - Binding inhibition of hACE2
  - Binding to different RBD mutants
  - Flow cytometry-based receptor-binding inhibition assay
  - SARS-CoV-2 neutralization assay
  - Pseudovirus neutralization assay based on the HIV platform
  - Computational modeling
- QUANTIFICATION AND STATISTICAL ANALYSIS

SUPPLEMENTAL INFORMATION

Supplemental information can be found online at https://doi.org/10.1016/j.isci.2023.106562.

ACKNOWLEDGMENTS

This project was supported by the Consejo Nacional de Ciencia y Tecnología (CONACyT), grant number 312677, the Swedish Research Council, the Knut and Alice Wallenberg Foundation, the European Union's Horizon 2020 research and innovation program under grant agreement no. 101003650 (ATAC), EU-OPENSCREEN ERIC and the European Union's Horizon Europe research and innovation programme ISIDORe under grant agreement No 10146133.

The authors are grateful to Verónica Vázquez García, Nilza Córdova, and Julia Real for their valuable technical assistance, Roberto Carente and Alejandra García from Analitek for the technical support during the single-cell experiments, and the CNRPyC-SENASICA, especially Fabiola Hernández, Mayrén Cristina Zamora Nava, and all the sequencing and bioinformatic staff for helping us to sequence our libraries.

AUTHOR CONTRIBUTIONS

Conceptualization, J.H.; Methodology, M.G.V., M.A.L.C., J.H., I.C., J.C.S., A.P., M.P., and L.S.; Formal analysis, M.G.V., M.A.L.C., M.L.L., M.A.H.O., M.R.S., R.S., F.Z., H.M., F.B., and L.V.; Investigation, M.G.V., E.A.M.G., S.H.V., D.H.T., M.R., A.A.F., M.S.H., M.R.S., I.C., J.C.S., A.F., M.P., L.S., and R.S.; Resources, A.S.G., O.V., V.M., F.B., L.V., and Q.P.H.; Writing—Original draft preparation, M.G.V. and J.H.; Writing—Review and Editing; L.V. and H.M.; Funding acquisition, J.H. and Q.P.H. All authors have read and agreed to the published version of the manuscript.

DECLARATION OF INTERESTS

M.G.V., M.R.S., E.A.M.G., V.M.H., and J.H. are coinventors of patent applications describing the neutralizing mAbs. The other authors declare no competing interests.

INCLUSION AND DIVERSITY

We support inclusive, diverse, and equitable conduct of research.

Received: September 18, 2022
Revised: November 21, 2022
Accepted: March 28, 2023
Published: April 1, 2023

REFERENCES

1. Yan, R., Zhang, Y., Li, Y., Xia, L., Guo, Y., and Zhou, Q. (2020). Structural basis for the recognition of SARS-CoV-2 by full-length human ACE2. Science *367*, 1444–1448. https://doi.org/10.1126/science.abb2762.

2. Lan, J., Ge, J., Yu, J., Shan, S., Zhou, H., Fan, S., Zhang, Q., Shi, X., Wang, Q., Zhang, L., and Wang, X. (2020). Structure of the SARS-CoV-2 spike receptor-binding domain bound to the ACE2 receptor. Nature *581*, 215–220. https://doi.org/10.1038/s41586-020-2180-5.

3. Harvey, W.T., Carabelli, A.M., Jackson, B., Gupta, R.K., Thomson, E.C., Harrison, E.M., Ludden, C., Reeve, R., Rambaut, A., COVID-19 Genomics UK COG-UK Consortium, et al.. (2021). SARS-CoV-2 variants, spike mutations and immune escape. Nat. Rev. Microbiol. *19*, 409–424. https://doi.org/10.1038/s41579-021-00573-0.

4. Tao, K., Tzou, P.L., Nouhin, J., Gupta, R.K., de Oliveira, T., Kosakovsky Pond, S.L., Fera, D., and Shafer, R.W. (2021). The biological and clinical significance of emerging SARS-CoV-2 variants. Nat. Rev. Genet. *22*, 757–773. https://doi.org/10.1038/s41576-021-00408-x.

5. Marcotte, H., Hammarström, L., and Pan-Hammarström, Q. (2022). Limited cross-variant neutralization after primary Omicron infection: consideration for a variant-containing booster. Signal Transduct. Target. Ther. *7*, 294. https://doi.org/10.1038/s41392-022-01146-0.

6. Gruell, H., Vanshylla, K., Tober-Lau, P., Hillus, D., Schommers, P., Lehmann, C., Kurth, F., Sander, L.E., and Klein, F. (2022). mRNA booster immunization elicits potent neutralizing serum activity against the SARS-CoV-2 Omicron variant. Nat. Med. *28*, 477–480. https://doi.org/10.1038/s41591-021-01676-0.

7. Viana, R., Moyo, S., Amoako, D.G., Tegally, H., Scheepers, C., Althaus, C.L., Anyaneji, U.J., Bester, P.A., Boni, M.F., Chand, M., et al. (2022). Rapid epidemic expansion of the SARS-CoV-2 Omicron variant in southern Africa. Nature *603*, 679–686. https://doi.org/10.1038/s41586-022-04411-y.

8. Bruel, T., Hadjadj, J., Maes, P., Planas, D., Seve, A., Staropoli, I., Guivel-Benhassine, F., Porrot, F., Bolland, W.H., Nguyen, Y., et al. (2022). Serum neutralization of SARS-CoV-2 Omicron sublineages BA.1 and BA.2 in patients receiving monoclonal antibodies. Nat. Med. *28*, 1297–1302. https://doi.org/10.1038/s41591-022-01792-5.

9. Wang, L., Zhou, T., Zhang, Y., Yang, E.S., Schramm, C.A., Shi, W., Pegu, A., Oloniniyi, O.K., Henry, A.R., Darko, S., et al. (2021). Ultrapotent antibodies against diverse and highly transmissible SARS-CoV-2 variants. Science *373*, eabh1766. https://doi.org/10.1126/science.abh1766.

10. Muik, A., Wallisch, A.K., Sänger, B., Swanson, K.A., Mühl, J., Chen, W., Cai, H., Maurus, D., Sarkar, R., Türeci, Ö., et al. (2021). Neutralization of SARS-CoV-2 lineage B.1.1.7 pseudovirus by BNT162b2 vaccine-elicited human sera. Science *371*, 1152–1153. https://doi.org/10.1126/science.abg6105.

11. Taylor, P.C., Adams, A.C., Hufford, M.M., de la Torre, I., Winthrop, K., and Gottlieb, R.L. (2021). Neutralizing monoclonal antibodies for treatment of COVID-19. Nat. Rev. Immunol. *21*, 382–393. https://doi.org/10.1038/s41577-021-00542-x.

12. Hammarström, L., Marcotte, H., Piralla, A., Baldanti, F., and Pan-Hammarström, Q. (2021). Antibody therapy for COVID-19. Curr. Opin. Allergy Clin. Immunol. *21*, 553–558. https://doi.org/10.1097/aci.0000000000000787.

13. Barnes, C.O., Jette, C.A., Abernathy, M.E., Dam, K.M.A., Esswein, S.R., Gristick, H.B., Malyutin, A.G., Sharaf, N.G., Huey-Tubman, K.E., Lee, Y.E., et al. (2020). SARS-CoV-2 neutralizing antibody structures inform therapeutic strategies. Nature *588*, 682–687. https://doi.org/10.1038/s41586-020-2852-1.

14. Greaney, A.J., Starr, T.N., Barnes, C.O., Weisblum, Y., Schmidt, F., Caskey, M., Gaebler, C., Cho, A., Agudelo, M., Finkin, S., et al. (2021). Mapping mutations to the SARS-CoV-2 RBD that escape binding by different classes of antibodies. Nat. Commun. *12*, 4196. https://doi.org/10.1038/s41467-021-24435-8.

15. Raybould, M.I.J., Kovaltsuk, A., Marks, C., and Deane, C.M. (2021). CoV-AbDab: the coronavirus antibody database. Bioinformatics *37*, 734–735. https://doi.org/10.1093/bioinformatics/btaa739.

16. Andreano, E., Paciello, I., Piccini, G., Manganaro, N., Pileri, P., Hyseni, I., Leonardi, M., Pantano, E., Abbiento, V., Benincasa, L., et al. (2021). Hybrid immunity improves B cells and antibodies against SARS-CoV-2 variants. Nature *600*, 530–535. https://doi.org/10.1038/s41586-021-04117-7.

17. Gupta, A., Gonzalez-Rojas, Y., Juarez, E., Crespo Casal, M., Moya, J., Falci, D.R., Sarkis, E., Solis, J., Zheng, H., Scott, N., et al. (2021). Early treatment for Covid-19 with SARS-CoV-2 neutralizing antibody sotrovimab. N. Engl. J. Med. *385*, 1941–1950. https://doi.org/10.1056/NEJMoa2107934.

18. Cao, Y., Wang, J., Jian, F., Xiao, T., Song, W., Yisimayi, A., Huang, W., Li, Q., Wang, P., An, R., et al. (2022). Omicron escapes the majority of existing SARS-CoV-2 neutralizing antibodies. Nature *602*, 657–663. https://doi.org/10.1038/s41586-021-04385-3.

19. Zhou, H., Dcosta, B.M., Landau, N.R., and Tada, T. (2022). Resistance of SARS-CoV-2 omicron BA.1 and BA.2 variants to vaccine-elicited sera and therapeutic monoclonal antibodies. Viruses *14*, 1334. https://doi.org/10.3390/v14061334.

20. Altarawneh, H.N., Chemaitelly, H., Ayoub, H.H., Tang, P., Hasan, M.R., Yassine, H.M., Al-Khatib, H.A., Smatti, M.K., Coyle, P., Al-Kanaani, Z., et al. (2022). Effects of previous infection and vaccination on symptomatic omicron infections. N. Engl. J. Med. *387*, 21–34. https://doi.org/10.1056/NEJMoa2203965.

21. Madhi, S.A., Kwatra, G., Myers, J.E., Jassat, W., Dhar, N., Mukendi, C.K., Nana, A.J., Blumberg, L., Welch, R., Ngorima-Mabhena, N., and Mutevedzi, P.C. (2022). Population immunity and Covid-19 severity with omicron variant in South Africa. N. Engl. J. Med. *386*, 1314–1326. https://doi.org/10.1056/NEJMoa2119658.

22. Medigeshi, G.R., Batra, G., Murugesan, D.R., Thiruvengadam, R., Chattopadhyay, S., Das, B., Gosain, M., Ayushi, Singh, J., Singh, J., Anbalagan, A., et al. (2022). Sub-optimal neutralisation of omicron (B.1.1.529) variant by antibodies induced by vaccine alone or SARS-CoV-2 Infection plus vaccine (hybrid immunity) post 6-months. EBioMedicine *78*, 103938. https://doi.org/10.1016/j.ebiom.2022.103938.

23. Andrews, N., Stowe, J., Kirsebom, F., Toffa, S., Sachdeva, R., Gower, C., Ramsay, M., and Lopez Bernal, J. (2022). Effectiveness of COVID-19 booster vaccines against COVID-19-related symptoms, hospitalization and death in England. Nat. Med. *28*, 831–837. https://doi.org/10.1038/s41591-022-01699-1.

24. Edara, V.V., Manning, K.E., Ellis, M., Lai, L., Moore, K.M., Foster, S.L., Floyd, K., Davis-Gardner, M.E., Mantus, G., Nyhoff, L.E., et al. (2022). mRNA-1273 and BNT162b2 mRNA vaccines have reduced neutralizing activity against the SARS-CoV-2 omicron variant. Cell Rep. Med. *3*, 100529. https://doi.org/10.1016/j.xcrm.2022.100529.

25. Zuo, F., Abolhassani, H., Du, L., Piralla, A., Bertoglio, F., de Campos-Mata, L., Wan, H., Schubert, M., Cassaniti, I., Wang, Y., et al. (2022). Heterologous immunization with inactivated vaccine followed by mRNA-booster elicits strong immunity against SARS-CoV-2 Omicron variant. Nat. Commun. *13*, 2670. https://doi.org/10.1038/s41467-022-30340-5.

26. Ullrich, F., Hanoun, C., Turki, A.T., Liebregts, T., Breuckmann, K., Alashkar, F., Reinhardt, H.C., von Tresckow, B., and von Tresckow, J. (2022). Early report on the severity of COVID-19 in hematologic patients infected with the SARS-CoV2 omicron variant. Eur. J. Haematol. *109*, 364–372. https://doi.org/10.1111/ejh.13818.

27. Bierle, D.M., Ganesh, R., Tulledge-Scheitel, S., Hanson, S.N., Arndt, L.L., Wilker, C.G., and Razonable, R.R. (2022). Monoclonal antibody treatment of breakthrough COVID-19 in fully vaccinated individuals with high-risk comorbidities. J. Infect. Dis. *225*, 598–602. https://doi.org/10.1093/infdis/jiab570.

28. Åberg, M., Smed-Sörensen, A., Thålin, C., and Pan-Hammarström, Q. (2022). Mucosal IgA against SARS-CoV-2 omicron infection. N. Engl. J. Med. *387*, e55. https://doi.org/10.1056/NEJMc2213153.

29. Tian, X., Liu, L., Jiang, W., Zhang, H., Liu, W., and Li, J. (2021). Potent and persistent antibody response in COVID-19 recovered patients. Front. Immunol. *12*, 659041. https://doi.org/10.3389/fimmu.2021.659041.

30. Wajnberg, A., Amanat, F., Firpo, A., Altman, D.R., Bailey, M.J., Mansour, M., McMahon, M., Meade, P., Mendu, D.R., Muellers, K., et al. (2020). Robust neutralizing antibodies to SARS-CoV-2 infection persist for months. Science *370*, 1227–1230. https://doi.org/10.1126/science.abd7728.

31. Windsor, I.W., Tong, P., Lavidor, O., Moghaddam, A.S., McKay, L.G.A., Gautam, A., Chen, Y., MacDonald, E.A., Yoo, D.K., Griffiths, A., et al. (2022). Antibodies induced by an ancestral SARS-CoV-2 strain that cross-neutralize variants from Alpha to Omicron BA.1. Sci. Immunol. *7*, eabo3425. https://doi.org/10.1126/sciimmunol.abo3425.

32. Xiaojie, S., Yu, L., Lei, Y., Guang, Y., and Min, Q. (2020). Neutralizing antibodies targeting SARS-CoV-2 spike protein. Stem Cell Res. *50*, 102125. https://doi.org/10.1016/j.scr.2020.102125.

33. Andreano, E., Paciello, I., Marchese, S., Donnici, L., Pierleoni, G., Piccini, G., Manganaro, N., Pantano, E., Abbiento, V., Pileri, P., et al. (2022). Anatomy of Omicron BA.1 and BA.2 neutralizing antibodies in COVID-19 mRNA vaccinees. Nat. Commun. *13*, 3375. https://doi.org/10.1038/s41467-022-31115-8.

34. Yuan, M., Wang, Y., Lv, H., Wilson, I.A., and Wu, N.C. (2022). Molecular analysis of a public cross-neutralizing antibody response to SARS-CoV-2. Preprint at bioRxiv. https://doi.org/10.1101/2022.05.17.492220.

35. Zhou, H., Tada, T., Dcosta, B.M., and Landau, N.R. (2022). Neutralization of SARS-CoV-2 omicron BA.2 by therapeutic monoclonal antibodies. Preprint at bioRxiv. https://doi.org/10.1101/2022.02.15.480166.

36. Kumar, S., Chandele, A., and Sharma, A. (2021). Current status of therapeutic monoclonal antibodies against SARS-CoV-2. PLoS Pathog. *17*, e1009885. https://doi.org/10.1371/journal.ppat.1009885.

37. Cao, Y., Yisimayi, A., Jian, F., Song, W., Xiao, T., Wang, L., Du, S., Wang, J., Li, Q., Chen, X., et al. (2022). BA.2.12.1, BA.4 and BA.5 escape antibodies elicited by Omicron infection. Nature *608*, 593–602. https://doi.org/10.1038/s41586-022-04980-y.

38. De Gasparo, R., Pedotti, M., Simonelli, L., Nickl, P., Muecksch, F., Cassaniti, I., Percivalle, E., Lorenzi, J.C.C., Mazzola, F., Magrì, D., et al. (2021). Bispecific IgG neutralizes SARS-CoV-2 variants and prevents escape in mice. Nature *593*, 424–428. https://doi.org/10.1038/s41586-021-03461-y.

39. Robbiani, D.F., Gaebler, C., Muecksch, F., Lorenzi, J.C.C., Wang, Z., Cho, A., Agudelo, M., Barnes, C.O., Gazumyan, A., Finkin, S., et al. (2020). Convergent antibody responses to SARS-CoV-2 in convalescent individuals. Nature *584*, 437–442. https://doi.org/10.1038/s41586-020-2456-9.

40. Schmidt, F., Weisblum, Y., Muecksch, F., Hoffmann, H.H., Michailidis, E., Lorenzi, J.C.C., Mendoza, P., Rutkowska, M., Bednarski, E., Gaebler, C., et al. (2020). Measuring SARS-CoV-2 neutralizing antibody activity using pseudotyped and chimeric viruses. J. Exp. Med. *217*, e20201181. https://doi.org/10.1084/jem.20201181.

41. Melgoza-González, E.A., Hinojosa-Trujillo, D., Reséndiz-Sandoval, M., Mata-Haro, V., Hernández-Valenzuela, S., García-Vega, M., Bravo-Parra, M., Arvizu-Flores, A.A., Valenzuela, O., Velázquez, E., et al. (2022). Analysis of IgG, IgA and IgM antibodies against SARS-CoV-2 spike protein S1 in convalescent and vaccinated patients with the Pfizer-BioNTech and CanSinoBio vaccines. Transbound. Emerg. Dis. *69*, e734–e745. https://doi.org/10.1111/tbed.14344.

42. Percivalle, E., Cambiè, G., Cassaniti, I., Nepita, E.V., Maserati, R., Ferrari, A., Di Martino, R., Isernia, P., Mojoli, F., Bruno, R., et al. (2020). Prevalence of SARS-CoV-2 specific neutralising antibodies in blood donors from the lodi red zone in lombardy, Italy, as at 06 April 2020. Euro Surveill. *25*, 2001031. https://doi.org/10.2807/1560-7917.

43. Sircar, A., Kim, E.T., and Gray, J.J. (2009). RosettaAntibody: antibody variable region homology modeling server. Nucleic Acids Res. *37*, W474–W479. https://doi.org/10.1093/nar/gkp387.

44. Pedotti, M., Simonelli, L., Livoti, E., and Varani, L. (2011). Computational docking of antibody-antigen complexes, opportunities and pitfalls illustrated by influenza hemagglutinin. Int. J. Mol. Sci. *12*, 226–251. https://doi.org/10.3390/ijms12010226.

45. Simonelli, L., Beltramello, M., Yudina, Z., Macagno, A., Calzolai, L., and Varani, L. (2010). Rapid structural characterization of human antibody-antigen complexes through experimentally validated computational docking. J. Mol. Biol. *396*, 1491–1507. https://doi.org/10.1016/j.jmb.2009.12.053.

46. Van Der Spoel, D., Lindahl, E., Hess, B., Groenhof, G., Mark, A.E., and Berendsen, H.J.C. (2005). GROMACS: fast, flexible, and free. J. Comput. Chem. *26*, 1701–1718. https://doi.org/10.1002/jcc.20291.

STAR★METHODS

KEY RESOURCES TABLE

REAGENT or RESOURCE	SOURCE	IDENTIFIER
Antibodies		
Brilliant Violet 421 anti-human CD19 Antibody	BioLegend	Cat# 302233; Clone HIB19; RRID: AB_10897802
PE/Cyanine7 anti-human CD27 Antibody	BioLegend	Cat#302837; Clone O323; RRID: AB_2561918
FITC anti-human IgD Antibody	BioLegend	Cat#348205; Clone IA6-2; RRID: AB_10613638
THE DYKDDDDK Tag Antibody [HRP], mAb, Mouse	GenScript	Cat# A01428; Clone 5A8E5; RRID: AB_1720817
Goat Anti-Human IgG Antibody, HRP conjugate	Sigma-Aldrich	Cat# 32160702
Goat Anti-Mouse IgG, Human ads-AP	Southern Biotech	Cat# 1030-04; RRID:AB_2794293
LY-CoV1404	ProteoGenix	Cat# PX-TA1750-100UG
Bacterial and virus strains		
SARS-CoV-2 G614	Isolated from patients	N/A
SARS-CoV-2 Alpha	Isolated from patients	N/A
SARS-CoV-2 Beta	Isolated from patients	N/A
SARS-CoV-2 Delta	Isolated from patients	N/A
SARS-CoV-2 Omicron BA.1	Isolated from patients	N/A
SARS-CoV-2 Omicron BA.2	Isolated from patients	N/A
SARS-CoV-2 Omicron BA.5	Isolated from patients	N/A
Biological samples		
Human COVID-19 convalescent patient serum	This paper	N/A
Human COVID-19 convalescent patient PBMCs	This paper	N/A
Chemicals, peptides, and recombinant proteins		
APC Streptavidin	Biolegend	Cat# 405207
PE Streptavidin	Biolegend	Cat# 405203
SARS-CoV-2 Spike protein RBD, Omicron Variant, His Tag (BA.1/Omicron)	GenScript	Cat# Z03728
SARS-CoV-2 Spike RBD, His Tag (BA.4&BA.5/Omicron)	Acro Biosystems	Cat# SPD-C522r
Critical commercial assays		
MojoSort™ Human B Cell ($CD43^-$) Isolation Kit	Biolegend	Cat# 480062
LYNX Rapid RPE Antibody Conjugation Kit	BioRad	Cat# LNK022RPE
Chromium Next GEM Single Cell 5′ Kit v2	10x Genomics	Cat# 1000263
Library Construction Kit	10x Genomics	Cat# 1000190
Chromium Single Cell Human BCR Amplification Kit	10x Genomics	Cat# 1000253
Chromium Next GEM Chip K Single Cell Kit	10x Genomics	Cat# 1000287
Dual Index Kit TT Set A	10x Genomics	Cat# 1000215
Dual Index Kit TN Set A	10x Genomics	Cat# 1000250
EZ-Link™ Sulfo-NHS-LC-Biotinylation Kit	ThermoFisher	Cat# 21435
Experimental models: Cell lines		
Expi293F cells	ThermoFisher	Cat# A14527
VERO E6 cells	ATCC	Cat# CRL-1586

(*Continued on next page*)

Continued

REAGENT or RESOURCE	SOURCE	IDENTIFIER
293FT Cells	ThermoFisher	Cat# R70007
$293T_{ACE2}$ Cells	Robbiani et al. 2020[39]	https://doi.org/10.1038/s41586-020-2456-9
Recombinant DNA		
pSARS-CoV-2 $S_{\Delta 19}$	Schmidt et al. 2020[40]	https://doi.org/10.1084/jem.20201181
pCCNanoLuc2AEGFP	Schmidt et al. 2020[40]	https://doi.org/10.1084/jem.20201181
$pHIV_{NL}GagPol$	Schmidt et al. 2020[40]	https://doi.org/10.1084/jem.20201181
Software and algorithms		
Cell Ranger Software (version 5.0.0)	10x Genomics	https://support.10xgenomics.com/single-cell-gene-expression/software/downloads/latest?
Loupe V(D)J Browser (version 4.0.0)	10x Genomics	https://www.10xgenomics.com/products/loupe-browser/downloads
GraphPad Prism (version 8.4.2)		https://www.graphpad.com/
RosettaDock (version 3.1)		https://www.rosettacommons.org/

RESOURCE AVAILABILITY

Lead contact

Further information and requests for resources and reagents should be directed to and will be fulfilled by the Lead Contact, Jesús Hernández (jhdez@ciad.mx).

Materials availability

19n01 antibody plasmid is available with a material transfer agreement (MTA).

Data and code availability

- Data reported in this paper will be shared by the lead contact upon reasonable request.
- This paper does not report original code.
- Any additional information required to reanalyze the data reported in this paper is available from the lead contact upon request.

EXPERIMENTAL MODEL AND SUBJECT DETAILS

Study design

This study performed scRNA-seq of B cells from convalescent patients with COVID-19 with different clinical manifestations (mild, moderate, severe, and critical) to obtain and produce broadly neutralizing antibodies against emerging SARS-CoV-2 variants. For this purpose, we collected blood samples from nine convalescent patients with a PCR-confirmed SARS-CoV-2 infection 3 to 8 weeks from the onset of symptoms: mild (n=1), moderate (n=3), severe (n=3), and critical illness (n=2) (Figure S1). These patients had COVID-19 from October to November 2020, before the emergence and circulation of the first variants. The selection criteria were an IgG titer $\geq$ 1: 640 against the S1 protein of SARS-CoV-2. The classification of disease severity was performed according to the National Institute of Health (NIH). A second blood sample was collected from these patients, and scRNA-Seq was performed from sorted S1/RBD-specific B cells and enriched S1/RBD-specific B cells. The study was evaluated and approved by the Ethics Committee of the CIAD, AC (C.E.I./012-2/2020), and all patients signed informed consent forms.

METHOD DETAILS

Isolation of B cells

Peripheral mononuclear blood cells (PBMCs) were isolated from EDTA whole blood by density gradient centrifugation using Ficoll-Paque Plus (GE Healthcare Life Sciences, Massachusetts, USA). B cells were obtained from PBMCs using the MojoSort™ Human B-Cell (CD43-) isolation Kit (BioLegend, San Diego, CA, USA) according to the manufacturer's protocols. Isolated B cells were resuspended in RPMI-1640 medium

supplemented with 40% fetal bovine serum (FBS), and 2X freezing medium (30% DMSO in RPMI-1640 supplemented with 40% FBS) was added at a ratio of 1:1. Immediately, the cell suspension was dispensed in cryovials and kept at -80°C for 4 hours, and the cryovials were stored in liquid nitrogen until use.

S1/RBD-specific B-cell enrichment

Cryopreserved B cells from the nine convalescent patients were thawed in RPMI-1640 supplemented with 10% FBS tempered at 37°C; cells were centrifuged 300 x g for 8 min and resuspended for counting, and the viability of each sample was > 90%. Cells were centrifuged and resuspended in MojoSort Buffer (BioLegend, San Diego, CA, USA). S1 and RBD proteins were biotinylated using EZ-Link™ Sulfo-NHS-LC-Biotinylation Kit (Thermo Fisher Scientific); then the biotinylated proteins were incubated with the cells for 15 min at 4°C and then washed with 2 ml of Cell Staining Buffer (BioLegend, San Diego, CA, USA) and centrifuged at 300 x g for 8 min. Once labeled with SARS-CoV-2 proteins, the samples from each group of three patients were pooled. Streptavidin nanobeads (BioLegend, San Diego, CA, USA) were added to the cell pools, mixed well, and incubated for 15 min on ice. Then, 2.5 mL of MojoSort Buffer was added, and the sample tubes of each pool were placed in MojoSort Magnet (BioLegend, San Diego, CA, USA) for 5 min. The tubes were decanted without removing them from the magnet, 2.5 mL of MojoSort Buffer was added, and the last step was repeated. Finally, a positive selection of magnetically separated cells was collected and resuspended in Cell Staining Buffer; these were the enriched S1/RBD-specific B cells.

S1/RBD-specific B-Cell sorting

For protein-specific B-cell sorting, cryopreserved B cells from five convalescent patients (rAbCOVID29, rAbCOVID27, rAbCOVID09, rAbCOVID07, and rAbCOVID19) were selected due to the availability of cells from these patients for this experiment (Figure S1). The cells were thawed, washed with Cell Staining Buffer (BioLegend, San Diego, CA, USA), and then incubated at 4°C for 20 min with a cocktail of antibodies and protein S1 and RBD (WT) tetramers. The cocktail consisted of CD19-BV421 (BioLegend clone HIB19), CD27-PeCy7 (BioLegend clone O323), IgD-FITC (BioLegend clone IA6-2), RBD-APC, and S1-PE tetramers. After incubation, the cells were washed twice, and then the stained cells from each patient were pooled. Finally, protein-specific B cells were gated as $CD19^+CD27^+IgD^-RBD^+S1^+$, $CD19^+CD27^+IgD^-RBD^+S1^-$ and $CD19^+CD27^+IgD^-S1^+RBD^-$ and sorted using a BD FACS Aria III (BD Biosciences, San Jose, CA, USA).

Production and purification of recombinant proteins

A synthetic gene of hACE2 (805 aa) was cloned into a pcDNA3.1(+) vector by GenScript (GenScript, New Jersey, U.S.A.), soluble hACE2 (603 aa), SARS-CoV-2 S1 (633 aa) and RBD (229 aa) were synthesized and cloned into a pcDNA3.1(-) vector (GenScript, New Jersey, U.S.A.). To produce the RBD of SARS-CoV-2 variants, direct-site mutagenesis was performed by GenScript, using the RBD from the original strain as an initial sequence and inserting the mutations corresponding to each variant (except for Omicron sublineages). The expression gene constructs were preceded by a signal peptide and a Hist-tag (6xHis) C-terminal domain.[41] The expression of the recombinant proteins was performed in the Expi293 Expression System following the manufacturer's instructions (Thermo Fisher Scientific, Waltham, MA, USA). Briefly, Expi293F cells were grown in Expi293 expression medium. The transfection complex was prepared by mixing 30 μg of each plasmid and 81 μg of Expifectamine 293 reagent (both diluted in OptiMEM-I) and incubated for 20 min at room temperature. The complex was added to a 125 mL polycarbonate Erlenmeyer flask (Corning, Corning, NY, USA) with 75 x 10^6 Expi293F cells in 25.5 mL of Expi293 expression medium and incubated at 37°C and 125 rpm with 8% CO_2. After 20 hours, Expifectamine 293 Transfection Enhancers 1 and 2 were added to the medium, and the cells were incubated for four days until harvesting.

After four days of transfection, the culture supernatant was harvested and clarified by centrifugation at 4000 x g for 10 min. Then, the clarified supernatant was filtered through a 0.22 μm filter, followed by purification on immobilized metal affinity chromatography (IMAC) using a HisTrap HP 1 mL column (Cytiva, Marlborough, MA, USA). The elution was carried out in the chromatograph ÄKTA GO (GE Healthcare Life Sciences, Massachusetts, USA) by a linear gradient from 0 to 100% elution buffer (Imidazole 500 mM, NaCl 500 mM, and 20 mM NaH_2PO_4). The proteins were quantified by a Bradford assay, concentrated, and desalted with an Amicon Ultra15 (10 kDa cutoff) (Millipore, Massachusetts, USA) followed by dilution in phosphate-buffered saline (PBS) pH 7.4.

For the selected scFv sequences, the genes were synthesized and cloned into the pcDNA3.1 (-) vector by GenScript. The sequences comprise a signal peptide and a Flag-tag (DYKDDDDK) sequence in the

N-terminal domain, followed by the variable regions of the heavy (VH) and light (VL) chains joined by a linker peptide (3xGGGGS) and a Hist-tag (6xHist) C-terminal domain. Similar to the proteins mentioned above, scFv was expressed in the Expi293F expression system. The supernatants were harvested on the fourth day of transfection, and ELISAs evaluated the reactivity against the RBD of SARS-CoV-2 variants.

The heavy and light chain genes of selected antibodies for full-length IgG production were synthesized and cloned into the pcDNA3.1 (-) vector and expressed in the Expi293F expression system as the mentioned genes. Purification was carried out by protein G affinity chromatography using HiTrap Protein G HP 1 mL columns (Cytiva, Massachusetts, USA) in ÄKTA GO (GE Healthcare).

The antibody heavy and light chain sequences have been deposited into the GenBank database (accession numbers: OQ447224 to OQ447311).

Other recombinant proteins as RBD Omicron BA.1 was purchased from GenScript (Piscataway NJ, USA) and BA. BA.4/5 was purchased from Acro Biosystems (Newark, DE, USA).

Single-cell RNA-Seq

Single-cell suspensions of enriched or sorted S1 and RBD protein-specific B cells for single-cell RNA-seq library preparation were generated using 10x Genomics technology (10X Genomics, Pleasanton, CA, USA). The cell suspension for each pool was prepared with the Chromium Next GEM Single Cell 5′ v2 and Chromium Next GEM Chip K Single-Cell Kit and loaded into Chromium Controller equipment. Once the single cells were obtained by the formation of gel bead emulsions (GEMs), libraries were prepared using a Chromium Single Cell Human BCR Amplification Kit, Library Construction Kit, Dual Index Kit TT and Dual Index Kit TN according to manufacturer's instructions. Then, the libraries were sequenced on a NextSeq 550 sequencer (Illumina, San Diego, CA, USA).

Data processing

The FASTQ files obtained from sequencing were processed for alignment, filtering, barcode counting, and UMI counting using Cell Ranger Software (version 5.0.0) (10x Genomics Pleasanton, CA, USA) with the pipeline cell ranger multi and the GRCh38 reference genome. The output files were selected and used in Loupe V(D)J Browser (version 4.0.0) (10x Genomics) for data visualization, clonotype analysis, and selection of antibody sequences.

ELISA

Recombinant S1 and RBD proteins were coated in Nunc Maxosorp 96-well plates (Thermo Fisher Scientific, Massachusetts, USA) with 50 mM carbonate buffer pH 9.6 at a concentration of 2 μg/mL and incubated overnight at 4°C. Then, plates were washed with PBS and blocked with PBS 0.05% Tween (PBST) and 2% BSA for 1 hour at room temperature, followed by another wash. To evaluate the 44 scFvs, 50 μL of supernatant from each was incubated for 30 min at room temperature. Subsequently, the wells were washed four times with PBST, and then the DYKDDDDK Tag Antibody [HRP] (GenScript, New Jersey, U.S.A.) (0.2 μg/ml) was added and incubated for 30 min; after that, the wells were washed 4 times as previously described. Next, 50 μL of tetramethylbenzidine (TMB) (Immunochemistry, Minnesota, USA) was added and incubated for 20 min, the reaction was stopped with 50 μL of H_2SO_4, and the optical density (OD) was measured at 450 nm on an automated spectrophotometer (Thermo Scientific Multiskan FC Microplate Photometer). The ELISA procedure was identical for full-length IgG antibodies, only modifying the detection antibody using anti-human IgG-HRP (Sigma–Aldrich Missouri, USA).

Surface plasmon resonance

The antibody binding properties were analyzed at 25 °C using a Biacore 8K instrument (GE Healthcare) with 10 mM HEPES pH 7.4, 150 mM NaCl, 3 mM EDTA, and 0.005% Tween-20 as running buffer. SARS-CoV-2 antigens (different RBDs or full S) were immobilized (15 nM) on the surface of CM5 chips (Cytiva) through standard amine coupling. Increasing concentrations of antibody (6.25, 12.5, 25, 50, 100, 200 nM) were injected using a single-cycle kinetics setting, and dissociation was followed for 10 min. Analyte responses were corrected for nonspecific binding and buffer responses. Curve fitting and data analysis were performed with Biacore Insight Evaluation Software v.2.0.15.12933.

Competition experiments were performed to obtain information on the antibody-binding region. The first antibody was immobilized (50 nM) on the surface of CM5 chips (Cytiva) through standard amine coupling; RBD-SD1 was flowed (100 nM) to form the RBD-SD1/Ab complex, and suddenly after, the second antibody was injected (50 nM). If a binding event is detected in the final step, the second antibody has a different epitope from the first antibody (immobilized). If no binding event is detected, the two antibodies share overlapping epitopes.

Binding inhibition of hACE2

ELISAs were used to investigate the antibody's ability to inhibit the binding of RBD and full S protein to hACE2. We used 96-well ELISA plates coated at 4 °C with 158 nM RBD or 37 nM full S protein, washed and blocked with PBS + 10% fetal calf serum (FCS). Antibodies were then added at different dilutions (starting from 340 nM and serially diluted 1 to 3) and incubated for 1 hour at 25 °C; after washing, hACE2–mouse Fc was added at a constant saturating concentration (160 nM) and left for 1 hour at 25 °C. After further washing, bound hACE2 was detected using standard protocols with goat anti-mouse IgG coupled to alkaline phosphatase (dilution 1:500, Southern Biotech). ELISA plates were measured with the reader software Gen5 version 1.11.5 (BioTek Instruments). Data were analyzed with GraphPad Prism version 8.4.2.

Binding to different RBD mutants

To obtain information about the 19n01 binding region on the RBD, ELISAs were used to assess the effect of different RBD mutations on 19n01 binding. Ninety-six-well ELISA plates were coated at 4 °C with 158 nM RBD, washed, and blocked with PBS + 10% FCS. The 19n01 antibody was then added at different dilutions (starting from 90 nM and serially diluted 1 to 3) and incubated for 1 hour at 25 °C; after washing, the bound antibody was detected using standard protocols with goat anti-human IgG coupled to alkaline phosphatase (dilution 1:500, Southern Biotech). ELISA plates were measured with the reader software Gen5 version 1.11.5 (BioTek Instruments). Data were analyzed with GraphPad Prism version 8.4.2.

Flow cytometry-based receptor-binding inhibition assay

The RBD-ACE2 cell surface inhibition assay used Expi293F cells expressing hACE2 (ExpiACE2 cells). The RBDs from each variant (Alpha, Beta, Gamma, Delta, WT, and Omicron BA.1 and BA.4/5) were conjugated using the LYNX Rapid RPE Conjugation kit® (Bio-Rad, Hercules, CA, USA). For the inhibition assay, mAbs were diluted in PBA (phosphate-buffered saline and 0.1% albumin), and 50 µL of each dilution was preincubated with 25 nM RBD-PE for 1 hour at room temperature with constant agitation. ExpiACE2 cells were washed with 2 mL of PBA and centrifuged 300 x g for 8 min. Cells were subsequently incubated with RBD-PE and mAb mixture for 15 min. Then, the cells were washed twice and resuspended in PBA for flow cytometry acquisition in a BD FACSCantoII (BD Biosciences, San Jose, CA, USA) and data analysis. The results were expressed as the percentage of inhibition = (1-(RBD-ACE2 binding cells in the presence of mAbs/RBD-ACE2 binding cells in the positive control)) * 100. The IC_{50} was calculated using GraphPad Prism 9.

SARS-CoV-2 neutralization assay

The SARS-CoV-2 G614 strain and VOCs (Alpha, Beta, Delta, and Omicron BA.1, BA2, and BA.5 were isolated from patients in Pavia, Italy, and identified through next-generation sequencing. The neutralizing activities of antibodies were tested by a SARS-CoV-2 microneutralization test, as previously described.[42] Briefly, 50 µl of antibody, starting from 25 µg/ml in a serial two fold dilution series, was mixed in a flat-bottom tissue-culture microtiter plate (COSTAR, Corning Incorporated) with an equal volume of 100 median tissue culture infectious dose of infectious virus (TCID50) of a SARS-CoV-2 strain, previously titrated. All dilutions were made in Eagle's minimum essential medium with the addition of 1% penicillin, streptomycin, and glutamine and 5 µg/ml trypsin. After 1 hour of incubation at 33°C in 5% CO2, VERO E6 cells (VERO C1008 [Vero 76, cloneE6, Vero E6]; ATCC® CRL-1586™) were added to each well. After 3 days of incubation, the cells were stained with Gram's crystal violet solution (Merck) plus 5% formaldehyde 40% m/v (Carlo Erba S.p.A.) for 30 min. Microtiter plates were then washed in running water. Wells were analyzed to evaluate the degree of cytopathic effect compared to the untreated control. Each experiment was performed in triplicate. The IC_{50} was determined using four-parameter nonlinear regression (GraphPad Prism 8.3.0).

Pseudovirus neutralization assay based on the HIV platform

The human-codon optimized gene coding for the S protein of G614, BA.1, BA.2 and BA.4/5 lacking the C-terminal 19 codons ($S_{\Delta 19}$) was synthesized by GenScript. To generate (HIV-1/NanoLuc2AEGFP)-SARS-CoV-2 particles, three plasmids were used, with a reporter vector (pCCNanoLuc2AEGFP), HIV-1 structural/regulatory proteins ($pHIV_{NL}GagPol$) and SARS-CoV-2 $S_{\Delta 19}$ carried by separate plasmids as previously described[40] 293FT cells were transfected with 7 μg of $pHIV_{NL}GagPol$, 7 μg of pCCNanoLuc2AEGFP, and 2.5 μg of a pSARS-CoV-2 $S_{\Delta 19}$ carrying the $S_{\Delta 19}$ gene from G614 or Omicron variants (at a molar plasmid ratio of 1:1:0.45) using 66 μl 1 mg/ml of polyethylenimine (PEI).

Fivefold serially diluted of 19n01 and positive control LY-CoV1404 (ProteoGenix) were incubated with pseudotyped SARS-CoV-2 virus (G614, BA.1, BA.2, and BA.4/BA.5) for 1 hour at 37 °C. The mixture was subsequently incubated with $293T_{ACE2}$[39] cells for analyses of G614 or Omicron pseudoviruses for 48 hours, after which the cells were washed with PBS and lysed with Luciferase Cell Culture Lysis reagent (Promega). NanoLuc luciferase activity in the lysates was measured using the Nano-Glo Luciferase Assay System (Promega) with a Tecan Infinite microplate reader. The relative luminescence units were normalized to those derived from cells infected with pseudotyped virus in the absence of monoclonal antibodies. The IC_{50} values for the monoclonal antibodies were determined using four-parameter nonlinear regression (the least squares regression method without weighting) (GraphPad Prism 7.04 software).

Computational modeling

The 19n01 variable fragment was modeled according to the canonical structure method with the program RosettaAntibody[43] as previously described.[44] Docking was performed using RosettaDock v3.1 as previously described.[45] In summary, 19n01 model was docked to WT RBD experimental structure (PDBid: 6m17). Among the thousands of computationally generated complexes, the decoy in better agreement with experimental data (competition with hACE2 and differential neutralization activity against SARS-CoV-2 variants) was selected and further refined by computational docking.

The selected model was subjected to a 350ns molecular dynamics (MD) simulation to adjust the local geometry and verify that the structure was energetically stable. MD was performed with GROMACS.[46] The system was initially set up and equilibrated through standard MD protocols: proteins were centered in a triclinic box, 0.2 nm from the edge, filled with extended simple point charge (SPCE) water model and 0.15 m Na+Cl- ions using the AMBER99SB-ILDN protein force field. Energy minimization was performed in order to let the ions achieve a stable conformation. Temperature and pressure equilibration steps, respectively at 310 K and 1 Bar, of 100 ps each were completed before performing the full MD simulations with the above-mentioned force field. MD trajectory files were analyzed after the removal of Periodic Boundary Conditions. The stability of each simulated complex was verified by root mean square deviation and visual analysis.

QUANTIFICATION AND STATISTICAL ANALYSIS

We used GraphPad Prism 8.4.2 for data visualization, to determine the IC_{50} using four-parameter nonlinear regression, and for statistical analysis. Where applicable, statistical parameters are reported in the figure legends.

3. SINGLE-CELL TRANSCRIPTOMIC ANALYSIS OF B CELLS REVEALS NEW INSIGHTS INTO ATYPICAL MEMORY B CELLS IN COVID-19

Melissa García-Vega,[1] Mara Anais Llamas-Covarrubias,[2] Martin Loza,[3] Mónica Reséndiz-Sandoval,[1] Diana Hinojosa-Trujillo,[1] Edgar Melgoza-González,[1] Olivia Valenzuela,[4] Verónica Mata-Haro,[1] Miguel Hernández-Oñate,[1] Alan Soto-Gaxiola,[5] Karina Chávez-Rueda,[6] Kenta Nakai,[3] Jesús Hernández[1]

[1]Centro de Investigación en Alimentación y Desarrollo, A.C. Hermosillo, Sonora, Mexico, 83304.
[2]Research Institute for Microbial Diseases, Osaka University, 3-1 Yamadaoka, Suita, Japan, 565-0871.
[3]The Institute of Medical Science, The University of Tokyo, 4-6-1 Shirokanedai, Minato-ku, Tokyo, Japan, 108-0071.
[4]Departamento de Ciencias Químico Biológicas, División de Ciencias Biológicas y de la Salud, Universidad de Sonora, Hermosillo, Sonora, Mexico, 83000.
[5]Hospital General del Estado de Sonora "Dr. Ernesto Ramos Bours", Secretaria de Salud del Estado de Sonora. Hermosillo, Sonora, Mexico, 83000.
[6]Unidad de Investigación Médica en Inmunología, UMAE, Hospital de Pediatría, Centro Médico Nacional Siglo XXI, Instituto Mexicano del Seguro Social, Ciudad de México, Mexico, 06720.

Publicado en:
Journal of Medical Virology

Fecha de publicación:
12 de agosto del 2024

DOI: 10.1002/jmv.29851

Received: 15 May 2024 | Accepted: 31 July 2024

DOI: 10.1002/jmv.29851

RESEARCH ARTICLE

JOURNAL OF MEDICAL VIROLOGY WILEY

Single-cell transcriptomic analysis of B cells reveals new insights into atypical memory B cells in COVID-19

Melissa García-Vega[1] | Mara Anais Llamas-Covarrubias[2] | Martin Loza[3] | Mónica Reséndiz-Sandoval[1] | Diana Hinojosa-Trujillo[1] | Edgar Melgoza-González[1] | Olivia Valenzuela[4] | Verónica Mata-Haro[5] | Miguel Hernández-Oñate[6] | Alan Soto-Gaxiola[7] | Karina Chávez-Rueda[8] | Kenta Nakai[3] | Jesús Hernández[1]

[1]Laboratorio de Inmunología, Centro de Investigación en Alimentación y Desarrollo, A.C, Hermosillo, Sonora, Mexico

[2]Research Institute for Microbial Diseases, Osaka University, Suita, Japan

[3]The Institute of Medical Science, The University of Tokyo, Minato-ku, Tokyo, Japan

[4]Departamento de Ciencias Químico Biológicas, División de Ciencias Biológicas y de la Salud, Universidad de Sonora, Hermosillo, Sonora, Mexico

[5]Laboratorio de Microbiología e Inmunología, Centro de Investigación en Alimentación y Desarrollo, A.C, Hermosillo, Sonora, Mexico

[6]CONAHCYT-Laboratorio de Fisiología y Biología Molecular de Plantas, Centro de Investigación en Alimentación y Desarrollo, A.C, Hermosillo, Sonora, Mexico

[7]Hospital General del Estado de Sonora "Dr. Ernesto Ramos Bours", Secretaria de Salud del Estado de Sonora, Hermosillo, Sonora, Mexico

[8]Unidad de Investigación Médica en Inmunología, UMAE, Hospital de Pediatría, Centro Médico Nacional Siglo XXI, Instituto Mexicano del Seguro Social, Ciudad de México, Mexico

Correspondence
Kenta Nakai, The Institute of Medical Science, The University of Tokyo, Minato-ku, Tokyo, Japan.
Email: knakai@ims.u-tokyo.ac.jp

Jesús Hernández, Laboratorio de Inmunología, Centro de Investigación en Alimentación y Desarrollo, A.C. Hermosillo, Sonora 83304, Mexico.
Email: jhdez@ciad.mx

Funding information
The Centro Estatal de la Transfusión Sanguínea (Sonora); SENASICA; The Advanced Genomics Unit-Langebio of CINVESTAV; The Consejo Nacional de Ciencia y Tecnología, Grant/Award Number: 312677

Abstract

Here, we performed single-cell RNA sequencing of S1 and receptor binding domain protein-specific B cells from convalescent COVID-19 patients with different clinical manifestations. This study aimed to evaluate the role and developmental pathway of atypical memory B cells (MBCs) in response to severe acute respiratory syndrome coronavirus 2 (SARS-CoV-2) infection. The results revealed a proinflammatory signature across B cell subsets associated with disease severity, as evidenced by the upregulation of genes such as *GADD45B*, *MAP3K8*, and *NFKBIA* in critical and severe individuals. Furthermore, the analysis of atypical MBCs suggested a developmental pathway similar to that of conventional MBCs through germinal centers, as indicated by the expression of several genes involved in germinal center processes, including *CXCR4*, *CXCR5*, *BCL2*, and *MYC*. Additionally, the upregulation of genes characteristic of the immune response in COVID-19, such as *ZFP36* and *DUSP1*, suggested that the differentiation and activation of atypical MBCs may be influenced by exposure to SARS-CoV-2 and that these genes may contribute to the immune response for COVID-19 recovery. Our study contributes to a better understanding

Melissa García-Vega and Mara Anais Llamas-Covarrubias are contributed equally to this study.

of atypical MBCs in COVID-19 and the role of other B cell subsets across different clinical manifestations.

KEYWORDS
atypical memory B cells, B cells, COVID-19, SARS-CoV-2, single-cell RNAseq

1 | INTRODUCTION

A broad spectrum of B cell subsets has been described, such as transitional B cells, naive B cells, memory B cells (MBCs), atypical MBCs, and antibody secreting cells (ASCs).[1–3] All these cells have different derived subsets and antibody-independent functions with regulatory roles or are involved in the control of viral infections.[4–6] In the context of COVID-19, B cells have been extensively studied,[7–10] however, little attention has been given to atypical MBCs.

During the COVID-19 pandemic, different studies reported alterations in B cell subsets and suggested signatures associated with disease severity.[11–15] Critical and severe COVID-19 patients displayed aberrantly high proportions of ASCs, double-negative B cells ($CD27^-$ IgD^-), atypical MBCs, and activated naive B cells. Furthermore, some of these subsets have been associated with an extrafollicular response in critically ill patients, along with the expression of B cell receptor (BCR) inhibitory genes (*FCGR2B*, *CD72*, and *PTPN6*), which could affect the correct activation and functioning of B cells.[11,12,16]

The activation and differentiation of B cells in response to infectious diseases can lead to the development of atypical MBCs, as reported in malaria, human immunodeficiency virus (HIV), and COVID-19.[14,15,17,18] These cells are part of a heterogeneous population with a $CD19^+CD21^-CD27^-$ phenotype, and according to protein levels, transcripts of *CR2* and *CD27* are significantly lower in atypical MBCs than in conventional MBCs.[17,19] Since atypical MBCs are heterogeneous in individuals and diseases, their functions and developmental pathways are still controversial. Therefore, it remains unclear whether this differentiation is indicative of a productive role in the immune response or a malfunction of the immune system in COVID-19.

Here, we performed single-cell RNA-sequencing (scRNA-seq) of B cells from convalescent COVID-19 donors who experienced critical, severe, moderate, or mild symptoms. Our results revealed a wide heterogeneity of B cells across the different conditions, and the differential gene expression (DGE) analysis highlighted features associated with disease severity. Additionally, we identified a potential developmental pathway and possible function of atypical MBCs in COVID-19.

2 | MATERIAL AND METHODS

2.1 | Study design

This study performed a scRNA-seq analysis of B cells from convalescent patients with different clinical manifestations of COVID-19. For this purpose, we collected peripheral blood samples from nine participants who experienced critical ($n = 2$), severe ($n = 3$), moderate ($n = 3$), or mild symptoms ($n = 1$) (Figure 1A). All participants tested positive for severe acute respiratory syndrome coronavirus 2 (SARS-CoV-2) PCR between October and November 2020 before the first report of new variants in Hermosillo, Sonora, Mexico. Detailed clinical and demographic characteristics of the subjects are presented in Supporting Information S1: Figure 1a. Blood samples were collected 3–8 weeks after symptom onset and scRNA-seq of enriched S1 and receptor binding domain (RBD) protein-specific B cells was performed. The study was evaluated and approved by the Ethics Committee of CIAD, A.C. (C.E.I./012-2/2020), and all patients signed informed consent forms.

2.1.1 | Isolation of S1 and RBD protein-specific B cells

B cells were obtained from PBMCs using a MojoSort™ Human B Cell (CD43-) isolation Kit (BioLegend) according to the manufacturer's protocols and stored in liquid nitrogen until use. Cryopreserved B cells were thawed and resuspended in Cell Staining Buffer (BioLegend) and blocked with Human TruStain FcX™ (BioLegend) for 10 min at 4°C. Three different TotalSeq™ antibodies (BioLegend) were used for cell hashing: TotalSeq™-C0251, TotalSeq™-C0252, and TotalSeq™-C0253. The nine samples were divided into three groups, with each group containing three different samples. Before pooling, each sample was labeled with a different cell hashing antibody. They were incubated for 20 min at 4°C, followed by two washes with 1 mL of Cell Staining Buffer and centrifugation at 300*g* for 8 min.

Each pool was incubated with biotinylated S1 and RBD proteins for 15 min at 4°C and washed. The production of the SARS-CoV-2 proteins has been previously described.[20] Streptavidin nanobeads (BioLegend) were added to the pools and incubated for 15 min on ice. Then, 2.5 mL of MojoSort™ Buffer was added, and the tubes with the samples of each pool were placed in a MojoSort™ Magnet for 5 min. The tubes were decanted without removing them from the Magnet, 2.5 mL of MojoSort™ Buffer was added, and the previous step was repeated. Finally, a positive selection of magnetically separated cells was collected; these were the enriched S1 and RBD protein-specific B cells.

2.2 | scRNA libraries preparation and sequencing

Single-cell suspensions of enriched S1 and RBD protein-specific B cells and library preparation were generated using 10x Genomics technology (10x Genomics Pleasanton). For this, a suspension of ~10 000 cells per

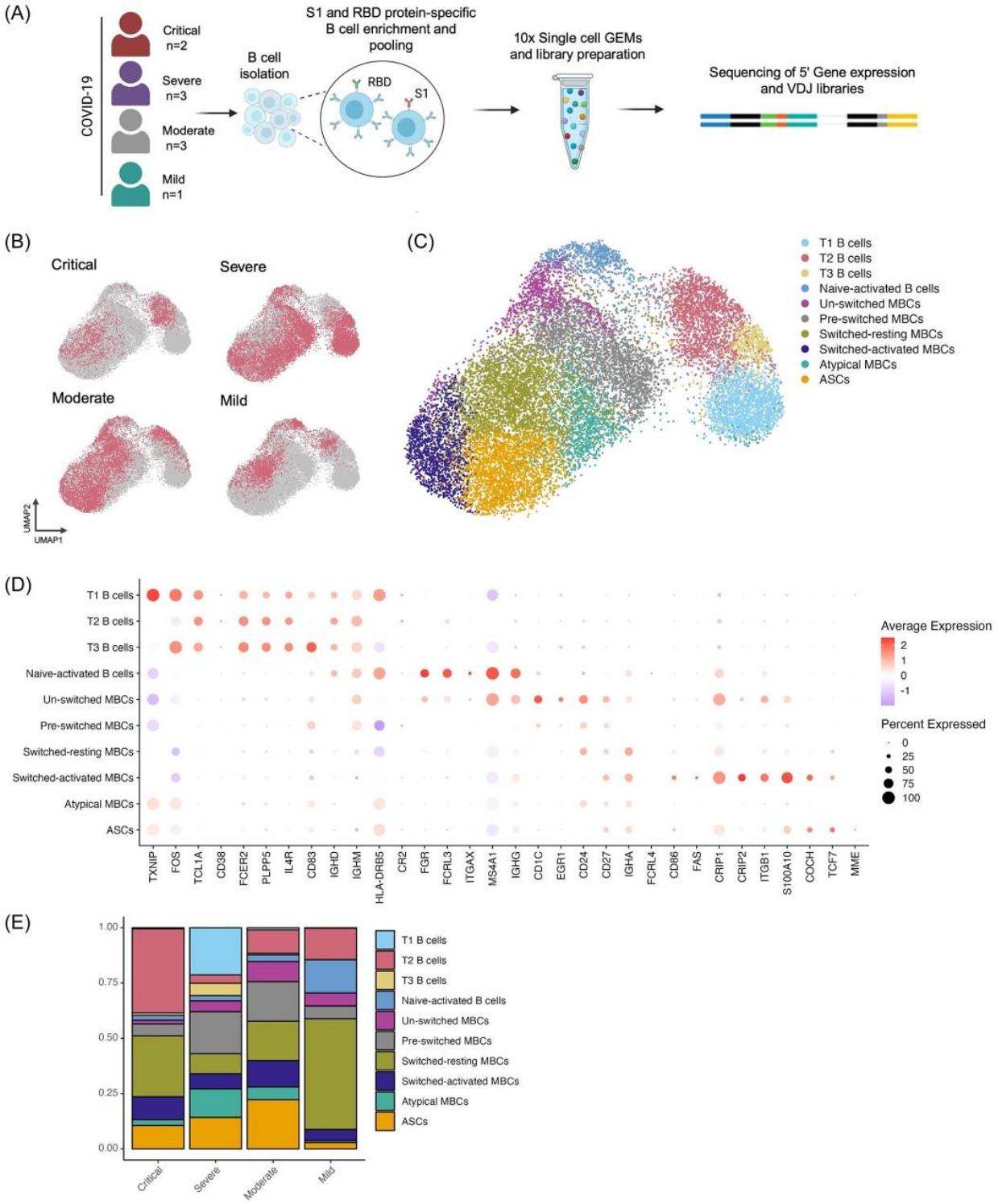

FIGURE 1 (See caption on next page).

pool was prepared with the Chromium Next GEM Single Cell 5' Reagent Kits v2 (Dual Index) and Chromium Next GEM Chip K Single Cell Kit to be loaded into the Chromium Controller equipment. Once the single cells were obtained by the formation of gel beads in emulsions (GEMs) the libraries were prepared using the Chromium Single Cell Human BCR Amplification Kit, 5' Feature Barcode Kit, and Library Construction Kit, according to the manufacturer's instructions. Then, the libraries were sequenced on a NextSeq. 550 system (Illumina).

2.3 | scRNA-seq data processing

FASTQ files were processed with cellranger (v 5.0) multi pipeline for alignment, filtering, barcoding, and (unique molecular identifier) counting using the GRCh38 genome as reference. For quality control, those cells with more than 5% of their total counts coming from mitochondrial genes were filtered out. Then, hashtag oligo demultiplexing was performed following Seurat's R-package pipeline.[21] Next, the workflow of the Seurat R package (v 4.0) was followed with default parameters,[22] and technical differences between samples were corrected using the Canek R package (v 0.2.5).[23] The corrected counts were scaled, and a principal component analysis (PCA) was performed. After inspecting the variability captured by the first PCs we decided to use the first 12 PCs for the subsequent analysis.

2.3.1 | Clustering and cell type annotation

To cluster the cells, the Leiden clustering algorithm implemented in the Seurat R package was applied for increasing values of resolutions. After selecting the best clustering resolution, we performed DGE analysis on the resulting clusters and obtained their top markers. The differentially expressed genes (DEGs) were obtained using *FindAllMarkers* from Seurat R package which compares gene expression between all clusters defined in the data set. Using these markers, clusters containing cells different from B cells were identified and filtered out. Then the clusters of B cells were annotated based on expressions of canonical markers.

2.3.2 | Functional enrichment analysis and trajectory analysis

Functional enrichment analysis on the Molecular Signatures Database (MSigDB) Hallmark gene sets,[24] and Gene Ontology (GO) Biological Process database[25] was performed using pre-ranked gene lists with the fast gene enrichment analysis (fgsea)[26] package in R (v 1.24.0), from the DEGs, indicating the NES (normalized enrichment score) and the adjusted *P*-value. The GO terms and Hallmark gene sets with adjusted p-value < 0.05 were considered significantly enriched and Dot plots were used to visualize enriched terms and sets. For the B cells trajectory analysis, the Slingshot[27] R package (v 2.6.0) was implemented using the clustered annotated T1 B cells as a starting point.

2.3.3 | Repertoire analysis

V(D)J libraries were processed using CellRanger v5.0 for contig assembly, annotation and clonotype calling. Downstream analysis was conducted using the Immcantation framework: ChangeO[28] was used for reannotation, and SHazaM was employed for somatic hypermutation analysis. Gene usage was analyzed by determining the proportion of the repertoire represented by each gene or gene pair combination in a weighted manner, and figures were generated by customized R code.

2.4 | Results

2.4.1 | Single-cell profiling of B cells in COVID-19 convalescent donors identifies a subset of atypical MBCs

After quality control and filtering, 18,190 cells were selected for subsequent analysis. We obtained the uniform manifold approximation and projection (UMAP) representation of cells based on the PCA results to visualize the cell clusters. These analyses revealed distinct cell distributions among convalescent donors with critical, severe, moderate, or mild diseases, and together resulted in the identification of 10 clusters (Figure 1B,C).

To obtain cellular identities, manual cell type annotation was performed based on the typical marker expression of B cell subsets,[1,17,29,30] followed by the analysis of frequency distribution for each subset by condition and individual donors (Figure 1D,E and Supporting Information S1: Figure 1b). We identified three clusters as transitional B cells based on their expression of *TCL1A*, *CD38*, and *FCER2* (CD23). The differential expression levels of these genes facilitated the distinction between T1, T2, and T3 transitional B cells

FIGURE 1 Transcriptomic analysis of B cells from convalescent COVID-19 patients. (A) Schematic overview of the experimental design for scRNA-seq, illustrating the workflow and steps involved in the experimental processes. (B) UMAP visualization of B cell distribution split by condition (critical, severe, moderate, and mild). The data includes 1752 cells from critical donors, 8647 cells from severe donors, 5399 cells from moderate donors, and 2392 cells from the mild donor. (C) UMAP visualization of 18 190 integrated and clustered B cells revealing clustering into 10 distinct groups (enumerated by cluster) and annotated with their identified subsets. (D) Dot plot visualization of expression of canonical B cell subtypes genes within the 10 subsets of B cells. Subsets are listed on the x-axis, while a selection of genes used for cell annotation is listed on the y-axis. The scale color represents the relative average expression based on log1p normalized data. (E) Proportion of B cell subsets distributed by condition. scRNA-seq, single-cell RNA-sequencing.

revealing a higher expression of *CD38* in T1 and lower in T3 B cells. Additionally, the expression levels of *FCER2* range from highest in T3, intermediate in T2, and lowest in T1 B cells, which aligns with previously reported protein levels of these cell subsets[1,30] (Figure 1D, Supporting Information S1: Figure 1c and 2a). Interestingly, the clusters from T1 and T3 B cells had a high frequency in donors with severe disease, while the cluster corresponding to T2 B cells was notably higher in donors with critical disease.

Additionally, to observe other distinctive characteristics of T1, T2, and T3, we performed a DGE analysis between these three subsets (Supporting Information S1: Figure 2b). T1 was characterized by high expression of *TXNIP* and *ZFP36L2*, genes related to cellular senescence.[31,32] In contrast, T2 showed expression of genes related to antigen presentation, such as *HLA-DQA1*, in addition to the upregulation of *CD40*. Finally, T3 was characterized by the expression of *NFKBIA*, *CD83*, and *JUN*, mostly expressed in proinflammatory cells.

Continuing with cell annotation, a cluster of naive-activated B cells showed high expression of *MS4A1* (CD20), *FCRL3*, and *ITGAX*, and low expression of *IGHM* and *IGHD*. This subset also had high expression of *IGHG*, suggesting it may undergo class switch recombination through the extrafollicular pathway.[33] Naive-activated B cells were most frequent in the donor with mild disease. Then, we identified five distinct clusters of MBCs,[1] one of which was characterized as un-switched MBCs, based on its expression of *CD24*, *CR2* (CD21), *CD27*, and *CD1C*, along with low expression of *MS4A1*. The subsequent cluster was annotated as pre-switched MBCs, due to its expression of *CD24*, *CR2*, *CD27*, and low expression of *IGHM*. A high frequency of these cells was observed in donors with severe and moderate symptoms. The switched-resting MBCs was identified by their expression of *CD24*, *CD27*, *IGHA*, and low levels of *IGHG*, with most cells in this cluster originating from the donor with mild disease.

Another cluster of MBCs was switched-activated MBCs which expressed *CD27*, *FAS*, *ITGB1*, *CD86*, and *IGHA*. Next, the fifth cluster of MBCs was identified as atypical MBCs. Although the transcriptional profile of this cluster exhibited similarities to the previously identified subsets of MBCs, a DGE analysis was conducted exclusively on all MBC clusters to refine their annotation. It was observed that the transcriptional levels of *CD27* and *CR2* in the fifth cluster of MBCs were notably lower compared to conventional MBCs (un-switched, pre-switched, switched-resting, and switched-activated MBCs) (Supporting Information S1: Figure 2c). These signatures enabled us to annotate this cluster as atypical MBCs, supported by the co-expression of other genes previously reported in these cells, such as *CD24* and *CXCR5*.[17] Donors with severe symptoms predominantly exhibited a higher frequency of atypical MBCs. The last identified clusters showed high expression of *TCF7*, along with co-expression of *IGHA*, *IGHG* and *HLA-DRB5*, which were annotated as ASCs, and the highest frequency of these cells came from donors with moderate disease. These results provide a comprehensive view of B cell heterogeneity in convalescent COVID-19 donors, and differences in cell compositions were noted across disease conditions.

2.4.2 | Proinflammatory signatures are differentially expressed between critical/severe versus moderate/mild

To further explore the transcriptomic characteristics of B cell subsets across different COVID-19 conditions, we conducted a DGE analysis. Figure 2A displays the heatmap visualization of the seven subsets with the highest number of DEGs between conditions. Interestingly, genes related to the proinflammatory response were upregulated in severe donors, including *GADD45B*, *MAP3K8*, *NFKBIA*, *JUNB*, *AREG*, *PPP1R15A*, and *FOSB*, and were expressed across the different subsets (Figure 2A). Additionally, it was confirmed that some of these genes displayed a characteristic signature overall in donors with severe symptoms (Figure 2B). Furthermore, *NFKBIA*, *CD69*, and *CD83* were upregulated in severe and critical conditions (Figures 2B,C). In contrast, mild to moderate symptoms exhibited increased expression of antiviral genes (*IFI16*, *IFI30*, *ISG20*, and *AIM2*) and activation-related genes (*SPIB*, *PTPRCAP*) (Figure 2A–C, Supporting Information S1: Figure 3a).

Next, we conducted gene set enrichment analysis (GSEA) to identify biological processes from GO and hallmark gene sets from the MSigDB across donor severity (Figure 2D and Supporting Information S1: Figure 3b). The results showed that donors with severe symptoms were mainly involved in tumor necrosis factor alpha (TNF-α) signaling via nuclear factor kappa B (NF-κB) and hypoxia pathways in most of the cell subsets, including atypical MBCs. In donors with critical conditions, these pathways were specifically upregulated in T2 B cells while simultaneously being downregulated in ASCs.

Then, we aimed to analyze the induced and repressed genes in critical and severe donors as compared to moderate and mild donors (Figure 2E). The atypical MBCs in moderate/mild groups expressed *IGHG* and *IGHG1*, meanwhile critical/severe groups expressed *CXCR4*, *PELI1* and *RGS2* genes. In T2 B cells the moderate/mild conditions showed induced expression of *S1PR4* and *CCR7* genes, which are involved in the differentiation and migration of B cells, respectively. In naive-activated B cells, the predominant genes in moderate/mild groups were *IGHM*, *IGHG2*, and *CD72*, meanwhile critical/severe group showed a high expression of genes like *PPP1R15A*, and *MAP3K8*. In addition, the genes *FOS*, *CD83*, *NFKBIA*, and *CD69*, were characteristically induced in most of the B cell subsets from critical/severe condition. (Figure 2E, Supporting Information S1: Figure 3c, and Supporting Information S2: Data 1).

2.4.3 | Atypical MBCs shows characteristic somatic hypermutation levels and a diverse BCR repertoire

To better understand the B cell response in SARS-CoV-2 infection, we analyzed the BCR repertoire across cell subsets and clinical manifestations. Initially, we assessed somatic hypermutation (SHM) levels, revealing distinct rates correlating with cell phenotype (Figure 3A). This observation is supported by Figure 3B, where mutated B cell distribution increased with cell differentiation. Specifically, SHM

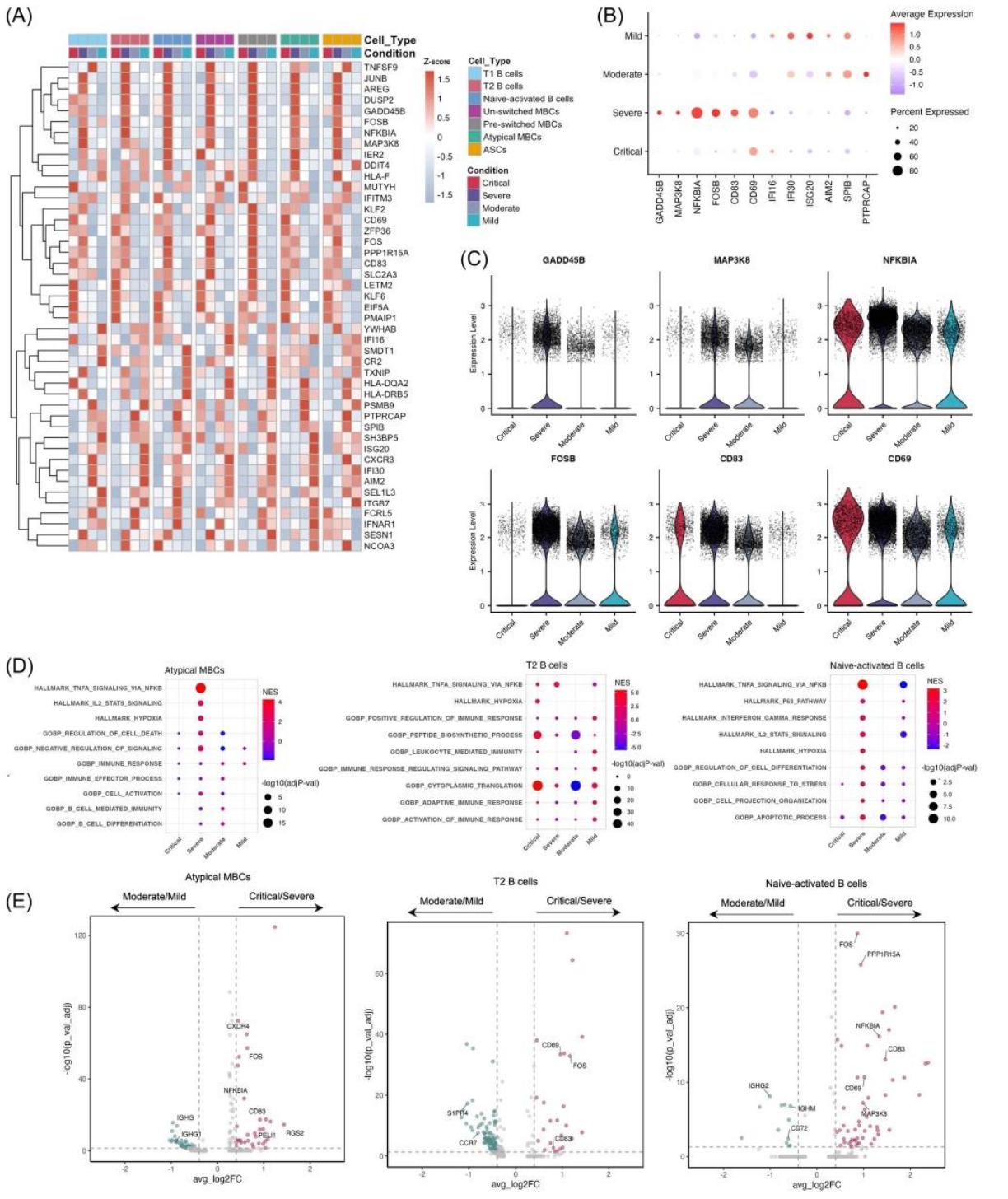

FIGURE 2 (See caption on next page).

rate < 1 is predominantly associated with transitional B cells (which are still immature B cells), while SHM rate > 7 is mainly observed in switched-activated MBCs and ASCs (Figures 3A,B). Additionally, we observed that atypical MBCs showed lower SHM levels compared to switched MBCs (switched-resting and switched-activated MBCs) but higher levels than nonswitched MBCs (un-switched and preswitched MBCs) (Figure 3A).

For comparative analyses across conditions, transitional B cells (T1, T2, and T3) were excluded as these cells are undergoing maturation processes (Figure 3C and Supporting Information S1: Figure 4a). The results showed a similar distribution of SHM rates across. However, we observed a slightly higher proportion of SHM rates < 1 in the critical condition and a lower proportion of SHM rates > 7 in the mild condition as compared with other groups (Figure 3C).

We then assessed the distribution of BCR isotype genes in each condition and the usage of Immunoglobulin heavy chain variable region (IGHV) and Immunoglobulin heavy chain joining region (IGHJ) genes in conventional MBCs, atypical MBCs, and ASCs (Figures 3D,E, and Supporting Information S1: Figures 4b-g). Among conventional MBCs, *IGHM* was the predominant gene isotype across groups. In critical and mild conditions, *IGHA1* emerged as the second most predominant, while the abundance of *IGHG1* and *IGHG2* increased in the severe and moderate groups. We observed a similar prevalence of IGHM in atypical MBCs with less diversity of isotype genes in critical and mild conditions. This may be attributed to the limited number of atypical MBCs identified in these two groups. In ASCs, both severe and moderate groups exhibited high frequencies of *IGHG1*, and exclusive association with *IGHA2* (Figure 3D).

The IGHV gene usage revealed a prevalence of *IGHV3-23* in both conventional and atypical MBCs (Supporting Information S1: Figure 4b, and 3c). In conventional MBCs, particularly within the severe and moderate groups, *IGHV3-33* was predominant. Conversely, in ASCs, a dominance of the *IGHV1-18* and *IGHV4-39* genes was observed in critical conditions (Supporting Information S1: Figure 4d). In Figure 3E, we highlight the overrepresentation of IGHV/IGHJ combinations in atypical versus conventional MBCs. Atypical MBCs exhibit a predominant frequency of *IGHV1-18/IGHJ5*, *IGHV1-69D/IGHJ6*, and *IGHV3-21/IGHJ3* in mild conditions, while *IGHV3-11/IGHJ4* and *IGHV6-1/IGHJ4* are overrepresented in critical cases. Conversely, conventional MBCs display a predominant frequency, mainly of *IGHV1-69/IGHJ1*, *IGHV3-13/IGHJ2*, and *IGHV3-20/IGHJ4*, in critical conditions (Figure 3E). The *IGHJ4* gene emerged as the most frequently used across conventional MBCs, atypical MBCs, and ASCs (Supporting Information S1: Figures 4e-g). This gene is recognized for its heightened occurrence in both healthy and pathological conditions.[34]

Overall, the results demonstrate that preferential gene usage plays an important role in antibody production against SARS-CoV-2 across different conditions, as previously reported.[35,36] Moreover, variations in gene usage and SHM were noted between conventional MBCs and atypical MBCs.

2.4.4 | Differentiation of atypical MBCs in response to SARS-CoV-2 infection

Atypical MBCs have been relatively underexplored in the context of the response against SARS-CoV-2, as well as in other diseases. Although we observe some differences between classical and atypical MBCs in the results above, we further dissected potential factors driving the differentiation of these cells during COVID-19 infection. Additionally, we sought to analyze their characteristics and possible functions. We first delineated the differentiation trajectories of cell subsets, starting from the least differentiated cluster (T1). We found three lineages culminating into switched-activated MBCs, ASCs, and atypical MBCs (Figure 4A, and Supporting Information S1: Figure 5). Interestingly, all lineages branched at the switched-resting MBCs group, suggesting a strong relationship between the final subsets and these cells.

We further investigate genes potentially involved in differentiating atypical MBCs by performing DGE analysis. The volcano plot in Figure 4B displays the genes upregulated in the atypical MBCs compared to the other two final subsets (switched-activated MBCs and ASCs). Specifically, 172 genes were upregulated, including genes involved in germinal center (GC) processes such as *CXCR4*, *MCL1*, *BCL2*, and *MYC*. Interestingly, we observe the upregulation of genes such as *CD79B* and *NR4A2*, which have previously been reported in atypical MBCs in malaria.[37] Additionally, we identified the induction

FIGURE 2 Gene expression differences in B cell subsets across different conditions. (A) Heatmap showing DEGs in the seven main analyzed subsets derived from convalescent donors with critical, severe, moderate, and mild conditions. The top color annotation above the heatmap represents the cell types (B cell subsets), while the second color annotation represents the COVID-19 conditions. The expression scale, represented by the Z-score, indicates the number of standard deviations from the mean expression of each normalized gene expression across conditions within each cell type. (B) Dot plot highlighting genes widely expressed mainly in severe conditions, associated with a proinflammatory response, as well as genes primarily expressed in moderate and mild conditions, associated with an antiviral response. The scale color represents the relative average expression based on log1p normalized data. (C) Violin plots represent the absolute normalized expression levels of selected proinflammatory response genes, divided by condition. (D) GSEA analysis of DEGs across the different conditions in T2 B cells, naive-activated B cells and atypical MBCs. Circle colors represent the normalized enrichment score (NES) scores whereas circle size represents the -log10 of adjusted *p* Values. (E) Volcano plots illustrating the upregulated genes in critical/severe (purple) versus moderate/mild (green) from T2 B cells, naive-activated B cells and atypical MBCs. Horizontal dotted line indicates the adjusted *p* Value cutoff of 0.05, and vertical dotted lines indicate the log fold-change of the average expression (avg_log2FC) cutoff of 0.4. DEGs, differentially expressed genes; GSEA, gene set enrichment analysis; MBCs, memory B cells.

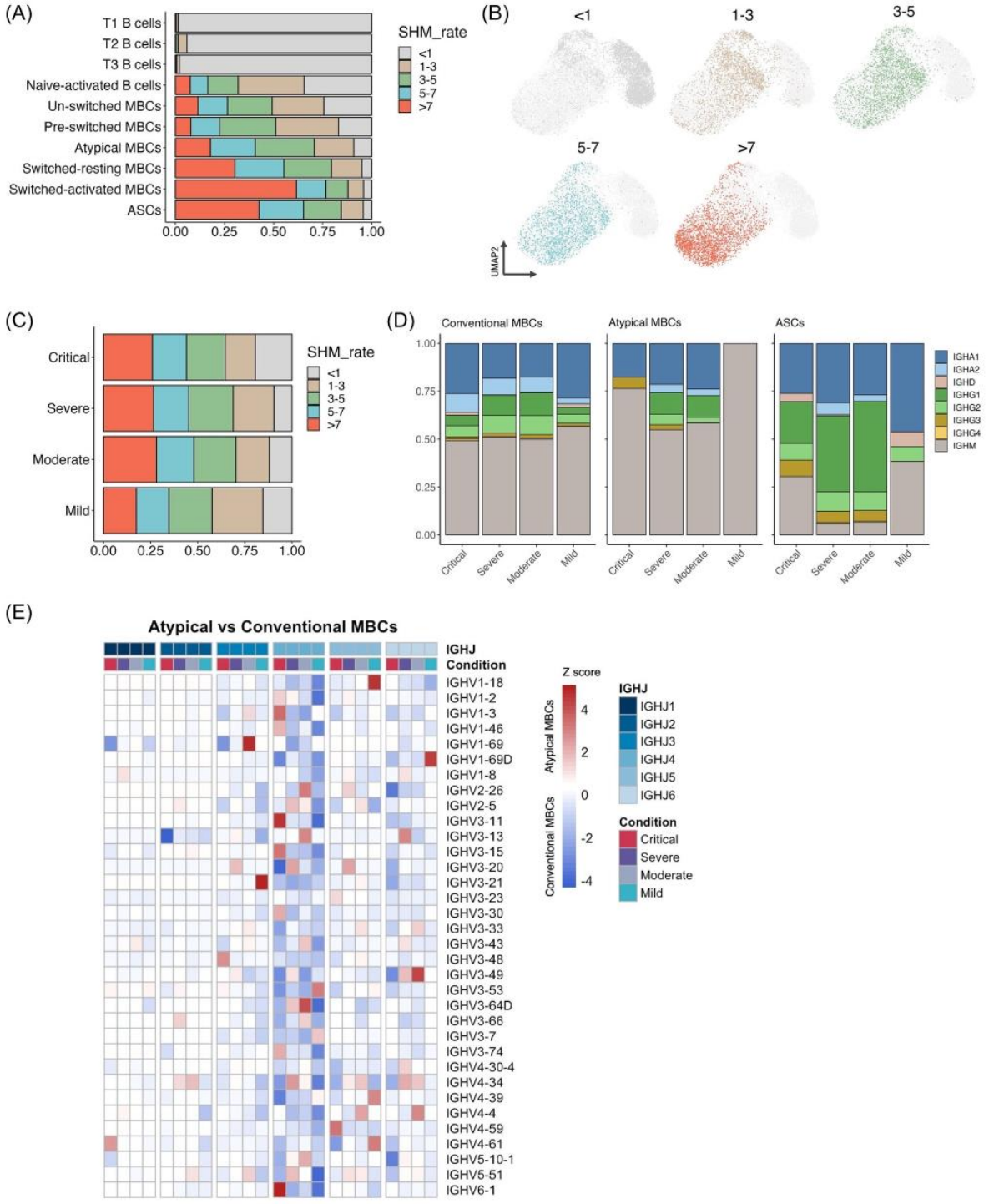

FIGURE 3 BCR repertoire analysis. (A) SHM rates across the 10 different B cell subsets, showing correlation of SHM levels with cell phenotype). (B) UMAP visualization of B cells from COVID-19 patients colored by SHM rates. (C) Distribution of SHM rates among critical, severe, moderate, and mild conditions, excluding transitional B cells (T1, T2, and T3 B cells). (D) Bar plots showing the isotype gene proportion in conventional MBCs, atypical MBCs, and ASCs across the different conditions. (E) Heatmap showing IGHV/IGHJ gene pairing frequencies in atypical versus conventional MBCs, across the different conditions. The Z-score scale shows in positive values (light red to deep red) the IGHV/IGHJ combinations in atypical MBCs, with deeper red color indicating more frequent combinations in these cells. Conversely, negative Z-score values (light blue to deep blue) depict the IGHV/IGHJ combinations in conventional MBCs, with deeper blue color representing a highly frequent combinations in these cells. ASCs, antibody secreting cells; MBCs, memory B cells; SHM, somatic hypermutation.

of *BTG1*, *FOXP1*, and *KLF2* genes, which are related to B cell differentiation. In contrast, 250 genes were upregulated in switched-activated MBCs and ASCs, including *HHEX* and *SUB1*, which are involved in MBC and plasma cell differentiation, respectively, as well as *MEF2C* and *ZBTB38*, essential genes for proliferation and efficient humoral response (Figure 4B, and Supporting Information S3: Data 2).

Moreover, GO enrichment analyses linked these upregulated genes from atypical MBCs with BCR signaling, activation, proliferation, and differentiation of B cells, as well as regulation of the MAPK cascade (Figure 4C). On the contrary, genes differentially expressed in switched-activated MBCs and ASCs were predominantly associated in processes related to ATP synthesis, cellular respiration, and oxidative phosphorylation (Figure 4C-left). Finally, we observed significant overexpression of certain genes closely involved in the COVID-19 response, such as *IRF1*, *IFNGR2*, *DUSP1*, *ZFP36L2*, *JUND*, and *FOS*, in atypical MBCs, and some of these genes also expressed in transitional B cells. This overexpression was noted in comparison with the rest of the subsets (Figure 4D). These data indicate that atypical MBCs have undergone GC processes, and their differentiation is involved in the antiviral response against SARS-CoV-2.

3 | DISCUSSION

Our study aimed to analyze B cells at single-cell resolution from convalescent COVID-19 donors, with a specific focus on conducting comprehensive analyzes on atypical MBCs to enhance our understanding of these cells in the context of COVID-19.

The transcriptomic profiling of B cells revealed cellular heterogeneity across conditions, notably indicating an increase in transitional B cells among donors who experienced critical and severe symptoms. The high frequency of these cells could be associated with antigenic persistence to develop mature B cells. Previous studies have found an increase in transitional B cells during COVID-19, in patients with mild/moderate symptoms, linked to ASCs maturation and viral clearance.[12–14] However, our results show a high frequency of these cells in severe/critical convalescent donors, suggesting they were generated in response to SARS-CoV-2 but remained arrested in the transitional stage. This is particularly evident in T1 cells, which exhibited high expression of *TXNIP* and *ZFP36L2*, indicating they were in a state of senescence.[31,32] This state can be attributed to the stress and cellular damage caused by the severity of COVID-19. Atypical MBCs were another remarkable subset mainly found in severe convalescent donors, though they were also present in minor frequency across mild, moderate, and critical conditions. This suggests that atypical MBCs play a role in the response of COVID-19.[14,15]

The severity of COVID-19 involves a proinflammatory response, primarily driven by monocytes, macrophages, and T cells.[38–40] While B cells are primarily known for antibody production, our findings reveal a proinflammatory signature in convalescents with critical/severe symptoms. This is evidenced by the upregulation of certain genes such as *GADD45B*, *MAP3K8*, *PPP1R15A*, and *NFKBIA*,[41–43] expressed across B cell subsets. Consistent with these results, we also observed that the expressed genes in subsets from severe conditions were associated with TNF-α signaling via NF-κB, a pathway involved in producing inflammatory cytokines.[44] Notably, genes such as *GADD45B*, *NFKBIA* and *TNFSF9* directly participate in this pathway.[42,45] Thus, our data suggest that B cells, including transitional, naive, memory, and ASC, may play a role in the proinflammatory response in severe COVID-19. On the other hand, donors who had mild/moderate symptoms exhibited high expression of IFN-response genes such as *IFI16*, *IFI30*, and *ISG20*, which are associated with an antiviral response,[46] which may have contributed to better outcomes.

Given the limited understanding of atypical MBCs, we employ multiple bioinformatic approaches to elucidate fundamental features and potential developmental pathways of these cells in COVID-19. The results suggest that atypical MBCs follow a developmental pathway similar to conventional MBCs in response to SARS-CoV-2. However, at some point during differentiation, these cells diverge to take a different route and become atypical MBCs. Several studies on malaria, HIV, and other pathologies have reported possible mechanisms of differentiation.[6,18,19,47] Among these, some results suggest that poor T follicular helper (Tfh) cooperation during processes in the GC may drive B cell differentiation into atypical MBCs. Another proposed mechanism is that the upregulation of inhibitory receptors and reduced BCR signaling may promote the development of atypical MBCs from classical MBCs. Additionally, these cells could arise during the normal activation of conventional MBCs in response to infection via an unknown mechanism. Finally, another potential pathway is the generation of atypical MBCs via extrafollicular activation, which may represent a population of pre-antibody-secreting cells, such as double negative 2 (DN2) B cells.

In this context, the trajectory analysis conducted on our data confirms that atypical MBCs follow a differentiation trajectory like conventional MBCs, indicating that these atypical cells also undergo GC processes. This is supported by their SHM levels and high expression of genes associated with the GC, including *CXCR5*, *CXCR4*, and *MYC*, which are essential for the circulation and maintenance of the dark and light zones, as well as for interaction with Tfh cells.[48,49] Additionally, *BCL2* and *MCL1*, which are increased in GC B cells, play crucial roles in GC maintenance and apoptosis prevention.[50,51] Furthermore, the GO analysis reveals that atypical MBCs are involved in BCR signaling, activation, and proliferation pathways. This indicates that these cells are not anergic or exhausted, and their mechanism is opposite to that associated with reduced BCR signaling. Then, we identified several characteristic genes widely reported in COVID-19 and that were found to be upregulated in atypical MBCs, such as *IFNGR2*, *DUSP1*, *ZFP36*, and *IFITM3*.[52–54] This suggests that their development could be influenced by antigen exposure and the resulting immune environment. Additionally, the results indicate that these cells may serve as a functional class of B cells actively contributing to the immune response. They appear to be active cells, exhibiting high BCR signaling, and expressing genes such as *ZFP36* and *DUSP1*, which play immune regulatory roles in COVID-19 infection and recovery.

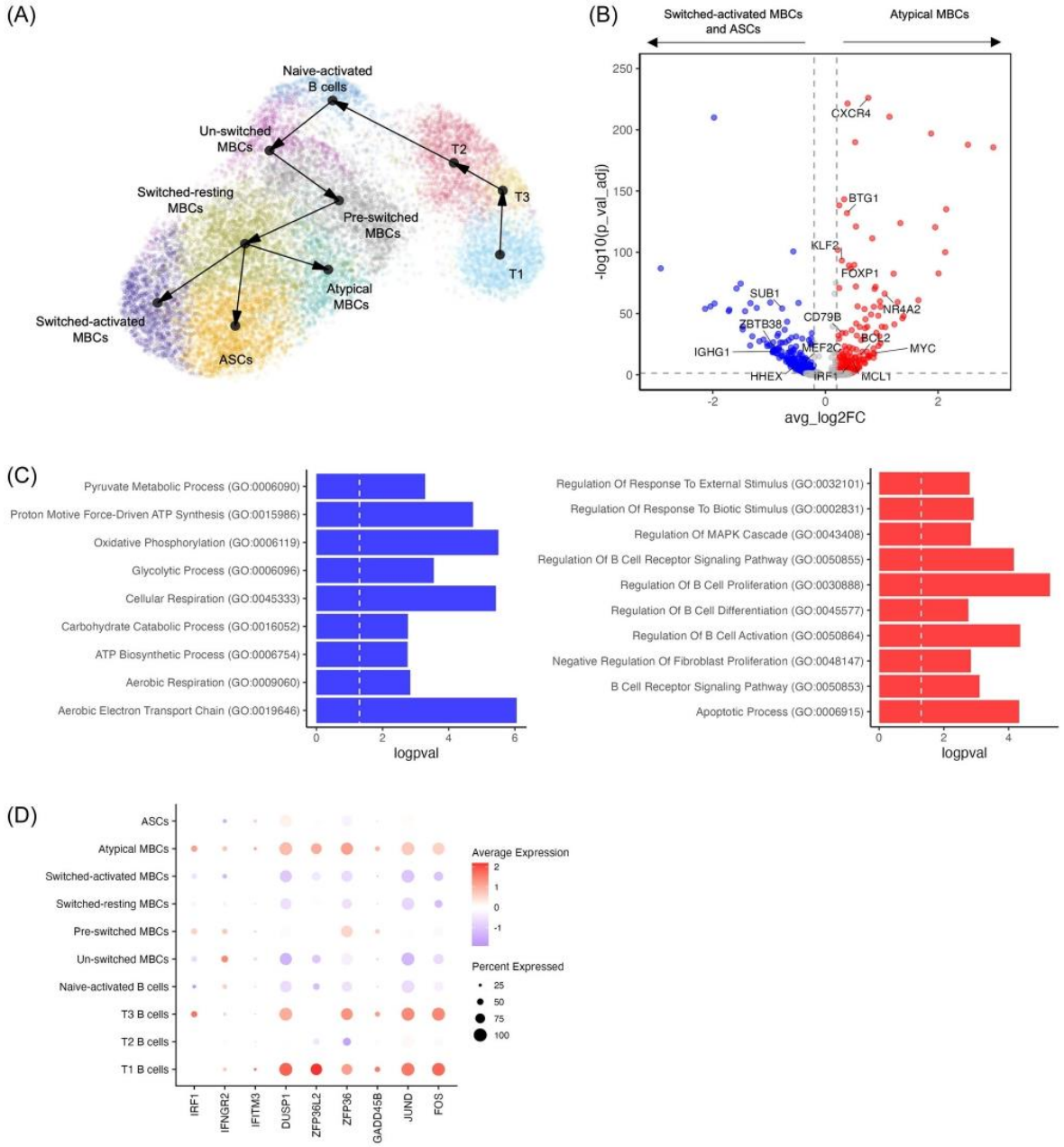

FIGURE 4 Transcriptomic features of atypical MBCs. (A) Trajectory analysis revealing the stages of differentiation of B cell subsets, starting with the less differentiated T1 B cells, and concluding in three different lineages: atypical MBCs, ASCs, and switched-activated MBCs. (B) Volcano plot showing DEGs in atypical MBCs (red) versus switched-activated MBCs and ASCs (blue), a total of 172 and 250 DEGs are shown respectively. Horizontal dotted line indicates the adjusted *P*-value cutoff of 0.05, and vertical dotted lines indicate the log fold-change of the average expression (avg_log2FC) cutoff of 0.2. (C) Gene Ontology analysis from the DEGs in atypical MBCs (red) versus switched-activated MBCs and ASCs (blue). (D) Heatmap of DEGs compared in atypical MBCs, ASCs, and switched-activated MBCs. (E) Dot plot displaying the expression levels of specific genes involved in the COVID-19 response across different B cell subsets. The scale color represents the relative average expression based on log1p normalized data. ASCs, antibody secreting cells; DEGs, differentially expressed genes; GSEA, gene set enrichment analysis; MBCs, memory B cells.

One limitation of this study is the small number of donors (mild $n = 1$, moderate $n = 3$, severe $n = 3$, and critical $n = 2$). This may explain the low number of cells and DEGs observed in the critical and mild groups. However, despite having only two donors, the critical group exhibited the lowest number of cells, which could be attributed to the lymphopenia characterized in the most critical cases. Additionally, this study lacked medical history from the donors. Future studies with a larger sample size and comprehensive clinical data could be crucial for further investigating the B cell response and in COVID-19. Moreover, while the study employed magnetic enrichment of S1 and RBD-specific B cells from convalescent donors, using FACS will increase the purity of the cells.

In summary, the transcriptomic analysis of B cells from convalescent COVID-19 patients revealed cell heterogeneity across different conditions. The results highlight the capacity of B cell subsets to contribute to the proinflammatory response, particularly in severe and critical cases. Additionally, the findings on atypical MBCs suggest a developmental pathway through the GC, similar to conventional MBCs. However, their differentiation and activation may be influenced by exposure to SARS-CoV-2, and they may play a role in contributing to the immune response for COVID-19 recovery. These results provide a better understanding of atypical MBCs in COVID-19 and a better understanding of the role of other B cell subsets in different clinical manifestations.

AUTHOR CONTRIBUTIONS

Conceptualization: Jesús Hernández. *Data curation*: Melissa García-Vega, Mara Anais Llamas-Covarrubias, Martin Loza, and Miguel Hernández-Oñate. *Formal analysis*: Melissa García-Vega, Mara Anais Llamas-Covarrubias, and Martin Loza. *Investigation*: Melissa García-Vega, Mara Anais Llamas-Covarrubias, Martin Loza, Mónica Reséndiz-Sandoval, and Diana Hinojosa-Trujillo, Edgar Melgoza-González. *Methodology*: Jesús Hernández, Melissa García-Vega, Mara Anais Llamas-Covarrubias, and Martin Loza. *Visualization*: Jesús Hernández. *Funding acquisition*: Jesús Hernández and Kenta Nakai. *Project administration*: Jesús Hernández. *Supervision*: Jesús Hernández. *Resources*: Jesús Hernández and Alan Soto-Gaxiola. *Writing—original draft*: Melissa García-Vega, Mara Anais Llamas-Covarrubias, Martin Loza, and Jesús Hernández. *Writing—review and editing*: Melissa García-Vega, Mara Anais Llamas-Covarrubias, Martin Loza, Verónica Mata-Haro, Miguel Hernández-Oñate, Jesús Hernández, Mónica Reséndiz-Sandoval, Olivia Valenzuela, Karina Chávez-Rueda, and Kenta Nakai.

ACKNOWLEDGMENTS

The authors thank Julia Real and Dr. Edgar Velázquez from the Centro Estatal de la Transfusión Sanguínea (Sonora) for supporting the project with the sample collection. Roberto Carvente and Alejandra García from Analitek for their technical support in the Single-cell experiments and sequencing. We also thank SENASICA for helping with the sequencing process, especially Fabiola Hernández, and the Advanced Genomics Unit-Langebio of CINVESTAV for access to the computing cluster. This project was funded by the Consejo Nacional de Ciencia y Tecnología grant 312677.

CONFLICT OF INTEREST STATEMENT

The authors declare no conflict of interest.

DATA AVAILABILITY STATEMENT

The scRNA-seq data that support the findings of this study are available on Zenodo data repository at https://zenodo.org/records/12519679. The R codes used to analyze the data are available from corresponding authors upon request.

ORCID

Jesús Hernández http://orcid.org/0000-0002-5131-3600

REFERENCES

1. Sanz I, Wei C, Jenks SA, et al. Challenges and opportunities for consistent classification of human B cell and plasma cell populations. *Front Immunol*. 2019;10:2458.
2. Zhou Y, Zhang Y, Han J, Yang M, Zhu J, Jin T. Transitional B cells involved in autoimmunity and their impact on neuroimmunological diseases. *J Transl Med*. 2020;18:131.
3. Suan D, Sundling C, Brink R. Plasma cell and memory B cell differentiation from the germinal center. *Curr Opin Immunol*. 2017;45:97-102.
4. Oliviero B, Mantovani S, Ludovisi S, et al. Skewed B cells in chronic hepatitis C virus infection maintain their ability to respond to virus-induced activation. *J Viral Hepatitis*. 2015;22:391-398.
5. Burton AR, Pallett LJ, McCoy LE, et al. Circulating and intrahepatic antiviral B cells are defective in hepatitis B. *J Clin Invest*. 2018;128:4588-4603.
6. Moir S, Ho J, Malaspina A, et al. Evidence for HIV-associated B cell exhaustion in a dysfunctional memory B cell compartment in HIV-infected viremic individuals. *J Exp Med*. 2008;205:1797-1805.
7. Dugan HL, Stamper CT, Li L, et al. Profiling B cell immunodominance after SARS-CoV-2 infection reveals antibody evolution to non-neutralizing viral targets. *Immunity*. 2021;54:1290-1303.e7.e1297.
8. Scharf L, Axelsson H, Emmanouilidi A, et al. Longitudinal single-cell analysis of SARS-CoV-2-reactive B cells uncovers persistence of early-formed, antigen-specific clones. *JCI Insight*. 2023;8:e165299.
9. Sokal A, Chappert P, Barba-Spaeth G, et al. Maturation and persistence of the anti-SARS-CoV-2 memory B cell response. *Cell*. 2021;184:1201-1213.e1214.
10. Jin X, Zhou W, Luo M, et al. Global characterization of B cell receptor repertoire in COVID-19 patients by single-cell V(D)J sequencing. *Brief Bioinform*. 2021;22:bbab192.
11. Kaneko N. Loss of Bcl-6-Expressing T Follicular Helper Cells and Germinal Centers in COVID-19. *Cell*. 2020;183:143-157.e113.
12. Woodruff MC, Ramonell RP, Nguyen DC, et al. Extrafollicular B cell responses correlate with neutralizing antibodies and morbidity in COVID-19. *Nat Immunol*. 2020;21:1506-1516.
13. Sosa-Hernández VA, Torres-Ruíz J, Cervantes-Díaz R, et al. B cell subsets as Severity-Associated signatures in COVID-19 patients. *Front Immunol*. 2020;11:611004.
14. Oliviero B, Varchetta S, Mele D, et al. Expansion of atypical memory B cells is a prominent feature of COVID-19. *Cell Mol Immunol*. 2020;17:1101-1103.
15. Wildner NH, Ahmadi P, Schulte S, et al. B cell analysis in SARS-CoV-2 versus malaria: increased frequencies of plasmablasts and atypical memory B cells in COVID-19. *J Leukoc Biol*. 2021;109:77-90.
16. Stephenson E, Reynolds G, Botting RA, et al. Single-cell multi-omics analysis of the immune response in COVID-19. *Nat Med*. 2021;27:904-916.

17. Sullivan RT, Kim CC, Fontana MF, et al. FCRL5 delineates functionally impaired memory B cells associated with plasmodium falciparum exposure. *PLoS Pathog*. 2015;11:e1004894.
18. Portugal S, Tipton CM, Sohn H, et al. Malaria-associated atypical memory B cells exhibit markedly reduced B cell receptor signaling and effector function. *eLife*. 2015;4:e07218.
19. Braddom AE, Batugedara G, Bol S, Bunnik EM. Potential functions of atypical memory B cells in plasmodium-exposed individuals. *Int J Parasitol*. 2020;50:1033-1042.
20. Melgoza-Gonzalez EA. Analysis of IgG, IgA and IgM antibodies against SARS-CoV-2 spike protein S1 in convalescent and vaccinated patients with the Pfizer-BioNTech and CanSinoBio vaccines. *Transbound Emerg Dis*. 2021.
21. Stoeckius M, Zheng S, Houck-Loomis B, et al. Cell hashing with barcoded antibodies enables multiplexing and doublet detection for single cell genomics. *Genome Biol*. 2018;19:224.
22. Satija R, Farrell JA, Gennert D, Schier AF, Regev A. Spatial reconstruction of single-cell gene expression data. *Nat Biotechnol*. 2015;33:495-502.
23. Loza M, Teraguchi S, Standley DM, Diez D. Unbiased integration of single cell transcriptome replicates. *NAR Geno Bioinform*. 2022;4:lqac022.
24. Liberzon A, Birger C, Thorvaldsdóttir H, Ghandi M, Mesirov JP, Tamayo P. The molecular signatures database hallmark gene set collection. *Cell Systems*. 2015;1:417-425.
25. Ashburner M, Ball CA, Blake JA, et al. Gene ontology: tool for the unification of biology. The Gene Ontology Consortium. *Nature Genet*. 2000;25:25-29.
26. Korotkevich G, et al. Fast gene set enrichment analysis. *bioRxiv*. 2021:060012.
27. Street K, Risso D, Fletcher RB, et al. Slingshot: cell lineage and pseudotime inference for single-cell transcriptomics. *BMC Genomics*. 2018;19:477.
28. Gupta NT, Vander Heiden JA, Uduman M, Gadala-Maria D, Yaari G, Kleinstein SH. Change-O: a toolkit for analyzing large-scale B cell immunoglobulin repertoire sequencing data. *Bioinformatics*. 2015;31:3356-3358.
29. Stewart A, Ng JCF, Wallis G, Tsioligka V, Fraternali F, Dunn-Walters DK. Single-Cell transcriptomic analyses define distinct peripheral B cell subsets and discrete development pathways. *Front Immunol*. 2021;12:602539.
30. Suryani S, Fulcher DA, Santner-Nanan B, et al. Differential expression of CD21 identifies developmentally and functionally distinct subsets of human transitional B cells. *Blood*. 2010;115:519-529.
31. Huy H, Song HY, Kim MJ, et al. TXNIP regulates AKT-mediated cellular senescence by direct interaction under glucose-mediated metabolic stress. *Aging cell*. 2018;17:e12836.
32. Suk FM, Chang CC, Lin RJ, et al. ZFP36L1 and ZFP36L2 inhibit cell proliferation in a cyclin d-dependent and p53-independent manner. *Sci Rep*. 2018;8:2742.
33. Stavnezer J, Schrader CE. IgH chain class switch recombination: mechanism and regulation. *J Immunol*. 2014;193:5370-5378.
34. Shi B, Dong X, Ma Q, et al. The usage of human IGHJ genes follows a particular non-random selection: the recombination signal sequence May affect the usage of human IGHJ genes. *Front Genet*. 2020;11:524413.
35. Xiaojie S, Yu L, Lei Y, Guang Y, Min Q. Neutralizing antibodies targeting SARS-CoV-2 spike protein. *Stem Cell Res*. 2021;50:102125.
36. García-Vega M, Melgoza-González EA, Hernández-Valenzuela S, et al. 19n01, a broadly neutralizing antibody against omicron BA.1, BA.2, BA.4/5, and other SARS-CoV-2 variants of concern. *iScience*. 2023;26:106562.
37. Holla P, Dizon B, Ambegaonkar AA, et al. Shared transcriptional profiles of atypical B cells suggest common drivers of expansion and function in malaria, HIV, and autoimmunity. *Sci Adv*. 2021;7:abg8384.
38. Vanderbeke L, Van Mol P, Van Herck Y, et al. Monocyte-driven atypical cytokine storm and aberrant neutrophil activation as key mediators of COVID-19 disease severity. *Nat Commun*. 2021;12:4117.
39. Wang Y, Luu LDW, Liu S, et al. Single-cell transcriptomic analysis reveals a systemic immune dysregulation in COVID-19-associated pediatric encephalopathy. *Signal Transduct Target Ther*. 2023;8:398.
40. Wang Y, Perlman S. COVID-19: inflammatory profile. *Annu Rev Med*. 2022;73:65-80.
41. Goel S, Saheb Sharif-Askari F, Saheb Sharif Askari N, et al. SARS-CoV-2 switches 'on' MAPK and NFκB signaling via the reduction of nuclear DUSP1 and DUSP5 expression. *Fronti Pharmacol*. 2021;12:631879.
42. Yang Z, Song L, Huang C. Gadd45 proteins as critical signal transducers linking NF-&;#954;B to MAPK cascades. *Curr Cancer Drug Targets*. 2009;9:915-930.
43. Li Y, Duche A, Sayer MR, et al. SARS-CoV-2 early infection signature identified potential key infection mechanisms and drug targets. *BMC Genomics*. 2021;22:125.
44. Wu Y, Zhou BP. TNF-α/NF-κB/Snail pathway in cancer cell migration and invasion. *Br J Cancer*. 2010;102:639-644.
45. Camblor DG, Miranda D, Albaiceta GM, et al. Genetic variants in the NF-κB signaling pathway (NFKB1, NFKBIA, NFKBIZ) and risk of critical outcome among COVID-19 patients. *Hum Immunol*. 2022;83:613-617.
46. Weiss CM, Trobaugh DW, Sun C, et al. The Interferon-Induced exonuclease ISG20 exerts antiviral activity through upregulation of type I interferon response proteins. *mSphere*. 2018;3:e00209-18.
47. Figueiredo MM, Costa PAC, Diniz SQ, et al. T follicular helper cells regulate the activation of B lymphocytes and antibody production during plasmodium vivax infection. *PLoS Pathog*. 2017;13:e1006484.
48. Allen CDC, Ansel KM, Low C, et al. Germinal center dark and light zone organization is mediated by CXCR4 and CXCR5. *Nature Immunol*. 2004;5:943-952.
49. Finkin S, Hartweger H, Oliveira TY, Kara EE, Nussenzweig MC. Protein Amounts of the MYC Transcription Factor Determine Germinal Center B Cell Division Capacity. *Immunity*. 2019;51:324-336.e325.
50. Vikstrom I, Carotta S, Lüthje K, et al. Mcl-1 is essential for germinal center formation and B cell memory. *Science*. 2010;330:1095-1099.
51. Li Y, Takahashi Y, Fujii S, et al. EAF2 mediates germinal centre B-cell apoptosis to suppress excessive immune responses and prevent autoimmunity. *Nat Commun*. 2016;7:10836.
52. Wauters E, Van Mol P, Garg AD, et al. Discriminating mild from critical COVID-19 by innate and adaptive immune single-cell profiling of bronchoalveolar lavages. *Cell Res*. 2021;31:272-290.
53. Lu J, Meng M, Zhou X, et al. Identification of COVID-19 severity biomarkers based on feature selection on single-cell RNA-Seq data of CD8(+) T cells. *Front Genet*. 2022;13:1053772.
54. Regino-Zamarripa NE, Ramírez-Martínez G, Jiménez-Álvarez LA, et al. Differential leukocyte expression of IFITM1 and IFITM3 in patients with severe pandemic influenza A(H1N1) and COVID-19. *J Interferon Cytokine Res*. 2022;42:430-443.

SUPPORTING INFORMATION

Additional supporting information can be found online in the Supporting Information section at the end of this article.

How to cite this article: García-Vega M, Llamas-Covarrubias MA, Loza M, et al. Single-cell transcriptomic analysis of B cells reveals new insights into atypical memory B cells in COVID-19. *J Med Virol*. 2024;96:e29851. doi:10.1002/jmv.29851

4. COMPARATIVE SINGLE-CELL TRANSCRIPTOMIC PROFILE OF HYBRID IMMUNITY INDUCED BY ADENOVIRUS VECTOR-BASED COVID-19 VACCINES

Melissa García-Vega[1], Hui Wan[2], Mónica Reséndiz-Sandoval[1], Diana Hinojosa-Trujillo[1], Olivia Valenzuela[3], Verónica Mata-Haro[1], Freddy Dehesa-Canseco[4], Mario Solís-Hernández[4], Harold Marcotte[2], Qiang Pan-Hammarström[2], Jesús Hernández[1*]

[1]Laboratorio de Inmunología, Centro de Investigación en Alimentación y Desarrollo, A.C. Hermosillo, Sonora, 83304, Mexico.
[2]Division of Immunology, Department of Medical Biochemistry and Biophysics, Karolinska Institutet, Solna, SE171 65, Sweden.
[3]Departamento de Ciencias Químico Biológicas, Universidad de Sonora, Hermosillo, Sonora, 83000, Mexico.
[4] Comisión México-Estados Unidos para la Prevención de la Fiebre Aftosa y otras Enfermedades Exóticas de los Animales (CPA), SENASICA, SADER, Ciudad de México 05010, Mexico.

Publicado en la revista:
Genes & Immunity

Fecha de publicación:
3 de abril del 2024

DOI: 10.1038/s41435-024-00270-x

ARTICLE

Check for updates

Comparative single-cell transcriptomic profile of hybrid immunity induced by adenovirus vector-based COVID-19 vaccines

Melissa García-Vega[1,5], Hui Wan[2,5], Mónica Reséndiz-Sandoval[1], Diana Hinojosa-Trujillo[1], Olivia Valenzuela[3], Verónica Mata-Haro[1], Freddy Dehesa-Canseco[4], Mario Solís-Hernández[4], Harold Marcotte[2], Qiang Pan-Hammarström[2]✉ and Jesús Hernández[1]✉

In this study, antibody response and a single-cell RNA-seq analysis were conducted on peripheral blood mononuclear cells from five different groups: naïve subjects vaccinated with AZD1222 (AZ) or Ad5-nCoV (Cso), individuals previously infected and later vaccinated (hybrid) with AZD1222 (AZ-hb) or Ad5-nCoV (Cso-hb), and those who were infected and had recovered from COVID-19 (Inf). The results showed that AZ induced more robust neutralizing antibody responses than Cso. The single-cell RNA data revealed a high frequency of memory B cells in the Cso and Cso-hb. In contrast, AZ and AZ-hb groups exhibited the highest proportion of activated naïve B cells expressing *CXCR4*. Transcriptomic analysis of $CD4^+$ and $CD8^+$ T cells demonstrated a heterogeneous response following vaccination, hybrid immunity, or natural infection. However, a single dose of Ad5-nCoV was sufficient to strongly activate $CD4^+$ T cells (naïve and memory) expressing *ANX1* and *FOS*, similar to the hybrid response observed with AZ. An interesting finding was the robust activation of a subset of $CD8^+$ T cells expressing *GZMB*, *GZMH*, and *IFNG* genes in the Cso-hb group. Our findings suggest that both vaccines effectively stimulated the cellular immune response; however, the Ad5-nCoV induced a more robust $CD8^+$ T-cell response in previously infected individuals.

Genes & Immunity; https://doi.org/10.1038/s41435-024-00270-x

INTRODUCTION

Since the onset of the pandemic in late 2019, an unprecedented global effort has been undertaken to develop safe and effective vaccines against SARS-CoV-2. The World Health Organization (WHO) has granted emergency approval to 12 vaccines that employ various technologies and exhibit varying efficacy rates. Adenovirus vector-based vaccines targeting SARS-CoV-2, such as Ad26.COV2-S (Johnson & Johnson), ChAdOx1 nCoV-19/AZD1222 (Oxford-AstraZeneca), and Ad5-nCoV (CanSinoBio) have demonstrated substantial protection against severe disease. However, their effectiveness against clinical manifestations may be lower than mRNA vaccines [1, 2].

Hybrid immunity, induced by natural infection against SARS-CoV-2 followed by vaccination, may provide more robust immune protection against SARS-CoV-2 and its circulating variants than infection or vaccination alone [3–7]. Most results of hybrid immunity come from mRNA vaccine studies, yet limited information is available on adenovirus vector-based vaccines, such as AZD1222 or Ad5-nCoV. For example, a single dose of the AZD1222 vaccine elicits higher antibody responses in people with prior SARS-CoV-2 infection compared to two doses in naïve individuals [8]. In addition, the humoral immune response induced by Ad5-nCoV is lower than that induced by other vaccines; nonetheless, people with prior SARS-CoV-2 infection and immunized with Ad5-nCoV exhibit a robust immune response similar to that induced by other vaccines [9]. These results are consistent with studies on different COVID-19 vaccines where "hybrid immunity" provides a potent immune response in vaccinated people with a history of SARS-CoV-2 infection [3].

Through single-cell RNA-seq (scRNA-seq) analysis in subjects vaccinated with Ad5-nCoV without previous infection, it was observed that Ad5-nCoV triggered a humoral immune response and expanded BCR clones. Nevertheless, immunoglobulin heavy chain variable region (*IGHV*) gene usage (*IGHV1-69D*, *IGHV1-18*, and *IGHV4-59*) differed [10] from those identified against SARS-CoV-2 infection (*IGHV3-53*, *IGHV1-69*, *IGHV1-2*) [11, 12]. The difference in *IGHV* gene usage may explain the lower level of neutralizing antibodies observed after a single dose of Ad5-nCoV. In contrast, Ad5-nCoV activated the cellular immune response, evidenced by an increased proportion of central memory (TCM) $CD4^+$ T cells, elevated IFN-γ level, and enhanced expression of proinflammatory genes on day 14 after vaccination, including interferon-stimulated genes (ISGs) in $CD4^+$ T cells, $CD8^+$ T cells, and natural killer (NK) cells [10]. However, no studies have evaluated the hybrid response induced by adenovirus vector-based vaccines at the single-cell level.

[1]Laboratorio de Inmunología, Centro de Investigación en Alimentación y Desarrollo, A.C, Hermosillo, Sonora 83304, Mexico. [2]Division of Immunology, Department of Medical Biochemistry and Biophysics, Karolinska Institutet, Solna SE171 65, Sweden. [3]Departamento de Ciencias Químico Biológicas, Universidad de Sonora, Hermosillo, Sonora 83000, Mexico. [4]Comisión México-Estados Unidos para la Prevención de la Fiebre Aftosa y otras Enfermedades Exóticas de los Animales (CPA), SENASICA, SADER, Ciudad de México 05010, Mexico. [5]These authors contributed equally: Melissa García-Vega, Hui Wan. ✉email: qiang.pan-hammarstrom@ki.se; jhdez@ciad.mx

Received: 9 January 2024 Revised: 20 March 2024 Accepted: 25 March 2024
Published online: 03 April 2024

Here, we report a single cell RNA sequencing (scRNA-seq) analysis of peripheral blood mononuclear cells (PBMCs) from individuals vaccinated with either the recommended two doses of the AZD1222 (AZ) vaccine or one dose of the Ad5-nCoV (Cso) vaccine, infected and subsequently vaccinated with AZD1222 (AZ-hb) or Ad5-nCoV (Cso-hb), and convalescent individuals of coronavirus disease 2019 (COVID-19) without vaccination (Inf). This study reveals the diversity of cell subsets in each group (natural infection, vaccine-induced, or hybrid), inducing a different immune response. Furthermore, these subsets play roles based on differentially expressed genes (DEGs) and the robust immune response induced during hybrid immunity.

MATERIALS AND METHODS

Subjects and sample collection

We obtained blood samples from 27 donors by non-probabilistic sampling. Eligibility criteria included age ≥18 vaccinated with AZD1222 or Ad5-nCoV with or without prior SARS-CoV-2 infection and 1−2 months since the last vaccination, or SARS-CoV-2 infection without vaccination and 3−8 weeks from the onset of symptoms. Peripheral mononuclear blood cells (PBMCs) were isolated from EDTA whole blood by density gradient centrifugation using Ficoll-Paque Plus (GE Healthcare Life Sciences, Massachusetts, USA). Isolated PBMC cells were resuspended in RPMI-1640 medium supplemented with 40% fetal bovine serum (FBS), and 2X freezing medium (30% DMSO in RPMI-1640 supplemented with 40% FBS) was added at a ratio of 1:1. Immediately, the cell suspension was dispensed in cryovials and kept at −80 °C for 4 h, and the cryovials were stored in liquid nitrogen until use. Samples were divided into five groups: vaccinated with Ad5-nCoV (Cso, $n = 6$), or AZD1222 (AZ, $n = 4$), infected (Inf, $n = 5$), and two hybrid groups, previously infected and vaccinated with Ad5-nCoV (Cso-hb, $n = 6$) or AZD1222 (AZ-hb, $n = 6$). The study was evaluated and approved by the Ethics Committee of the CIAD, AC (CEI/012-2/2020), and all patients signed informed consent forms.

ScRNA-seq and BCR sequencing

We performed scRNA-seq and single-cell BCR-sequencing (scBCRseq) using 10x Genomics technology (Fig. 1a). PBMCs from each donor were pooled into groups (AZ, AZ-hb, Cso, Cso-hb, or Inf), and incubated with TotalSeq™-C antibodies for cell hashing: TotalSeq™-C0251 (Cat# 394661), TotalSeq™-C0252 (Cat# 394663), TotalSeq™-C0254 (Cat# 394667), TotalSeq™-C0255 (Cat# 394669), TotalSeq™-C0256 (Cat# 394671) (BioLegend, San Diego, CA, USA). Then, labeled cells were divided into two groups and loaded into a 10x Chromium chip for Gel Bead-in-Emulsion (GEMs) generation and scRNAseq library preparation. A total of two libraries were prepared, including scRNA-seq and scVDJ-seq libraries. Briefly, scRNA-seq and VDJ-seq libraries were prepared on the Chromium platform using single-cell expression 5′ v2 profiling chemistry (10X Genomics, Pleasanton, CA, USA) and VDJ-B enrichment combined with cell hashing. HTO-labeled cells from 2 to 3 donors were pooled equally and washed twice with RPMI-1640 immediately before loading on the 10X controller. Complementary DNA amplification and library construction were conducted following the manufacturer's protocol, with additional steps for amplifying HTO barcodes. Libraries were sequenced to ~50,000 reads per cell on a Novaseq S2 (Illumina, San Diego, CA, USA) and BCR enrichment.

ScRNA-seq analysis

scRNA-seq and scBCR-seq data were aligned and quantified using cell ranger v5.0.1 multi (10X Genomics) against their corresponding human reference genome (GRCh38). Count matrices from the cell range output were preprocessed by filtering for cells and genes (minimum cells per gene, 10; minimum UMI per cell, 100). The filtered transcriptome data were normalized using default settings in the Seurat 4.3.0 package [13] (RNA expression by a factor of 10,000 with log-transformed, cell surface protein of Feature Barcode by a centered log ratio). Then, samples from patients vaccinated with different vaccines were demultiplexed based on the unique hashtag antibodies, and the threshold for classification was 0.99. Genes expressed in fewer than three cells were removed. Cells were filtered by removing low quality cells with (1) fewer than 200 expressed genes, (2) mitochondrial gene percentage >10%, and (3) ribosomal gene percentage <5%. The potential doublets were eliminated based on the following criteria: (1) expression of more than 4000 genes, (2) identification as doublets by DoubletFinder, and (3) detection of markers indicative of other cell types after reclustering of one specific cell type. The singlet was extracted for further analysis. The RNA expression data were then further scaled based on regressing the number of unique molecular identifiers (UMIs) detected, the percentage of mitochondrial counts per cell, and different cell cycle phases for each cell. Dimension reduction was performed using principal component analysis (PCA), and then the significant components were selected according to the p values. The top 20 main components were used to perform UMAP to visualize the cells. Clusters were identified by a shared nearest neighbors (SNN) modularity optimization-based clustering algorithm, and the clustering resolution was set to 0.75. Cellular identity was determined by finding differentially expressed genes for each cluster using Seurat's Mann–Whitney test (FindAllMarkers) implementation. Differentially expressed genes were selected with the threshold adjusted $p < 0.05$ and absolute logged fold-change (Log2FC) ≥ 0.585. The cells were first automatedly annotated by scPred using its PMBC reference, and then cell clusters were manually annotated according to scPred prediction. The B and T cells were isolated and processed separately for downstream clustering and gene analysis. The filtered contig annotation output from Cell Ranger VDJ analysis was merged using scRepertoire v1.3.5 [14] with default parameters. Shazam v1.1.0 was used to calculate the somatic hypermutation rate of heavy chain variable (*VH*) genes.

Microneutralization

Vero C1008 (Vero 76, clone E6, Vero E6) cells (ATCC-CRL-1586 cells) were cultured in 96-well cell culture plates to 80% confluence. Dilution of samples (previously inactivated) was prepared with Dulbecco's modified Eagle's medium (DMEM; Gibco, Grand Island, NY, USA) supplemented with 2% FBS and 2% penicillin–streptomycin-amphotericin B suspension (Sigma–Aldrich, St. Louis, MO, USA). Serial dilutions (1:10 to 1:5120) were prepared with virus (100 $TCID_{50}$) and incubated for 60 min at 37 °C in 5% CO_2. Later, samples (100 µL of each dilution) were incubated with Vero cells in DMEM for 72 h as previously described. Samples were considered positive when a serum dilution of at least 1:10 neutralized the 100% cytopathic effect of the virus adjusted to 100 $TCID_{50}$ [15].

ELISA

ELISA was performed as previously described [16]. Briefly, ELISA microwell plates (Thermo Fisher Scientific, Waltham, MA, USA) were coated with SARS-CoV-2 RBD using 100 nM carbonate-bicarbonate buffer. After blocking with 2% BSA (Sigma–Aldrich), serum samples were diluted 1:100 in PBS with 0.05% Tween 20 and 1% nonfat milk (American Bio) and incubated for 60 min at room temperature. After washing, anti-human IgG-HRP (Sigma–Aldrich) was incubated for 30 min, and after washing, 50 µL of TMB (Immunochemistry, Minnesota, USA) was added. The reaction was stopped with 50 µL of 1 M H_2SO_4, and the optical density (O.D.) was read at 450 nm using an automated spectrophotometer (Thermo Scientific Multiskan FC Microplate Photometer).

Statistical analysis

The chi-square test was used to compare the cell proportions and somatic hypermutation rate of *VH* genes between the two groups. The Mann–Whitney U test was used to compare the antibody response and *IGHV* gene usage between groups. The symbols indicating significance are as follows: $*p \le 0.05$, $**p \le 0.01$, $***p \le 0.001$, and $****p \le 0.0001$. Data analysis and visualization were performed using R v4.0.3.

RESULTS

Here, we assessed the single-cell transcriptomic profile of PBMCs from five groups of individuals: (1) vaccinated with AZD1222 (AZ; $n = 4$); (2) previously infected and vaccinated with AZD1222 (AZ-hb; $n = 6$); (3) vaccinated with Ad5-nCoV (Cso; $n = 6$); (4) previously infected and vaccinated with Ad5-nCoV (Cso-hb; $n = 6$); and (5) convalescent of COVID-19 without vaccination (Inf; $n = 5$) (Fig. 1a). The clinical characteristics of these individuals are outlined in Fig. 1b. The age of the patients ranged from 22 to 78 years old, with 17 females and 10 males. The duration between SARS-CoV-2 infection diagnosis and vaccine administration spanned from 4 to 14 months. All vaccinated individuals in the study adhered to the recommended vaccine regimen: receiving

a

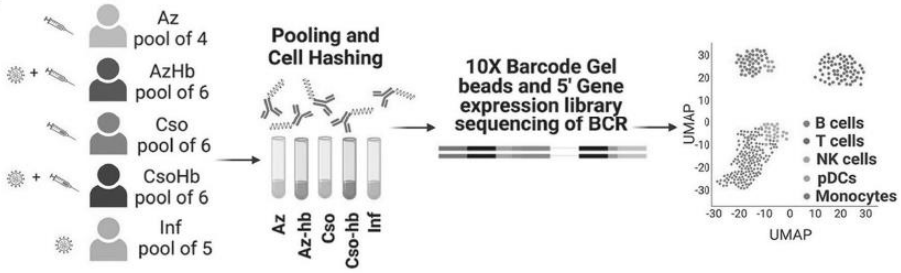

b

Table. Clinical and demografic characteristics of donors

Pool	ID	Sex	Age (Years)	Time since last vaccine (Months)	Time since COVID-19 Dx (Months)	Condition
Az	Az01	M	63	1	-	-
	Az02	F	61	1	-	-
	Az03	F	61	1	-	-
	Az04	F	65	1	-	-
Az-Hb	AzHyb01	M	61	1	12	Severe
	AzHyb02	M	79	1	13	Moderate
	AzHyb03	F	64	1	14	Severe
	AzHyb04	M	64	1	12	Mild
	AzHyb05	M	62	1	8	Moderate
	AzHyb06	F	78	1	6	Mild
Cso	Cso01	F	22	2	-	-
	Cso02	F	28	2	-	-
	Cso03	M	34	2	-	-
	Cso04	F	26	2	-	-
	Cso05	F	52	2	-	-
	Cso06	M	31	2	-	-
Cso-Hb	CsoHyb01	F	29	2	13	Mild
	CsoHyb02	F	38	2	14	Severe
	CsoHyb03	F	32	2	7	Mild
	CsoHyb04	M	49	2	6	Mild
	CsoHyb05	F	56	2	7	Mild
	CsoHyb06	F	52	2	12	Mild
Inf	Inf01	M	65	-	1	Mild
	Inf02	F	45	-	2	Moderate
	Inf03	M	40	-	1	Moderate
	Inf04	F	50	-	1	Severe
	Inf05	F	40	-	1	Severe

c

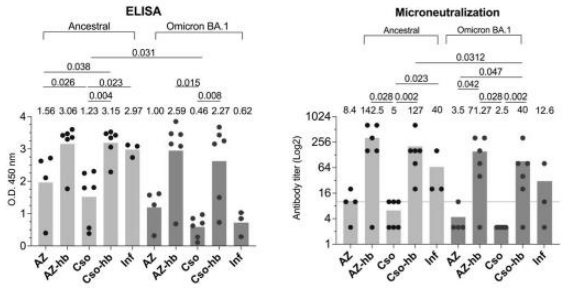

Fig. 1 Single-cell transcriptomic profile of hybrid immunity induced by Ad5-nCoV and AZD1222 vaccines. a Study design. Twenty-seven donors were enrolled in this study and divided into five groups: vaccinated with AZD1222 (AZ without prior infection and AZ-hb with prior infection), vaccinated with Ad5-nCov (Cso without prior infection and Cso-hb with prior infection), and convalescent from COVID-19 (Inf). PBMCs were collected from participants 1−2 months after the last vaccination or COVID-19 infection without vaccination and processed for scRNA-Seq experiments. **b** Clinical and demographic characteristics of donors. **c** Binding and neutralizing antibody titers against the ancestral virus of SARS-CoV-2 and Omicron BA.1 for each group. Each column represents the mean titers.

either one dose of Ad5-nCoV or two doses of AZD1222, with a 30-day interval between doses. Samples were collected one month after the second dose of AZD1222 (AZ and AZ-hb), two months after the dose of Ad5-nCoV (Cso and Cso-hb), and one to two months after infection (Inf group) (Fig. 1b). Although whole-genome sequencing of the viral samples was not conducted, SARS-CoV-2 variant surveillance data indicate that participants in this study were infected with ancestral SARS-CoV-2 (between May 2020 and January 2021) before the detection of any variants in Hermosillo, Sonora, Mexico.

Humoral immune response

Previous reports have shown that hybrid immunity induces a robust humoral immune response against SARS-CoV-2 variants [3, 17, 18]. In this study, the levels of IgG antibody and neutralizing antibody titres (nAbs) against the ancestral strain were significantly lower in the Cso group than in the Cso-hb group ($P < 0.04$) (Fig. 1c). The IgG antibody and nAb responses were also lower in the AZ group than in the AZ-hb group but the difference was significant only for the level of nAb titres against Omicron BA.1. In addition, the nAb response against Omicron BA.1 was significantly lower than the response against the ancestral strain in the Cso-hb group alone ($p = 0.0312$) (Fig. 1c). These results indicate that hybrid immunity resulting from either the AZD1222 or Ad5-nCoV vaccine was associated with a higher neutralizing antibody (nAb) response than those without previous infection, but the immune response against Omicron BA.1 was lower for the Ad5-nCoV vaccine (Cso-hb) than for the AZD1222 vaccine (Az-hb).

ScRNAseq analysis

We performed scRNAseq and scBCRseq on pooled PBMCs from each group (AZ, AZ-hb, Cso, Cso-hb, or Inf) using 10x Genomics technology. After library sequencing and data processing, we obtained a total of 8188 single cells with good quality. The RNA expression data were further scaled based on regressing the number of unique molecular identifiers (UMIs) detected and performing a uniform manifold approximation and projection (UMAP) in the five groups to visualize B cell, T cell, natural killer (NK) cell, monocyte, and plasmacytoid dendritic cell (pDC) clusters (Fig. 2a). The UMAP of individual cell types revealed a differential proportion of cells according to the group (Fig. 2b). We observed that the most abundant immune cells were T cells (median: 55.7%), followed by monocytes (median: 17.8%) and B cells (median: 15.4%). The Cso-hb group was characterized by a higher percentage ($P < 0.0001$) of B cells (36.8% vs. other groups: 13.3% −15.4%) and a lower abundance ($P < 0.0001$) of T cells compared to other groups including Cso (36.6% vs. other groups: 53.6% −58.1%) (Supplementary Fig. S1a–c). The other cells showed no difference among groups, and reclustering was subsequently performed within T- and B-cell types.

Profile of B cells

According to the transcriptional profile, four B-cell subclusters were identified: two clusters of naïve B cells ($IgM^+IgD^+CD27^-$), Bnaïve-1 and Bnaïve-2; one cluster of memory B cells ($IgD^-TNFRSF13B^+$, class-switched) and one cluster of plasmablasts ($CD9^+$) (Fig. 2a, c and Supplementary Fig. S2). A higher proportion of Bnaïve-1 cells, characterized by upregulation of the differentially expressed genes (DEGs) *JUN*, *FOS*, *CD83*, *CD69*, *NFKBIA*, and *CXCR4*, was found in the AZ, AZ-hb, and Cso groups ($p < 0.0001$) (Fig. 2c, d, and Supplementary Fig. 2b). In contrast, a higher proportion of Bnaïve-2 cells was found in the Cso-hb and Inf groups ($p < 0.01$) (Fig. 2e–g). Memory B cells were predominant in the Cso and Cso-hb groups (Cso and Cso-hb vs. Inf, $p < 0.05$; Cso-hb vs. AZ-hb ($p < 0.01$)) (Fig. 2e, g). Thus, Cso and Cso-hb induced the highest proportion of memory B cells, while AZ and AZ-hb induced the highest proportion of activated naïve B cells (Bnaïve-1). Furthermore, vaccination and hybrid immunity induced a higher proportion of Bnaïve and memory B cells than the Inf group. The samples were collected 1 month after infection, which may explain the lower proportion of memory B cells in the Inf group [19, 20].

The paired scBCRseq data showed that the hybrid groups had more class-switched memory B cells than the vaccinated-only groups, without preferences for a specific isotype other than *IGHA1*, which was more frequent in the AZ-hb group than in the Cso-hb group (Fig. 3a, b). The somatic hypermutation (SHM) rate of *IGHV* in switched or unswitched memory B cells was similar among the various groups ($p > 0.05$) (Fig. 3c). Furthermore, *IGHV3-33* gene usage was significantly increased in the Cso ($p = 0.018$) and Cso-hb ($p = 0.028$) groups compared to the Inf group, and *IGHV3-23* was higher ($p = 0.027$) in the Cso group than in the Cso-hb group, while IGHV1-18 was higher ($p = 0.04$) in AZ-hb group than AZ group (Fig. 3d). Although we did not sort antigen-specific B cells, we observed that memory B cells from the infected and hybrid groups highly expressed *IGHV4-39.J4*, *IGHV3-33.J4*, *IGHV3-74.J4*, and *IGHV3-23.J4*, as observed in other studies that sorted SARS-CoV-2 antigen-labeled B cells from infected individuals (Fig. 3e) [21]. Clonal BCR sequences were not detected, and therefore, the analysis of clonal diversity and abundance was not performed. Taken together, the differences in *IGHV* gene expression and the increased class switching in the hybrid groups suggest that certain clones were preferentially increased to enhance immunity upon a second encounter with the spike antigen.

Profile of T cells

We identified 17 distinct subclusters of T cells, including nine clusters of $CD4^+$ T cells and seven clusters of $CD8^+$ T cells (Fig. 4a, b). The $CD4^+$ T-cell clusters included five clusters of naïve cells (CD4.Tn-1 to CD4.Tn-5), three clusters of memory cells (CD4.Tm-1 to CD4.Tm-3 cells), and one cluster of regulatory T cells (expressing *IL2R*, *FOXP3*, *TIGIT*, and *CTLA4*) (Fig. 4c–e). The $CD8^+$ T-cell clusters included five clusters of CD8 cytotoxic effector T cells (CD8.Te-1 to CD8.Te-5) with different expression levels of cytotoxicity-associated genes and exhaustion-related genes, one naïve cluster (CD8.Tn cells expressing *CCR7*, *SELL*, *LEF1*, and *TCF7*) and one cluster expressing Tc17 markers (*RORC* and *KLRB1*) (Fig. 4c, i). The last cluster identified was γδ T cells ($CD3^+$ $CD4^-CD8^-$). The CD4/CD8 T-cell ratio was higher in AZ- and Cso-vaccinated individuals than in the respective hybrid groups (AZ-hb and Cso-hb) ($p < 0.0001$), suggesting that hybrid immunity induced a higher proportion of $CD8^+$ T cells (Fig. 4e).

The dominant $CD4^+$ T-cell subsets varied among the vaccination and hybrid groups (Fig. 4f, i, j and Supplementary Fig. 3). The CD4.Treg subset was found in similar proportions among all groups. The Inf group had a high proportion of CD4.Tm-1 memory T cells expressing high levels of *LTB* and *IL7R*, which are associated with the lymph node development pathway, as well as CD4.Tn-1 naïve T cells highly expressing genes involved in the "T-cell activation", "T-cell mediated immunity", and "positive regulation by host of viral transcription" pathways (Fig. 4f, i and Supplementary Fig. 3). In addition, the AZ group had a high proportion of CD4.Tm-2 cells highly expressing *LTB* and *IL7R*, which are involved in the "lymph node development" pathway, and CD4.Tn-4 cells highly expressing the ribosomal gene *RPS4Y1* and the mitochondrial gene *MTRNR2L8*. Cso and AZ-hb led to the expansion of CD4.Tn-2, which exhibited highest expression of activation genes (*JUN* and *FOS*). The Cso-hb group had a high proportion of CD4.Tn-5 cells expressing DEGs associated with the "T-cell activation" and "IL-12 production" pathways. Thus, specific imprints of CD4.Tn-1 and CD4.Tm-1 subsets in the Inf group and CD4.Tm-2 and CD4.Tn-4 subsets in the AZ group were observed, while the CD4.Tn-5 subset, expressing DEGs associated with the IL-12 production pathway, was dominant in the Cso-hb group.

The dominant CD8-positive subsets also differed among the groups. Vaccination (AZD1222 or Ad5-nCoV) or natural infection

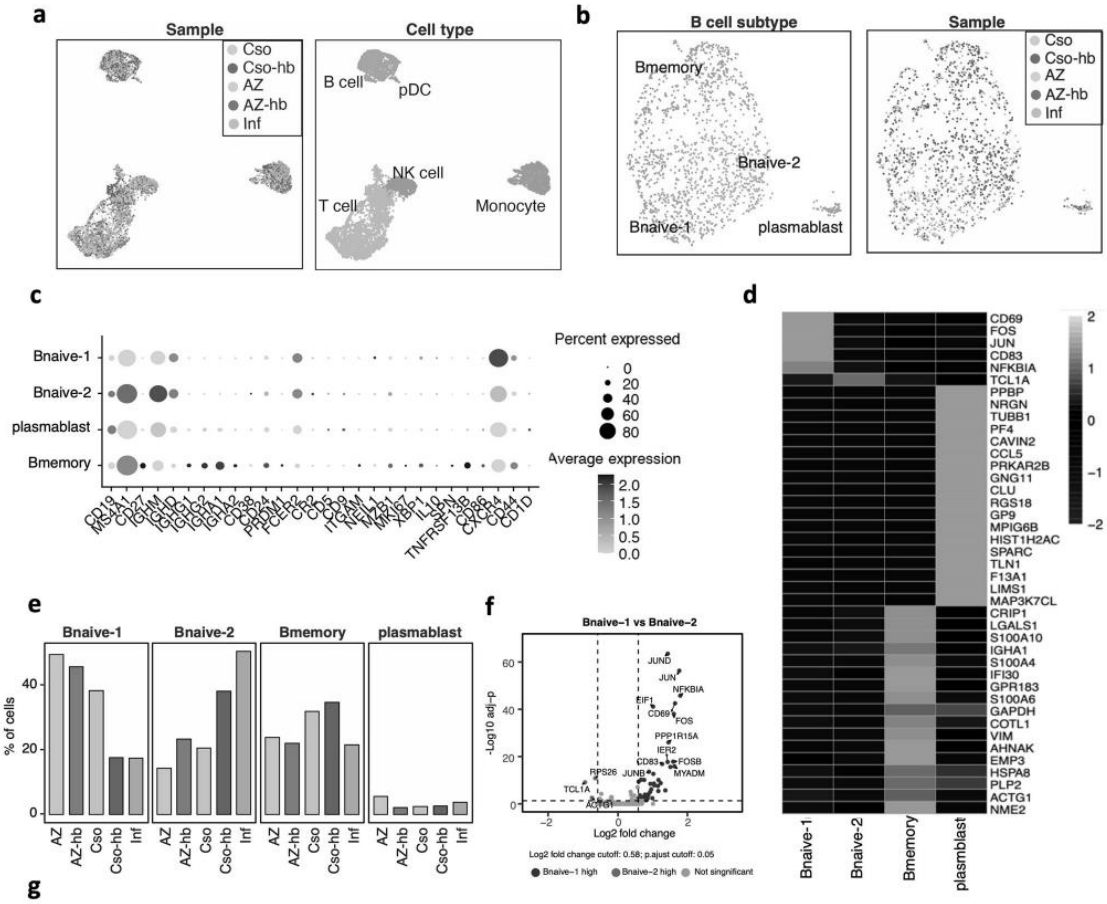

g

Cell_type	AZ vs AZ-hb	AZ vs Cso	AZ vs Inf	AZ-hb vs Cso-hb	AZ-hb vs Inf	Cso vs Cso-hb	Cso vs Inf	Cso-hb vs Inf
Bmemory	ns	ns	ns	***	ns	ns	**	****
Bnaive-1	ns	*	****	****	****	****	****	ns
Bnaive-2	*	ns	****	****	****	****	****	***
plasmablast	ns	ns	ns	ns	ns	ns	ns	ns

Fig. 2 Characterization of B cell response induced by vaccines (Ad5-nCoV and AZD1222) and hybrid immunity. a UMAP of all single cells, with each cell coloured for sample group, and major cell type. **b** UMAP of B cells, with each cell coloured for B cell subtype and group. **c** Mean expression of marker genes for B cell subsets. **d** Differentially Expressed Genes (DEGs) for each B cell subset. **e** Fraction of cells from different samples in each B cell subtype. **f** Volcano plot to identify the DEGs between the two naïve and plasma cell subsets. **g** Comparison of the proportion of B cell subsets between groups using Chi-square test. ns $p > 0.05$, *$p \le 0.05$, **$p \le 0.01$, ***$p \le 0.001$, and ****$p \le 0.0001$.

activated $CD8^+$ T-cell subsets expressing DEGs enriched in the cytolysis pathway (Fig. 4g–j and Supplementary Fig. 3). The proportion of cytotoxic CD8.Tc17 cells were higher in the Cso group. Most importantly, the Cso-hb hybrid immunity group predominantly exhibited CD8.Te-4 cells with elevated expression of interferon gamma (IFN-γ) genes and more than 78 DEGs enriched in pathways related to the response to type I IFN or IFN-γ signaling. Furthermore, the proportion of γδ T cells was higher in the AZ-hb group (Fig. 4h). These results suggest a differential expansion of clusters of $CD8^+$ T cells in response to vaccination and infection, with hybrid immunity-inducing T-cell subsets (CD8.Te-4 or γδ T cells) with potentially stronger antiviral properties.

DISCUSSION

This study employs single-cell transcriptomic analysis and antibody quantification to assess the immunity triggered by Ad5-nCoV and AZD1222 vaccines. Our findings reveal a diminished IgG antibody response to both the SARS-CoV-2 RBD of the ancestral virus and Omicron BA.1 in the Cso group compared to the AZ group. Nonetheless, the antibody response was substantially augmented in the hybrid groups (Cso-hb and AZ-hb) against both the ancestral and the Omicron variant. Omicron BA.1 was a variant of concern due to its high transmissibility and ability to evade the immune response, even in previously vaccinated individuals, which helped corroborate the robust humoral response generated in the hybrid groups, particularly in Az-hb. This underscores the capability of these adenoviral vaccines to provoke robust hybrid immunity. It is noteworthy, however, that the antibody response in the Cso-hb group was 1-log lower than that observed in the AZ-hb group.

The transcriptomic profile of B cells revealed that the principal subset in all the groups consisted of naïve B cells. The AZ and AZ-hb groups exhibited a high frequency of naïve B cells

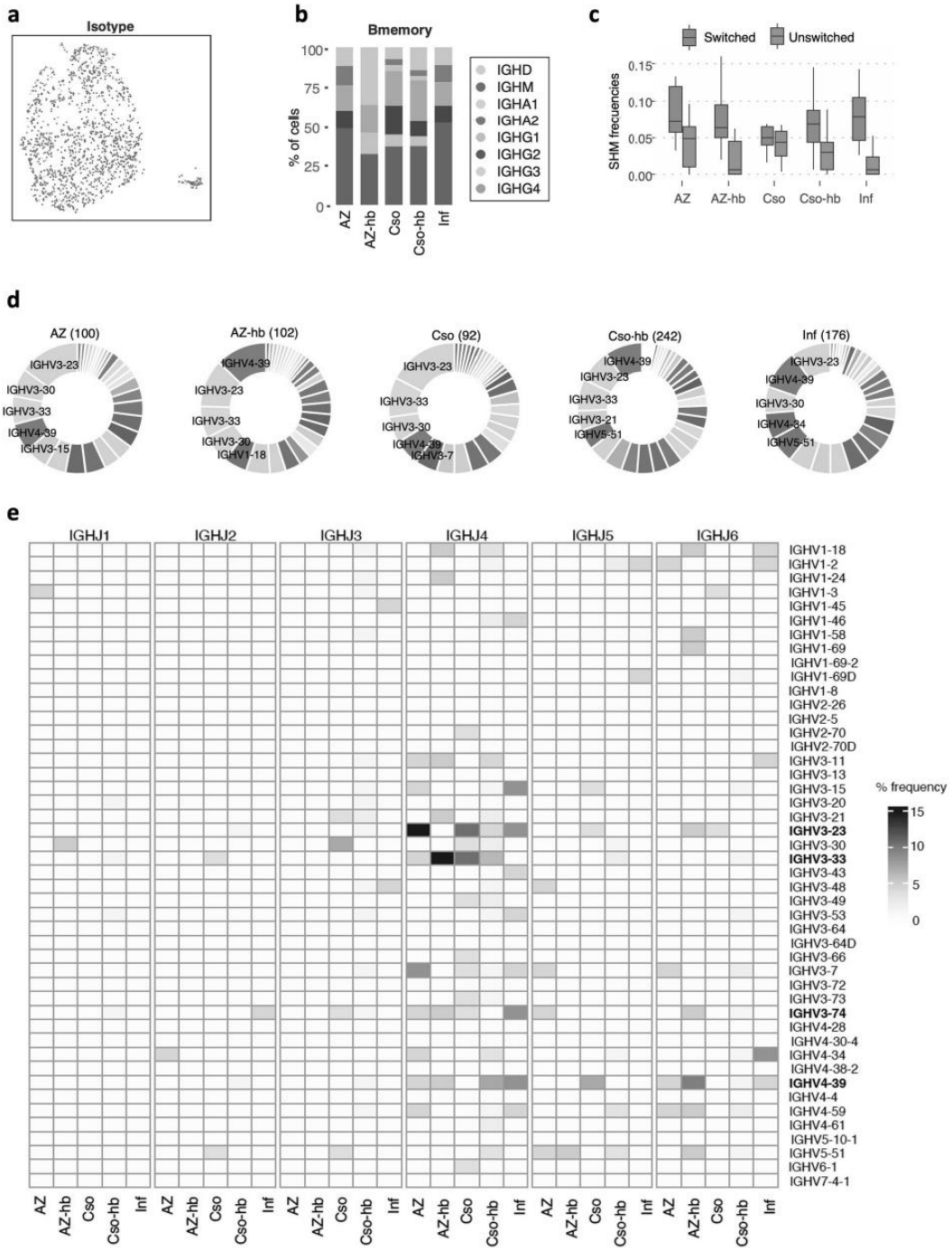

Fig. 3 BCR repertoire induced by vaccines (Ad5-nCoV and AZD1222) and hybrid immunity. a UMAP of B cells with each cell coloured for isotype. **b** Relative frequencies of scVDJ-derived antibody subclass in memory B cells of different immunization groups. **c** Somatic hypermutation (SHM) frequency in switched and unswitched memory B cells for each group. No statistical differences were observed between groups using Chi-square. **d** Top 5 *IGHV* genes of all identified B cell subsets in each group. **e** Frequencies of *IGHV/IGHJ* gene combination usage.

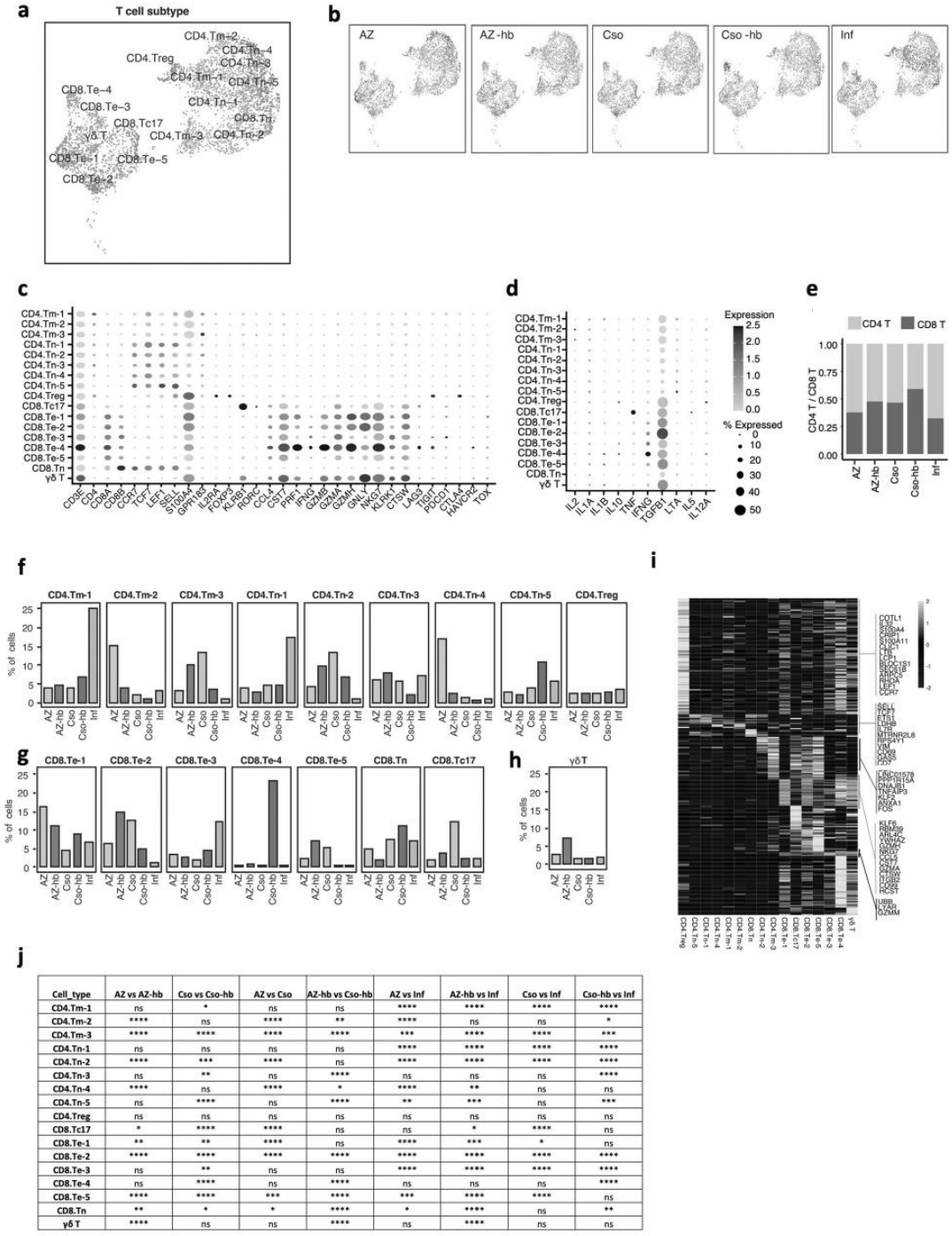

Cell_type	AZ vs AZ-hb	Cso vs Cso-hb	AZ vs Cso	AZ-hb vs Cso-hb	AZ vs Inf	AZ-hb vs Inf	Cso vs Inf	Cso-hb vs Inf
CD4.Tm-1	ns	*	ns	ns	****	****	****	****
CD4.Tm-2	****	ns	****	**	****	ns	ns	*
CD4.Tm-3	****	****	****	****	***	****	****	***
CD4.Tn-1	ns	ns	ns	ns	****	****	****	****
CD4.Tn-2	****	***	****	ns	****	****	****	****
CD4.Tn-3	ns	**	ns	****	ns	ns	ns	****
CD4.Tn-4	****	ns	****	*	****	**	ns	ns
CD4.Tn-5	ns	****	ns	****	**	***	ns	***
CD4.Treg	ns	ns	ns	ns	ns	ns	ns	ns
CD8.Tc17	*	****	****	ns	ns	*	****	ns
CD8.Te-1	**	**	****	ns	****	***	*	ns
CD8.Te-2	****	****	****	****	****	****	****	****
CD8.Te-3	ns	**	ns	ns	****	****	****	****
CD8.Te-4	ns	****	ns	****	ns	ns	ns	****
CD8.Te-5	****	****	***	****	***	****	****	ns
CD8.Tn	**	*	*	****	*	****	ns	**
γδ T	****	ns	ns	****	ns	****	ns	ns

Fig. 4 Characterization of T cell response induced by vaccines (Ad5-nCoV and AZD1222) and hybrid immunity. a UMAP of T cells with each cell coloured for T cell subtypes. **b** UMAP of T cells per group. **c** Mean expression of marker genes for T cell subsets. Seventeen T cell subsets were manually annotated based on the gene markers expression of the T cell types. **d** Mean expression of cytokine-related genes for T cell subsets. **e** Ratio of CD4/CD8 T cells for each group. Distribution and percentage of $CD4^+$ (**f**), $CD8^+$ (**g**), and γδ (**h**) T-cell subsets on total cells for each group. **i** Differentially expressed genes of each T cell subset. Only the top 5 genes are labeled. **j** Comparison of the proportion of T cell subsets between groups using Chi-square test. ns $p > 0.05$, *$p \le 0.05$, **$p \le 0.01$, ***$p \le 0.001$, and ****$p \le 0.0001$.

expressing high levels of *CXCR4* (Bnaïve-1). In contrast, within the Cso-hb and Inf groups, the Bnaïve-2 cluster predominated, characterized by a lower expression of *CXCR4*. This observation suggests that AZ and AZ-hb induce the production of naïve B cells with an enhanced migratory capability to secondary lymphoid tissues [22]. Furthermore, Cso and Cso-hb groups demonstrated a higher proportion of memory B cells than the Inf group. However, the variation in sample collection times could potentially account for these disparities, as the groups vaccinated with Ad5-nCoV were sampled two months after immunization. In contrast, the AZD1222 groups (AZ and AZ-hb) were sampled one month after receiving the booster dose.

The analysis of the usage of *IGHV* genes showed an overrepresentation of the *IGHV3* family in all groups using the vaccine (*IGHV3-23*, *IGHV3-30*, *IGHV3-33*), as observed in other studies, where *IGHV3-23* has been reported as a commonly used germline both in COVID-19 and healthy donors [21, 23]. Interestingly, Cso-hb and the Inf group shared a similar *IGHV* gene usage profile, especially by the expression of *IGHV5-51* and *IGHV3-11*. The *IGHV5-51* gene is associated with cross-reactive neutralizing antibodies [24, 25], suggesting that hybrid immunity elicited by Ad5-nCoV (Cso-hb) can produce neutralizing antibodies with a wider breadth compared to Cso vaccination only. Although our experimental design did not include the sorted antigen-specific B cells, *IGHV/IGHJ* combinations were similar to other studies evaluating SARS-CoV-2 antigen-labeled B cells from infected individuals [21]. For example, *IGHV3-23/IGHJ4*, which has been linked to SARS-CoV-2 and likely responds to the spike protein rather than other viral proteins [26], constituted the predominantly used *IGHV/IGHJ* combinations in our cohort. These results could suggest a high frequency SARS-CoV-2-specific B cells on recently vaccinated and infected individuals. It is noteworthy that when comparing Ad5-nCoV and AZD1222 vaccines, even in cases where similar *IGHV/IGHJ* combination frequencies were observed, the Ad5-nCoV vaccine elicits a diminished antibody response compared to AZD1222. This observation implies the involvement of other factors in explaining these discrepancies.

The transcriptional analysis of $CD4^+$ and $CD8^+$ T cells revealed a diverse response elicited by vaccination, hybrid immunity, or natural infection. Multiple memory and naïve T cell subsets exhibited expansion, including a shared population of memory $CD4^+$ T cells found in both the AZ-hb and Cso groups (CD4.Tm-3). In contrast, the Inf and AZ groups gave rise to distinct subpopulations (CD4.Tm-1 and CD4.Tm-2, respectively). CD4.Tm-3 represented a distinctive population, displaying a distinct gene expression profile in comparison to other memory $CD4^+$ T cells. *ANX1* and *FOS*, markers of robust activation, expressed in CD4.Tm-3 cells, along with upregulation of the IL-2 signaling pathway, are crucial for long-term memory T cells [27]. Conversely, CD4.Tm-2 exhibited signaling pathways associated with apoptosis. These findings imply that Cso and AZ-hb can foster a long-lasting population of memory CD4 T cells (CD4.Tm-3) compared to the AZ group (CD4.Tm-2). A similar trend emerged within naïve $CD4^+$ T cells, as Cso and AZ-hb expanded the same subset (CD4.Tn-2), distinct from the infection group (CD4.Tn-1) and AZ (CD4.Tn-4). In contrast, the subset observed in the Inf group (CD4. Tn-1) exhibited a signaling pathway linked to SARS-CoV-2 and coronavirus responses. Our data indicate that a single dose of Ad5-nCoV proved sufficient to induce a robust activation of $CD4^+$ T cells (both naïve and memory), resembling the hybrid response observed in the AZ-hb group.

In the case of effector $CD8^+$ T cells, a similar pattern was observed between the Cso and AZ-hb groups, indicated by a shared expansion of CD8.Te-2. This finding reinforces a comparable cellular response between these two groups, aligning with the observations made in the $CD4^+$ T-cell subsets. Notably, the Cso group exhibited a substantial proportion of Tc17 cells displaying moderate expression of effector genes (*GZMA* and *CST7*) and elevated expression of *TNF*. While these cells are predominantly known for their defence against bacteria and fungi, multiple studies have highlighted the role of effector cytotoxic Tc17 cells in antiviral immunity and inflammation [28, 29], including in COVID-19 patients with mild symptoms [30]. The stimulation of this particular subset in the Cso group could be attributed to the utilization of human adenoviral vector type 5 in the Ad5-nCoV vaccine. However, the role of Tc17 cells with heightened *TNF* expression warrants further investigation, as this phenomenon has not been reported with other COVID-19 vaccines.

Another intriguing observation pertained to the robust activation of CD8.Te-4 cells within the Cso-hb group. This subset of $CD8^+$ T cells displayed a cytotoxic profile, expressing *GZMB* and *GZMH* alongside significant expression of the IFN-γ gene (*IFNG*), crucial for viral infection clearance. Moreover, CD8.Te-4 exhibited elevated expression of inhibitory receptor genes such as PD-1 (*PDCD1*) and *LAG-3*, which are associated with T-cell exhaustion. Thus, the vigorous activation of CD8.Te-4 cells through the Ad5-nCoV vaccine led to the expression of exhaustion-related genes, potentially serving as a balancing mechanism to maintain immune system homeostasis and prevent immunopathology linked to these cells. These results parallel a separate study wherein $CD8^+$ T cells displayed a balanced phenotype, expressing proinflammatory genes (*TNF*, *IFNG*) and exhaustion genes (*TIGIT*, *PDCD1*) after Ad5-nCoV vaccine immunization [10]. In conclusion, our findings illustrate that both vaccines effectively stimulate the cellular immune response, yet the Ad5-nCoV vaccine induces a more robust $CD8^+$ T-cell response during hybrid immunity.

The average age of individuals vaccinated with AZD1222 differed from those receiving the Ad5-nCoV vaccine; this age difference may partly account for the observed differences in outcomes between the AZD1222 and Ad5-nCoV groups. These groups were selected based on the initial strategy of the vaccination campaigns in Mexico, where vaccines were administered according to age. Individuals aged 60 and older received the AZD1222 vaccine, while those under that age received the Ad5-nCoV vaccine. Nevertheless, it was observed that older individuals, vaccinated with AZD1222 vaccine, also developed strong hybrid immunity and a robust antibody response.

One limitation of this study is the variability in the time elapsed between SARS-CoV-2 infection diagnosis and vaccine administration, which differed across groups (ranging from 4 to 14 months), along with variations in the severity of COVID-19 infections and participant ages. These distinctions could influence the immune response. Furthermore, there were no pre-immunization or healthy people's data as a control for comparison. Also, pooling the samples limited the analysis and comparisons among the 5 different groups, preventing the correct assessment of intragroup variability that may arise from individual responses. Moreover, the relatively small number of B cells obtained from the bioinformatic analysis posed a constraint. Although the changes observed in the BCR of memory B cells are likely a response to SARS-CoV-2, using sorted SARS-CoV-2 antigen-labeled B cells along with more sampling time points may provide a better reflection of the immune response to SARS-CoV-2 vaccination and infection. Similarly, the distinct T cell subsets induced by AZD1222 and Ad5-nCoV vaccines might be a result of the T cell responses to the adenovirus vectors employed in these vaccines. Additionally, due to the limited number of cells, comprehensive analysis of other cell populations, such as NK cells, monocytes, and pDCs, proved challenging.

In summary, our study demonstrates that despite sharing a backbone, an adenovirus vector-based approach, two vaccines

can differentially induce hybrid immunity. Our results reveal that a single dose of the Ad5-nCoV regimen generates robust hybrid immunity and triggers a more pronounced cellular response than AZD1222. However, even among COVID-19-naïve subjects, AZD1222 elicits a more robust antibody response. The findings presented herein provide a high-resolution transcriptomic profile of both cellular and humoral immunity in response to AZD1222 and Ad5-nCoV vaccines, hybrid responses, and natural infections. This comprehensive understanding enhances our knowledge of the protective immune responses elicited by hybrid immunity and adenovirus-based COVID-19 vaccines.

DATA AVAILABILITY

The data supporting the findings of this study are available within the article and its Supplementary information files (Table Source data). The single-cell RNA-seq data and BCR-seq data can be accessed in Zenodo (https://doi.org/10.5281/zenodo.7904759).

CODE AVAILABILITY

The codes used to generate the results in the manuscript are available at: https://github.com/wanhui5867/adenovirus_C19_vaccines.

REFERENCES

1. Baden LR, El Sahly HM, Essink B, Kotloff K, Frey S, Novak R, et al. Efficacy and safety of the mRNA-1273 SARS-CoV-2 Vaccine. N Engl J Med. 2021;384:403–16.
2. Widge AT, Rouphael NG, Jackson LA, Anderson EJ, Roberts PC, Makhene M, et al. Durability of responses after SARS-CoV-2 mRNA-1273 vaccination. N Engl J Med. 2021;384:80–2.
3. Andreano E, Paciello I, Piccini G, Manganaro N, Pileri P, Hyseni I, et al. Hybrid immunity improves B cells and antibodies against SARS-CoV-2 variants. Nature. 2021;600:530–5.
4. Chen Y, Tong P, Whiteman N, Moghaddam AS, Zarghami M, Zuiani A, et al. Immune recall improves antibody durability and breadth to SARS-CoV-2 variants. Sci Immunol. 2022;7:eabp8328.
5. Stamatatos L, Czartoski J, Wan YH, Homad LJ, Rubin V, Glantz H, et al. mRNA vaccination boosts cross-variant neutralizing antibodies elicited by SARS-CoV-2 infection. Science. 2021;372:1413–8.
6. Reynolds CJ, Pade C, Gibbons JM, Butler DK, Otter AD, Menacho K, et al. Prior SARS-CoV-2 infection rescues B and T cell responses to variants after first vaccine dose. Science. 2021;372:1418–23.
7. Wratil PR, Stern M, Priller A, Willmann A, Almanzar G, Vogel E, et al. Three exposures to the spike protein of SARS-CoV-2 by either infection or vaccination elicit superior neutralizing immunity to all variants of concern. Nat Med. 2022;28:496–503.
8. Gelanew T, Mulu A, Abebe M, Bates TA, Wassie L, Tefer M, et al. A single dose ChAdOx1 nCoV-19 vaccine elicits high antibody responses in individuals with prior SARS-CoV-2 infection comparable to that of double dose vaccinated SARS-CoV-2 infection naive individuals. Vaccines. 2022;10:859.
9. Guzman-Lopez S, Darwich-Salazar A, Bocanegra-Ibarias P, Salas-Trevino D, Flores-Trevino S, Perez-Alba E, et al. Clinical and immunologic efficacy of the recombinant adenovirus Type-5-Vectored (CanSino Bio) vaccine in university professors during the COVID-19 delta wave. Vaccines. 2022;10:656.
10. Cao Q, Wu S, Xiao C, Chen S, Chi X, Cui X, et al. Integrated single-cell analysis revealed immune dynamics during Ad5-nCoV immunization. Cell Discov. 2021;7:64.
11. Xiaojie S, Yu L, Lei Y, Guang Y, Min Q. Neutralizing antibodies targeting SARS-CoV-2 spike protein. Stem Cell Res. 2020;50:102125.
12. Fagiani F, Catanzaro M, Lanni C. Molecular features of IGHV3-53-encoded antibodies elicited by SARS-CoV-2. Signal Transduct Target Ther. 2020;5:170.
13. Hao Y, Hao S, Andersen-Nissen E, Mauck WM 3rd, Zheng S, Butler A, et al. Integrated analysis of multimodal single-cell data. Cell. 2021;184:3573–87.e29.
14. Borcherding N, Bormann NL, Kraus G. scRepertoire: an R-based toolkit for single-cell immune receptor analysis. F1000Res. 2020;9:47.
15. Bewley KR, Coombes NS, Gagnon L, McInroy L, Baker N, Shaik I, et al. Quantification of SARS-CoV-2 neutralizing antibody by wild-type plaque reduction neutralization, microneutralization and pseudotyped virus neutralization assays. Nat Protoc. 2021;16:3114–40.
16. Melgoza-Gonzalez EA, Hinojosa-Trujillo D, Resendiz-Sandoval M, Mata-Haro V, Hernandez-Valenzuela S, Garcia-Vega M, et al. Analysis of IgG, IgA and IgM antibodies against SARS-CoV-2 spike protein S1 in convalescent and vaccinated patients with the Pfizer-BioNTech and CanSinoBio vaccines. Transbound Emerg Dis. 2022;69:e734–45.
17. Bates TA, McBride SK, Leier HC, Guzman G, Lyski ZL, Schoen D, et al. Vaccination before or after SARS-CoV-2 infection leads to robust humoral response and antibodies that effectively neutralize variants. Sci Immunol. 2022;7:eabn8014.
18. Hernández J, Dehesa-Canseco F, Vázquez-López AB, Reséndiz-Sandoval M, Caire-Juvera G, Solís-Hernández M, et al. Neutralization of Omicron BA.1, BA.5.1.6, BQ.1.3 and XBB1.1 induced by heterologous vaccination Ad5-nCoV and mRNA-1273. Signal Transduct Target Ther. 2023;8:174.
19. Sherina N, Piralla A, Du L, Wan H, Kumagai-Braesch M, Andréll J, et al. Persistence of SARS-CoV-2-specific B and T cell responses in convalescent COVID-19 patients 6-8 months after the infection. Med. 2021;2:281–95.e4.
20. Marcotte H, Piralla A, Zuo F, Du L, Cassaniti I, Wan H, et al. Immunity to SARS-CoV-2 up to 15 months after infection. iScience. 2022;25:103743.
21. He B, Liu S, Wang Y, Xu M, Cai W, Liu J, et al. Rapid isolation and immune profiling of SARS-CoV-2 specific memory B cell in convalescent COVID-19 patients via LIBRA-seq. Signal Transduct Target Ther. 2021;6:195.
22. Nie Y, Waite J, Brewer F, Sunshine MJ, Littman DR, Zou YR. The role of CXCR4 in maintaining peripheral B cell compartments and humoral immunity. J Exp Med. 2004;200:1145–56.
23. Xiang H, Zhao Y, Li X, Liu P, Wang L, Wang M, et al. Landscapes and dynamic diversifications of B-cell receptor repertoires in COVID-19 patients. Hum Immunol. 2022;83:119–29.
24. Yuan M, Wu NC, Zhu X, Lee CD, So RTY, Lv H, et al. A highly conserved cryptic epitope in the receptor binding domains of SARS-CoV-2 and SARS-CoV. Science. 2020;368:630–3.
25. Liu H, Yuan M, Huang D, Bangaru S, Zhao F, Lee CD, et al. A combination of cross-neutralizing antibodies synergizes to prevent SARS-CoV-2 and SARS-CoV pseudovirus infection. Cell Host Microbe. 2021;29:806–18.e6.
26. Wen W, Su W, Tang H, Le W, Zhang X, Zheng Y, et al. Immune cell profiling of COVID-19 patients in the recovery stage by single-cell sequencing. Cell Discov. 2020;6:31.
27. Kalia V, Sarkar S. Regulation of effector and memory CD8 T cell differentiation by IL-2-A balancing act. Front Immunol. 2018;9:2987.
28. Yeh N, Glosson NL, Wang N, Guindon L, McKinley C, Hamada H, et al. Tc17 cells are capable of mediating immunity to vaccinia virus by acquisition of a cytotoxic phenotype. J Immunol. 2010;185:2089–98.
29. Hamada H, de la Luz Garcia-Hernandez M, Reome JB, Misra SK, Strutt TM, McKinstry KK, et al. Tc17, a unique subset of CD8 T cells that can protect against lethal influenza challenge. J Immunol. 2009;182:3469–81.
30. Notarbartolo S, Ranzani V, Bandera A, Gruarin P, Bevilacqua V, Putignano AR, et al. Integrated longitudinal immunophenotypic, transcriptional and repertoire analyses delineate immune responses in COVID-19 patients. Sci Immunol. 2021;6:eabg5021.

ACKNOWLEDGEMENTS

This research was funded by Consejo Nacional de Ciencia y Tecnología (CONACyT), grant number 312677 (JH), the Swedish Research Council (2019-01302, 2020-06116, QPH), and the European Union's Horizon 2020 research and innovation program (ATAC, grant number 101003650, QPH). The authors thank Roberto Carvente and Analitek for technical support during the single-cell experiments and the SENASICA and WHO Collaborating Centre on Antimicrobial Resistance in Foodborne and Environmental Bacteria (MEX-33), especially Mayrén Zamora Nava and Fabiola Hernández Pérez, for helping us to sequence our libraries.

AUTHOR CONTRIBUTIONS

Conceptualization, JH; methodology, MGV, HW, MRS, DHT, OV, VMH, FDC, MSH; formal analysis, MGV, HW; investigation, MGV, HW; resources, MSH, QPH, JH; writing—original draft preparation, MGV and HW, and JH; writing—review and editing; HM, QPH, JH; funding acquisition, QPH, JH. All authors have read and agreed to the published version of the manuscript.

FUNDING

This work was supported by CONACyT (grant number 312677, JH), the Swedish Research Council (grants 2019-01302 and 2020-06116, QPH), and the European Union's Horizon 2020 research and innovation program through the ATAC project under grant number 101003650 (QPH).

COMPETING INTERESTS

The authors declare no competing interests.

ADDITIONAL INFORMATION

Supplementary information The online version contains supplementary material available at https://doi.org/10.1038/s41435-024-00270-x.

Correspondence and requests for materials should be addressed to Qiang Pan-Hammarström or Jesús. Hernández.

SPRINGER NATURE LICENSE
TERMS AND CONDITIONS

Jun 05, 2024

This Agreement between Centro de Investigación en Alimentación y Desarrollo -- Melissa García-Vega ("You") and Springer Nature ("Springer Nature") consists of your license details and the terms and conditions provided by Springer Nature and Copyright Clearance Center.

License Number	5802340961739
License date	Jun 05, 2024
Licensed Content Publisher	Springer Nature
Licensed Content Publication	Genes & Immunity
Licensed Content Title	Comparative single-cell transcriptomic profile of hybrid immunity induced by adenovirus vector-based COVID-19 vaccines
Licensed Content Author	Melissa García-Vega et al
Licensed Content Date	Apr 3, 2024
Type of Use	Thesis/Dissertation
Requestor type	academic/university or research institute
Format	print and electronic
Portion	full article/chapter
Will you be translating?	no

Circulation/distribution	1 - 29
Author of this Springer Nature content	yes
Title of new work	PRODUCCIÓN Y CARACTERIZACIÓN DE ANTICUERPOS CONTRA SARS-COV-2 Y ANÁLISIS DE EXPRESIÓN DIFERENCIAL A PARTIR DE LINFOCITOS B DE MEMORIA PERSONAS CONVALECIENTES DE COVID-19
Institution name	Centro de Investigación en Alimentación y Desarrollo A.C. (CIAD)
Expected presentation date	Aug 2024
Requestor Location	Centro de Investigación en Alimentación y Desarrollo Carretera Gustavo Enrique Astiazarán #46 Hermosillo, Sonora 83304 Mexico Attn: Centro de Investigación en Alimentación y Desarrollo
Total	0.00 USD

Terms and Conditions

Springer Nature Customer Service Centre GmbH Terms and Conditions

The following terms and conditions ("Terms and Conditions") together with the terms specified in your [RightsLink] constitute the License ("License") between you as Licensee and Springer Nature Customer Service Centre GmbH as Licensor. By clicking 'accept' and completing the transaction for your use of the material ("Licensed Material"), you confirm your acceptance of and obligation to be bound by these Terms and Conditions.

1. Grant and Scope of License

1. 1. The Licensor grants you a personal, non-exclusive, non-transferable, non-sublicensable, revocable, world-wide License to reproduce, distribute, communicate to the public, make available, broadcast, electronically transmit or create derivative works using the Licensed Material for the purpose(s) specified in your RightsLink Licence Details only. Licenses are granted for the specific use requested in the order and for no other use, subject to these Terms and Conditions. You acknowledge and

agree that the rights granted to you under this License do not include the right to modify, edit, translate, include in collective works, or create derivative works of the Licensed Material in whole or in part unless expressly stated in your RightsLink Licence Details. You may use the Licensed Material only as permitted under this Agreement and will not reproduce, distribute, display, perform, or otherwise use or exploit any Licensed Material in any way, in whole or in part, except as expressly permitted by this License.

1. 2. You may only use the Licensed Content in the manner and to the extent permitted by these Terms and Conditions, by your RightsLink Licence Details and by any applicable laws.

1. 3. A separate license may be required for any additional use of the Licensed Material, e.g. where a license has been purchased for print use only, separate permission must be obtained for electronic re-use. Similarly, a License is only valid in the language selected and does not apply for editions in other languages unless additional translation rights have been granted separately in the License.

1. 4. Any content within the Licensed Material that is owned by third parties is expressly excluded from the License.

1. 5. Rights for additional reuses such as custom editions, computer/mobile applications, film or TV reuses and/or any other derivative rights requests require additional permission and may be subject to an additional fee. Please apply to journalpermissions@springernature.com or bookpermissions@springernature.com for these rights.

2. Reservation of Rights

Licensor reserves all rights not expressly granted to you under this License. You acknowledge and agree that nothing in this License limits or restricts Licensor's rights in or use of the Licensed Material in any way. Neither this License, nor any act, omission, or statement by Licensor or you, conveys any ownership right to you in any Licensed Material, or to any element or portion thereof. As between Licensor and you, Licensor owns and retains all right, title, and interest in and to the Licensed Material subject to the license granted in Section 1.1. Your permission to use the Licensed Material is expressly conditioned on you not impairing Licensor's or the applicable copyright owner's rights in the Licensed Material in any way.

3. Restrictions on use

3. 1. Minor editing privileges are allowed for adaptations for stylistic purposes or formatting purposes provided such alterations do not alter the original meaning or intention of the Licensed Material and the new figure(s) are still accurate and representative of the Licensed Material. Any other changes including but not limited to, cropping, adapting, and/or omitting material that affect the meaning, intention or moral rights of the author(s) are strictly prohibited.

3. 2. You must not use any Licensed Material as part of any design or trademark.

3. 3. Licensed Material may be used in Open Access Publications (OAP), but any such reuse must include a clear acknowledgment of this permission visible at the same time as the figures/tables/illustration or abstract and which must indicate that the Licensed Material is not part of the governing OA license but has been

reproduced with permission. This may be indicated according to any standard referencing system but must include at a minimum 'Book/Journal title, Author, Journal Name (if applicable), Volume (if applicable), Publisher, Year, reproduced with permission from SNCSC'.

4. STM Permission Guidelines

4. 1. An alternative scope of license may apply to signatories of the STM Permissions Guidelines ("STM PG") as amended from time to time and made available at https://www.stm-assoc.org/intellectual-property/permissions/permissions-guidelines/.

4. 2. For content reuse requests that qualify for permission under the STM PG, and which may be updated from time to time, the STM PG supersede the terms and conditions contained in this License.

4. 3. If a License has been granted under the STM PG, but the STM PG no longer apply at the time of publication, further permission must be sought from the Rightsholder. Contact journalpermissions@springernature.com or bookpermissions@springernature.com for these rights.

5. Duration of License

5. 1. Unless otherwise indicated on your License, a License is valid from the date of purchase ("License Date") until the end of the relevant period in the below table:

Reuse in a medical communications project	Reuse up to distribution or time period indicated in License
Reuse in a dissertation/thesis	Lifetime of thesis
Reuse in a journal/magazine	Lifetime of journal/magazine
Reuse in a book/textbook	Lifetime of edition
Reuse on a website	1 year unless otherwise specified in the License
Reuse in a presentation/slide kit/poster	Lifetime of presentation/slide kit/poster. Note: publication whether electronic or in print of presentation/slide kit/poster may require further permission.
Reuse in conference proceedings	Lifetime of conference proceedings
Reuse in an annual report	Lifetime of annual report
Reuse in training/CME materials	Reuse up to distribution or time period indicated in License
Reuse in newsmedia	Lifetime of newsmedia
Reuse in coursepack/classroom materials	Reuse up to distribution and/or time period indicated in license

6. Acknowledgement

6. 1. The Licensor's permission must be acknowledged next to the Licensed Material in print. In electronic form, this acknowledgement must be visible at the

same time as the figures/tables/illustrations or abstract and must be hyperlinked to the journal/book's homepage.

6. 2. Acknowledgement may be provided according to any standard referencing system and at a minimum should include "Author, Article/Book Title, Journal name/Book imprint, volume, page number, year, Springer Nature".

7. Reuse in a dissertation or thesis

7. 1. Where 'reuse in a dissertation/thesis' has been selected, the following terms apply: Print rights of the Version of Record are provided for; electronic rights for use only on institutional repository as defined by the Sherpa guideline (www.sherpa.ac.uk/romeo/) and only up to what is required by the awarding institution.

7. 2. For theses published under an ISBN or ISSN, separate permission is required. Please contact journalpermissions@springernature.com or bookpermissions@springernature.com for these rights.

7. 3. Authors must properly cite the published manuscript in their thesis according to current citation standards and include the following acknowledgement: '*Reproduced with permission from Springer Nature*'.

8. License Fee

You must pay the fee set forth in the License Agreement (the "License Fees"). All amounts payable by you under this License are exclusive of any sales, use, withholding, value added or similar taxes, government fees or levies or other assessments. Collection and/or remittance of such taxes to the relevant tax authority shall be the responsibility of the party who has the legal obligation to do so.

9. Warranty

9. 1. The Licensor warrants that it has, to the best of its knowledge, the rights to license reuse of the Licensed Material. **You are solely responsible for ensuring that the material you wish to license is original to the Licensor and does not carry the copyright of another entity or third party (as credited in the published version).** If the credit line on any part of the Licensed Material indicates that it was reprinted or adapted with permission from another source, then you should seek additional permission from that source to reuse the material.

9. 2. EXCEPT FOR THE EXPRESS WARRANTY STATED HEREIN AND TO THE EXTENT PERMITTED BY APPLICABLE LAW, LICENSOR PROVIDES THE LICENSED MATERIAL "AS IS" AND MAKES NO OTHER REPRESENTATION OR WARRANTY. LICENSOR EXPRESSLY DISCLAIMS ANY LIABILITY FOR ANY CLAIM ARISING FROM OR OUT OF THE CONTENT, INCLUDING BUT NOT LIMITED TO ANY ERRORS, INACCURACIES, OMISSIONS, OR DEFECTS CONTAINED THEREIN, AND ANY IMPLIED OR EXPRESS WARRANTY AS TO MERCHANTABILITY OR FITNESS FOR A PARTICULAR PURPOSE. IN NO EVENT SHALL LICENSOR BE LIABLE TO YOU OR ANY OTHER PARTY OR ANY OTHER PERSON OR FOR ANY SPECIAL, CONSEQUENTIAL, INCIDENTAL, INDIRECT, PUNITIVE, OR EXEMPLARY DAMAGES, HOWEVER CAUSED, ARISING OUT OF OR IN CONNECTION WITH THE DOWNLOADING, VIEWING OR

USE OF THE LICENSED MATERIAL REGARDLESS OF THE FORM OF ACTION, WHETHER FOR BREACH OF CONTRACT, BREACH OF WARRANTY, TORT, NEGLIGENCE, INFRINGEMENT OR OTHERWISE (INCLUDING, WITHOUT LIMITATION, DAMAGES BASED ON LOSS OF PROFITS, DATA, FILES, USE, BUSINESS OPPORTUNITY OR CLAIMS OF THIRD PARTIES), AND WHETHER OR NOT THE PARTY HAS BEEN ADVISED OF THE POSSIBILITY OF SUCH DAMAGES. THIS LIMITATION APPLIES NOTWITHSTANDING ANY FAILURE OF ESSENTIAL PURPOSE OF ANY LIMITED REMEDY PROVIDED HEREIN.

10. Termination and Cancellation

10. 1. The License and all rights granted hereunder will continue until the end of the applicable period shown in Clause 5.1 above. Thereafter, this license will be terminated and all rights granted hereunder will cease.

10. 2. Licensor reserves the right to terminate the License in the event that payment is not received in full or if you breach the terms of this License.

11. General

11. 1. The License and the rights and obligations of the parties hereto shall be construed, interpreted and determined in accordance with the laws of the Federal Republic of Germany without reference to the stipulations of the CISG (United Nations Convention on Contracts for the International Sale of Goods) or to Germany's choice-of-law principle.

11. 2. The parties acknowledge and agree that any controversies and disputes arising out of this License shall be decided exclusively by the courts of or having jurisdiction for Heidelberg, Germany, as far as legally permissible.

11. 3. This License is solely for Licensor's and Licensee's benefit. It is not for the benefit of any other person or entity.

Questions? For questions on Copyright Clearance Center accounts or website issues please contact springernaturesupport@copyright.com or +1-855-239-3415 (toll free in the US) or +1-978-646-2777. For questions on Springer Nature licensing please visit https://www.springernature.com/gp/partners/rights-permissions-third-party-distribution

Other Conditions:

Version 1.4 - Dec 2022

Questions? customercare@copyright.com.

5. CONCLUSIONES GENERALES

En este trabajo se produjeron 44 anticuerpos recombinantes a partir de 25,621 secuencias VDJ, utilizando un criterio de selección desarrollado para este fin. El anticuerpo 19n01 destacó por su potente y amplia capacidad neutralizante contra diversas variantes del SARS-CoV-2, incluyendo Alfa, Beta, Gamma, Delta y subvariantes de Ómicron BA.1, BA.2, BA.4/5. Sin embargo, debido a que parte de su epítopo se encuentra en las posiciones K444 y V445 de la proteína S, las subvariantes de Ómicron con mutaciones en esas posiciones, como BQ.1.1, XBB.1.5, JN.1.7 y KP.3, ya no son susceptibles a su neutralización. Finalmente, la base de datos generada, que incluye 25,621 secuencias, podría ser de gran utilidad para seguir explorando potenciales anticuerpos neutralizantes contra variantes emergentes de preocupación. Además, las estrategias de selección y caracterización empleadas en este trabajo podrían servir para la identificación y estudio de futuros anticuerpos, no solo contra el SARS-CoV-2, sino también contra otros agentes infecciosos.

El estudio transcriptómico unicelular realizado en linfocitos B de sujetos convalecientes de COVID-19 permitió identificar la heterogeneidad de subpoblaciones en relación con distintos cuadros clínicos (leve, moderado, crítico y severo). Estos resultados revelan la capacidad de las subpoblaciones de linfocitos B para expresar genes proinflamatorios, especialmente en condiciones críticas y severas, que podrían contribuir a la gravedad de la enfermedad. Además, en este trabajo se muestra la identificación y caracterización de un grupo de linfocitos B de memoria atípicos. Los análisis indican que estas células presentan un perfil transcripcional y de repertorio distintos en comparación con los linfocitos B de memoria convencionales. Así mismo, los análisis muestran que estas células siguen una vía de diferenciación de centros germinales; no obstante, su diferenciación y activación podrían estar influenciadas por genes característicos a la exposición antigénica al SARS-CoV-2. Este estudio contribuye a una mejor comprensión del desarrollo de los linfocitos B de memoria atípicos en COVID-19 y el papel de otras subpoblaciones en las diferentes manifestaciones clínicas.

Los análisis realizados en el trabajo comparativo de la inmunidad híbrida generada por vacunas basadas en vectores adenovirales demostraron que ambas vacunas estimulan eficazmente la inmunidad híbrida, aunque con características distintas. La vacuna AZD1222 destaca por generar una robusta respuesta humoral con anticuerpos neutralizantes, mientras que Ad5-nCoV induce una

intensa respuesta celular incluso con una sola dosis. Estos hallazgos evidencian la diversidad en la respuesta inmune provocada por dos vacunas basadas en vectores adenovirales con esquemas de vacunación diferentes. Este estudio contribuye a la comprensión de la inmunidad híbrida en COVID-19 y podría ser valioso para el diseño de futuras estrategias de vacunación.

Finalmente, como resultado de esta tesis, se publicaron tres artículos titulados "*19n01, a broadly neutralizing antibody against Omicron BA.1, BA.2, BA.4/5, and other SARS-CoV-2 variants of concern*", "*Single-cell transcriptomic analysis of B cells reveals new insights into atypical memory B cells in COVID-19*" y "*Comparative single-cell transcriptomic profile of hybrid immunity induced by adenovirus vector-based COVID-19 vaccines*". Además, se ha presentado una patente bajo el título "*Anticuerpos contra el virus SARS-CoV-2 y sus variantes*", en la que se detalla el desarrollo de los 44 anticuerpos producidos con tecnología recombinante a partir de la secuenciación single-cell RNAseq de linfocitos B en sujetos convalecientes de COVID-19. Estos resultados también se han presentado de forma oral y en póster en el Congreso Internacional COVID and Beyond: Novel Approaches to Global Infectious Diseases, llevado a cabo en Bruselas, Bélgica, en octubre de 2022; así como en el Congreso Internacional de Inmunología (IUIS) en Ciudad del Cabo, Sudáfrica, en noviembre de 2023.

6. REFERENCIAS

Qiu, X. *et al.* Reversion of advanced Ebola virus disease in nonhuman primates with ZMapp. *Nature* 514, 47-53 (2014).

Wong, G., Bienes, K. M., Xiii, A., Fausther-Bovendo, H. & Kobinger, G. P. Ebola-specific therapeutic antibodies from lab to clinic: The example of ZMapp. *Antiviral Res* 226, 105873 (2024).

Tavakolpour, S. *et al.* A comprehensive review of rituximab therapy in rheumatoid arthritis patients. *Clin Rheumatol* 38, 2977-2994 (2019).

Taylor, P. C. *et al.* Neutralizing monoclonal antibodies for treatment of COVID-19. *Nat Rev Immunol* 21, 382-393 (2021).

Yamasoba, D. *et al.* Neutralisation sensitivity of SARS-CoV-2 omicron subvariants to therapeutic monoclonal antibodies. *Lancet Infect Dis* 22, 942-943 (2022).

Woodruff, M. C. *et al.* Extrafollicular B cell responses correlate with neutralizing antibodies and morbidity in COVID-19. *Nat Immunol* 21, 1506-1516 (2020).

Kaneko, N. *et al.* Loss of Bcl-6-Expressing T Follicular Helper Cells and Germinal Centers in COVID-19. *Cell* 183, 143-157 e113 (2020).

Oliviero, B. *et al.* Expansion of atypical memory B cells is a prominent feature of COVID-19. *Cell Mol Immunol* 17, 1101-1103 (2020).

Braddom, A. E., Batugedara, G., Bol, S. & Bunnik, E. M. Potential functions of atypical memory B cells in Plasmodium-exposed individuals. *Int J Parasitol* 50, 1033-1042 (2020).

Ebinger, J. E. *et al.* Antibody responses to the BNT162b2 mRNA vaccine in individuals previously infected with SARS-CoV-2. *Nature Medicine* 27, 981-984 (2021).

Sureshchandra, S. *et al.* Single-cell profiling of T and B cell repertoires following SARS-CoV-2 mRNA vaccine. *JCI Insight* 6 (2021).

Tan, Y. *et al.* Single-cell transcriptome atlas reveals protective characteristics of COVID-19 mRNA vaccine. *J Med Virol* 95, e28161 (2023).

Pulendran, B. & Arunachalam, P. S. Systems biological assessment of human immunity to BNT162b2 mRNA vaccination. *Res Sq* (2021).

Rabi, F. A., Al Zoubi, M. S., Kasasbeh, G. A., Salameh, D. M. & Al-Nasser, A. D. SARS-CoV-2 and Coronavirus Disease 2019: What We Know So Far. *Pathogens* 9 (2020).

Cai, Y. *et al.* Distinct conformational states of SARS-CoV-2 spike protein. *Science* 369, 1586-1592 (2020).

Almehdi, A. M. *et al.* SARS-CoV-2 spike protein: pathogenesis, vaccines, and potential therapies. *Infection* 49, 855-876 (2021).

Nishiura, H. *et al.* Estimation of the asymptomatic ratio of novel coronavirus infections (COVID-19). *Int J Infect Dis* 94, 154-155 (2020).

Cascella, M., Rajnik, M., Aleem, A., Dulebohn, S. C. & Di Napoli, R. in *StatPearls* (2024).

Russell, C. D., Lone, N. I. & Baillie, J. K. Comorbidities, multimorbidity and COVID-19. *Nature Medicine* 29, 334-343 (2023).

Sanyaolu, A. *et al.* Comorbidity and its Impact on Patients with COVID-19. *SN Compr Clin Med* 2, 1069-1076 (2020).

Silva, S. J. R. d., Kohl, A., Pena, L. & Pardee, K. Recent insights into SARS-CoV-2 omicron variant. *Reviews in Medical Virology* 33, e2373 (2023).

Tao, K. *et al.* The biological and clinical significance of emerging SARS-CoV-2 variants. *Nat Rev Genet* 22, 757-773 (2021).

Rahmani, K. *et al.* The effectiveness of COVID-19 vaccines in reducing the incidence, hospitalization, and mortality from COVID-19: A systematic review and meta-analysis. *Front Public Health* 10, 873596 (2022).

Korber, B. *et al.* Tracking Changes in SARS-CoV-2 Spike: Evidence that D614G Increases Infectivity of the COVID-19 Virus. *Cell* 182, 812-827.e819 (2020).

Fan, Y. *et al.* SARS-CoV-2 Omicron variant: recent progress and future perspectives. *Signal Transduct Target Ther* 7, 141 (2022).

Cui, Z. *et al.* Structural and functional characterizations of infectivity and immune evasion of SARS-CoV-2 Omicron. *Cell* 185, 860-871 e813 (2022).

Meng, B. *et al.* Altered TMPRSS2 usage by SARS-CoV-2 Omicron impacts infectivity and fusogenicity. *Nature* 603, 706-714 (2022).

Suzuki, R. *et al.* Attenuated fusogenicity and pathogenicity of SARS-CoV-2 Omicron variant. *Nature* 603, 700-705 (2022).

Balint, G., Voros-Horvath, B. & Szechenyi, A. Omicron: increased transmissibility and decreased pathogenicity. *Signal Transduct Target Ther* 7, 151 (2022).

Luo, X. H., Zhu, Y., Mao, J. & Du, R. C. T cell immunobiology and cytokine storm of COVID-19. *Scand J Immunol* 93, e12989 (2021).

Zanza, C. *et al.* Cytokine Storm in COVID-19: Immunopathogenesis and Therapy. *Medicina (Kaunas)* 58 (2022).

Li, Q. *et al.* Immune response in COVID-19: what is next? *Cell Death & Differentiation* 29, 1107-1122 (2022).

Diao, B. *et al.* Reduction and Functional Exhaustion of T Cells in Patients With Coronavirus Disease 2019 (COVID-19). *Front Immunol* 11, 827 (2020).

Zheng, H. Y. *et al.* Elevated exhaustion levels and reduced functional diversity of T cells in peripheral blood may predict severe progression in COVID-19 patients. *Cell Mol Immunol* 17, 541-543 (2020).

André, S. *et al.* T cell apoptosis characterizes severe Covid-19 disease. *Cell Death & Differentiation* 29, 1486-1499 (2022).

Kusnadi, A. *et al.* Severely ill COVID-19 patients display augmented functional properties in SARS-CoV-2-reactive CD8 + T cells. *bioRxiv* (2020).

Qin, X. *et al.* The seroprevalence and kinetics of IgM and IgG in the progression of COVID-19. *BMC Immunol* 22, 14 (2021).

Chvatal-Medina, M., Mendez-Cortina, Y., Patino, P. J., Velilla, P. A. & Rugeles, M. T. Antibody Responses in COVID-19: A Review. *Front Immunol* 12, 633184 (2021).

Ma, H. *et al.* Serum IgA, IgM, and IgG responses in COVID-19. *Cellular & Molecular Immunology* 17, 773-775 (2020).

Young, C. & Brink, R. The unique biology of germinal center B cells. *Immunity* 54, 1652-1664 (2021).

Crotty, S. Hybrid immunity. *Science* 372, 1392-1393 (2021).

Stamatatos, L. *et al.* mRNA vaccination boosts cross-variant neutralizing antibodies elicited by SARS-CoV-2 infection. *Science* (2021).

Reynolds, C. J. *et al.* Prior SARS-CoV-2 infection rescues B and T cell responses to variants after first vaccine dose. *Science* (2021).

Fonseca, M. H. G., de Souza, T. d. F. G., de Carvalho Araújo, F. M. & de Andrade, L. O. M. Dynamics of antibody response to CoronaVac vaccine. *Journal of medical virology* 94, 2139-2148 (2022).

Cao, Q. *et al.* Integrated single-cell analysis revealed immune dynamics during Ad5-nCoV immunization. *Cell Discov* 7, 64 (2021).

Chibwana, M. G. *et al.* AstraZeneca COVID-19 vaccine induces robust broadly cross-reactive antibody responses in Malawian adults previously infected with SARS-CoV-2. *BMC medicine* 20, 128 (2022).

Andreano, E. *et al.* Hybrid immunity improves B cells and antibodies against SARS-CoV-2 variants. *Nature* 600, 530-535 (2021).

Gelanew, T. *et al.* A single dose ChAdOx1 nCoV-19 vaccine elicits high antibody responses in individuals with prior SARS-CoV-2 infection comparable to that of double dose vaccinated SARS-CoV-2 infection naive individuals. *Res Sq* (2022).

Niyomnaitham, S. *et al.* Immunogenicity of a single dose of BNT162b2, ChAdOx1 nCoV-19, or CoronaVac against SARS-CoV-2 delta and omicron variants among previously infected adults: A randomized trial. *The Journal of Infection* 85, 436 (2022).

Rodda, L. B. *et al.* Imprinted SARS-CoV-2-specific memory lymphocytes define hybrid immunity. *Cell* 185, 1588-1601 e1514 (2022).